Magnetic domain structure in hexagonal crystals

Al-Bassam, T.S.

MAGNETIC DOMAIN STRUCTURE

IN HEXAGONAL CRYSTALS

by

T. S. Al-Bassam, B.Sc., M.Sc.

Presented in candidature for the

Degree of Doctor of Philosophy

October, 1969

CONTENTS

ABSTRACT

The domains structure of cobalt, gadolinium and terbium have been investigated; single crystals of gadolinium and terbium were obtained in which the oxide content was considerably reduced by a solid state electrolysis technique.

The Bitter technique has been used for most of the observations with a modified colloid, but a dry colloid technique has been used at temperatures below 240°K or higher than room temperature. Two different pieces of apparatus were designed for use at high or low temperatures. In the case of cobalt single crystals the results obtained at room temperature are similar to those obtained previously. The pattern at 77°K was as expected from the anisotropy data. The lengths of daggers of reverse magnetization and the widths of their bases were found to be in direct proportion (for simple and complex daggers). The variation of the exchange constant A with temperature was also determined. It was not possible to observe a closure domain structure, however this did not rule out the possibility of a partial structure being present on the basal plane, though the variation of domain width with temperature agrees best with that of Kittel model.

The domain structure of gadolinium was much easier to analyse than that of cobalt. At 274°K patterns on planes containing the c-axis showed parallel 180° walls with the development of partial closure

structures at the surface near the basal plane and at the oxide inclusions. Basal plane patterns indicate that the 180° walls are not plane and give more detailed information about the mixed nature of the basal structure. The change in domain structure has been studied as the temperature is reduced to 77°K and under the influence of magnetic fields up to 1400 Oe. Unexpected results were obtained when the normal field produced by a permanent magnet was applied to the basal plane. Such arrangements produced the well known honeycomb structure which was observed on other materials after an applied field of few K.Oe. was applied parallel or perpendicular to the c-axis. This was believed to be the result of a closure structure with magnetization laid freely in basal plane. The non-uniformity of the lines of force produced by such magnet will re-orient the direction of the magnetic moment within the closure region.

The domain structure in a cube shaped terbium single crystal was observed at 210°K and different possibilities for the internal configuration were given. Agreement between experimental observation and the proposed model which consists of plate type domains magnetized along the b_1 and b_2 axis but not along the third axis b_3-axis, which is perpendicular to one surface. The equilibrium width was measured and compared with the calculated one and they were in good agreement. The structure at lower temperatures was studied. However as in gadolinium it is still not clear whether the pattern observed at low temperature represents a true domain structure.

LIST OF ILLUSTRATIONS

Preceding Page

Preceding page

Preceding Page

CHAPTER 1

INTRODUCTION

1.1 Ferromagnetism

Magnetic materials are in some respects the most intriguing and exciting to study. In spite of the fact that a full understanding of the types of magnetic behaviour is still difficult, the progress that has been made is remarkable. In addition there are many technical applications which make them of obvious interest. The most known and important of these materials are ferromagnetic. A great variety of materials may be placed in this category being quite distinctly characterized by their magnetic properties. For such materials there exists a temperature called the Curie temperature, below which it is found to be possible to attain magnetic saturation by the application of small magnetic fields. At the same time it is possible for the magnetization of the specimen to be zero in a zero applied field. In order to align the magnetic moments at room temperature for a paramagnetic material it is found that a field of the order of 10^7 oersted is necessary while this field exists naturally with no applied field in a ferromagnetic body.

Weiss (1907) was the first to postulate the existence of a strong molecular field which aligned the individual magnetic moments parallel to each other. At the absolute zero of temperature this ordering will be perfect, but as the temperature is raised the alignment is gradually reduced by thermal fluctuations and the effect of this is to completely

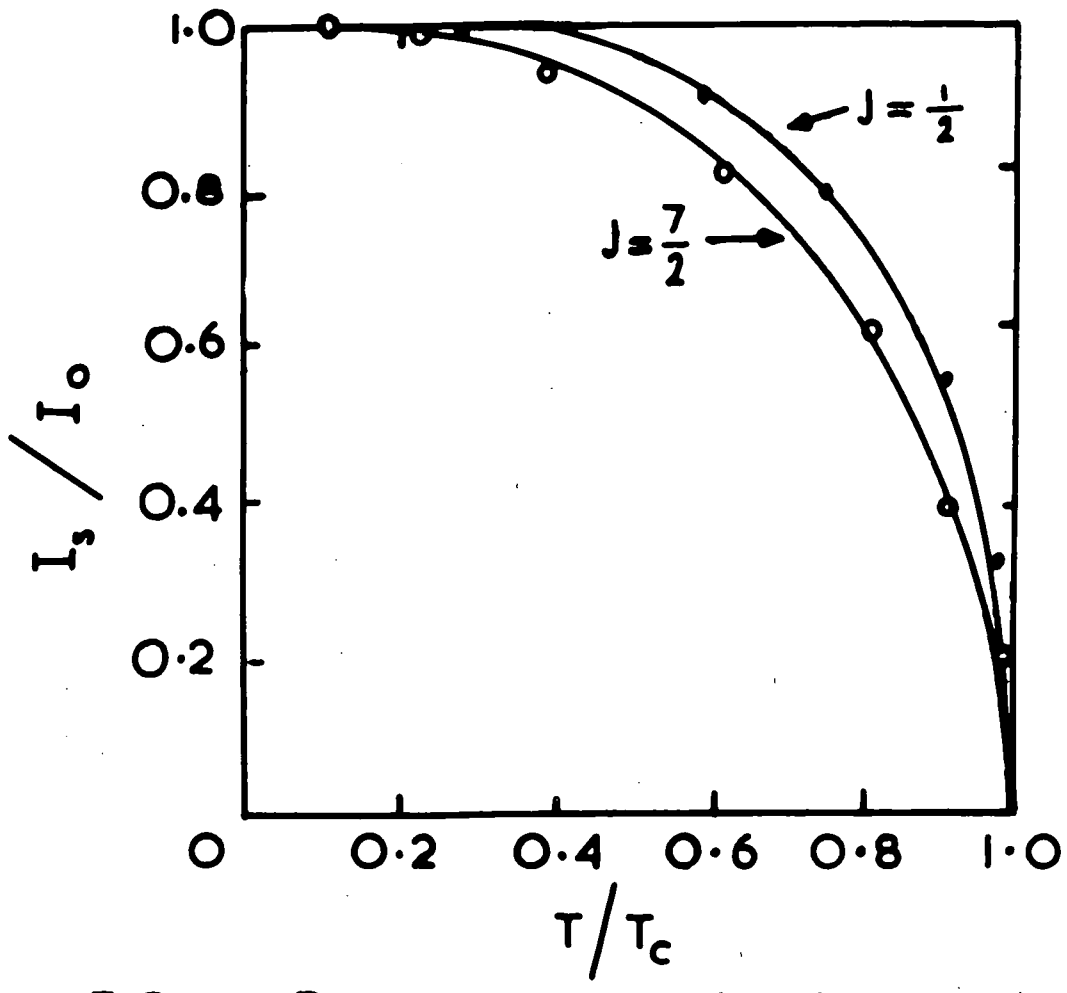

FIG. 1.1 Reduced magnetization curve as a function of temperature for

- • Cobalt
- o Gadolinium

destroy the ordering when the Curie temperature is reached. Fig.(1.1) shows the variation of spontaneous magnetization with temperature for Cobalt and Gadolinium, similar shaped curves being obtained for all ferromagnetic elements if the variation is plotted against temperature in reduced units. Above the Curie point the ordering breaks down and the material becomes paramagnetic. By this theory Weiss demonstrated clearly the reason for the easy magnetization of ferromagnetic materials, but it would not however give an explanation for the fact that ferromagnetic substances may exist in a state of zero magnetization; they are usually found with a zero demagnetized state. Weiss therefore advanced a second hypothesis which leads to a possible explanation of this point. He postulated that a ferromagnetic material divided up into small regions called domains, in each of which the atomic moments are always spontaneously aligned, but the direction of alignment varies from domain to domain to produce a zero resultant.

The origin of the molecular field (Weiss field ~ 10^7 oersted) is not explained by this theory. It was not until (1928) that Heisenberg postulated the existence of the exchange force. This is a purely quantum-mechanical force and has no classical counterpart, so any attempt to explain this force by non-mathematical representation will be somewhat incorrect. This force provides a physical explanation for the large magnitude of molecular field. Heisenberg showed that the force is due to an electrostatic term arising from the overlapping of

orbital wave functions of electrons associated with neighbouring atoms which leads to effective spin-spin coupling. This electrostatic energy term also depends on the relative orientation of the spins of the adjacent particles and therefore gives rise to the ferromagnetic effect. This effect, in a crystal in which each ion has a non zero spin, is large enough to account for the magnitude of the Weiss field.

There are a variety of ways in which the moments can align themselves. These different types of magnetic order give rise to different categories of materials. Ferromagnetics include the transition metals iron, nickel and cobalt, the heavy rare earth metals, and a few oxide compounds such as europium oxide. In these materials the moments align parallel to each other and thus produce a large moment per unit volume, so we should expect to find these ferromagnetic materials with high magnetization. The moment arises as a result of positive exchange interaction. Another category of materials is that in which, owing to negative exchange interaction, the spins are arranged in an anti-parallel pattern so that the atomic moments cancel and the resultant magnetic moment will be zero. Such material is called anti-ferromagnetic and examples are found amongst the rare earth metals and in many transition and rare earth compounds. A third class of alignment which arises through negative exchange interaction is that known as ferrimagnetic in which anti-parallel arrangement exists but there is a net moment which arises from a situation in which the moment pointing in one direction

is larger than that pointing in the other. This kind may occur when two or more kinds of magnetic atom of different moments are mixed together, or in complex crystals where there may be more elementary moments pointing in one direction than in the other. Examples of this type of alignment are found in the ferrites $MO.Fe_2O_3$ where M represents a metallic ion. These are non-metallic and of high resistivity. Even though the ferrimagnets possess a net magnetization it is much lower than that of the ferromagnetic materials.

The spontaneous alignment arises as a result of the exchange interaction which operates between uncompensated electron spins in the partially filled electron shells. The intrinsic magnetic moment of a ferromagnet is almost entirely due to the spins of these electrons. Electron orbital motion does not contribute a large moment to the intrinsic magnetization of solid magnetic materials based on transition metals. Owing to an interaction between the orbital motion and crystalline fields the orbital moments very nearly cancel out. This is known as quenching. The magnetic behaviour has been shown by Van Vleck (1952) to be mainly due to the electron spin. Unfilled electron shells are responsible for ferromagnetism rather than valence electrons. Since in a filled shell the electrons are paired off with as many spins up as spins down, they will average to zero moments. Thus only atoms with incomplete shells can have a net magnetic moment. The

arrangement of the spins is such that it will produce the highest possible net magnetic moment. For this to be consistent with the rule for filled shells means that once the shell is half filled additional electrons must point the other way. Thus in the case of transition metal the electrons responsible for the magnetization are those in the unfilled 3d band while the magnetic properties of the rare earth metals are closely related to the character of the unfilled 4f shell. The unfilled shell in the transition metals, is the outermost in the metallic ion. Interaction of the electron orbits with the crystalline field as in the transition metals quenches the orbital angular momentum, while in the case of the rare earths the unfilled 4f shell is screened from the crystalline field by the 5s and 5p shells. This will be discussed in Chapter 4. Thus the orbital angular momentum contributes to the total magnetic moment.

1.2 The Domain Hypothesis

The question of why the majority of ferromagnetics are not actually found in the spontaneously magnetized state, but are much more likely to have approximately zero magnetization, was answered by Weiss' hypothesis of domains. This hypothesis proposes that the interior of the material is divided into many magnetic domains, each of which is spontaneously magnetized. Since only the direction of domain magnetization varies from domain to domain the resultant magnetization can be changed from zero to the full value of spontaneous magnetization.

This direction of spontaneous magnetization is not constant within the material but varies between different domains. The domains in most substances are seen to be magnetized in one or more of a small number of directions called easy direction in which there is a strong tendency for the intrinsic magnetization to lie. The region in which the transition from one direction to the other occurs is called the domain wall. Domains vary in size but typical dimensions lie between 10^{-2} and 10^{-5} cm.

Application of a magnetic field to a ferromagnetic material, will affect the domains as suggested by Becker (1939). In a weak applied field the volume of domains which are favourably oriented with respect to the field will increase at the expense of unfavourably oriented domains. This process takes place by means of domain boundary displacements, while in a strong field the volume of the domains increases by means of the rotation of the direction of magnetization towards the direction of the field. The first direct observation of domains was made by Bitter (1931) and independently by Van Hamos and Thiessen (1932), using a colloidal suspension of small magnetic particles to make the boundary walls visible. This technique later became known as the Bitter technique. However, Bitter was unable to provide a direct relationship between the pattern observed on the surface and the internal structure for two reasons, firstly mechanical polishing has produced too great a strain on the surface of the specimen and secondly, because of their large size, the magnetic particles used were not sufficiently responsive

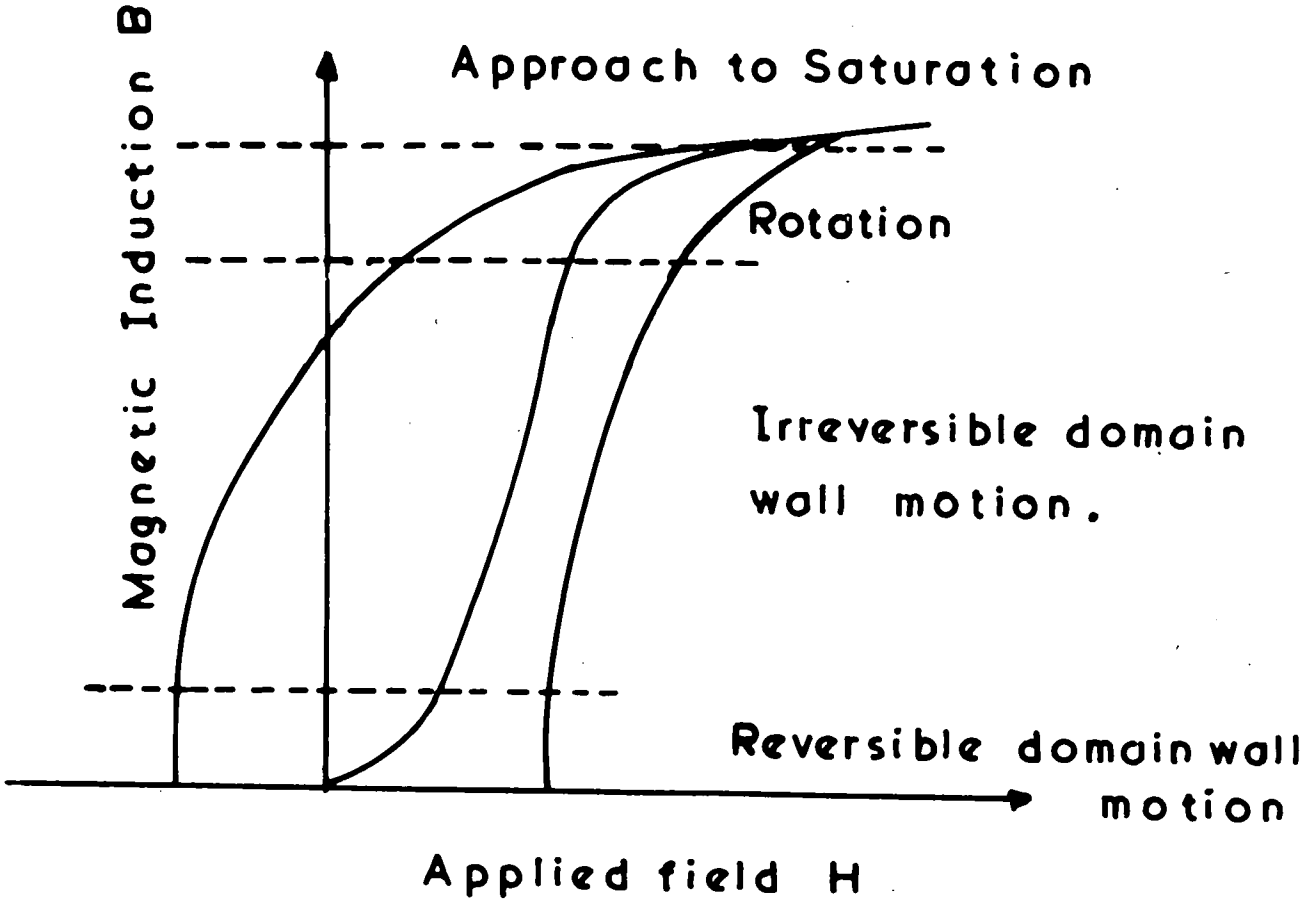

FIG. 1.2 Magnetization Curve and the Classification of Magnetization Mechanisms.

to the stray fields at the surface. The first acceptable theoretical explanation of domain structure was proposed by Landau and Lifshitz (1935). Working on the assumption that a ferromagnetic body with a large number of domains is a system of minimum energy, they calculated the different energy terms which will contribute to the total energy of the system and from which a minimum energy value may be obtained. Following the theoretical studies of Landau and Lifshitz, Elmore (1938) conducted the first experiments to observe clear domain patterns. By electropolishing a cobalt specimen he eliminated the strain previously resulting from mechanical polishing and thus observed the true domain structure of cobalt. This structure could be clearly distinguished from the pattern observed on the mechanically polished surface.

1.3 Magnetization curve

An important characteristic of any magnetic material is its magnetization curve when an increasing field is applied to an initially demagnetized specimen. The curve obtained is shown in figure 1.2. This behaviour of spontaneous magnetization with the applied field may be interpreted in terms of domain wall movement. In a narrow range of magnetization starting from the demagnetized state ($I = 0$, $H = 0$) the size of the domain, which is oriented nearest to the direction of the applied field, will increase by domain wall motion and the magnetization

will increase. At this stage the change in wall position is reversible (initial permeability range). If the magnetic field is increased beyond the initial permeability range the intensity of magnetization will increase rapidly until the domain growth is complete. This range is achieved mainly by irreversible displacement of domain walls from one stable position to another. When an external field of sufficient magnitude has been applied and the domain growth is completed, thus forming a material of a single domain, a further magnetization increase takes place slowly by the rotation of the magnetic moment in the direction of the applied field. The ferromagnetic materials show hysteresis, in that if the magnetizing field is reduced to zero, the total magnetization in the direction of the field still has a finite value. That is to say, the domain distribution has not returned to its original state. The area enclosed by the hysteresis loop is approximately given by the product of the saturation induction B_s times coercive force, that is, the energy dissipated on going once around a hysteresis loop. This is one of the major losses in magnetic materials and is believed to be due to energy dissipated by irreversible domain wall motions. This hysteresis loss is controlled principally by controlling impurities since impurities tend to pin domain walls. Reducing the number of impurities reduces the energy needed to move the walls which in turn reduces the losses. In order to understand the real

character of a magnetization curve, it is necessary to know the distribution of directions of domain magnetization at each point on the curve. It should also be recognised that the distribution of domain magnetization is quite different from the demagnetized state and the point of zero magnetization at the coercive force, though both states have equally $I = 0$.

1.4 Contributions to the Free Energy of a Magnetic System

The energy contributions to the system in a stress free state and with no applied external field are: exchange energy, magnetocrystalline anisotropy energy, wall energy, magnetostatic energy and magnetostrictive energy.

1.4.1 Exchange Energy

In the case of a ferromagnetic material where the fundamental moments are due to electron spin alone it is reasonable to consider only interaction between the electron spin of a given atom and that of its nearest neighbours. The force involved is of sufficiently short range to make this approximation adequate for the purpose of calculating the exchange energy between two atoms, i, j

$$E_{ex} = - 2J S^2 \sum_{i>j} \cos \phi_{ij} \quad \ldots\ldots\ldots (1.1)$$

where J is the exchange integral which may take either positive or negative sign depending on the spin alignment (parallel or anti-parallel), ϕ_{ij} is the angle between the direction of the spin momentum vector of atoms i and j, S is the total spin momentum per atom. Because the exchange energy has a minimum value when ϕ_{ij} is zero it can be assumed that the exchange energy in the domains is the zero level, therefore only the excess in the walls need be considered. If we assume that $\phi_{ij} \ll 1$ then the exchange energy varies with the angle between spins reducing to

$$\Delta E_{ex} = J S^2 \phi^2 \quad \text{.....(1.2)}$$

In order to calculate the exchange energy density it is necessary to estimate the energy exchange constant

$$A = \frac{2JS^2}{a} \quad \text{.....(1.3)}$$

where a is the lattice parameter. Estimating the value of A is very useful since it enters into the theoretical expressions for both the width and energy of a domain boundary.

1.4.2
Magnetocrystalline Anisotropy

In treating the exchange energy the crystal is considered to be isotropic, that is the exchange energy does not depend on the

coordinates of the system. However the experimental magnetization curves in a single crystal show that in certain directions, (easy directions) only a very small field is required to induce a given magnetization whereas a much larger field is needed to induce the same value of magnetization along the hard direction. Thus the magnetization tends to lie along certain crystallographic axes. It therefore becomes clear that the magnetic properties of the crystal are anisotropic and that the magnetic energy of the system will be dependent upon the direction of the magnetization vector relative to the crystal axes. This effect is known as magnetocrystalline anisotropy. When magnetization within the domains lies parallel to the easy direction the magnetocrystalline energy will be minimum.

The anisotropy energy density E_k in hexagonal crystals may be expressed by a power series expansion of the form:-

$$E_k = \sum_n K_n \sin^{2n} \theta \quad \ldots\ldots\ldots\ldots\ldots\ldots (1.4)$$

where K_n is an anisotropy constant independent of θ, the angle between the magnetization vector and the C-axis. Usually the first three terms of the expansion are sufficient to represent the actual anisotropy energy; higher powers are negligible in the case of cobalt, so

$$E_k(\theta) = K_o + K_1 \sin^2 \theta + K_2 \sin^4 \theta \quad \ldots\ldots\ldots (1.5)$$

The anisotropy constants of ferromagnetic materials are strongly temperature dependent. The angle θ does not specify completely the direction of the magnetization in the crystal, this is also dependent on the azimuthal angle ϕ about the c-axis. No term in ϕ appears in the energy expression in (1.4) but symmetry shows that the lowest term in which ϕ will be involved will be a term of sixth order so that,

$$E_k(\theta,\phi) = K_o + K_1 \sin^2\theta + K_2 \sin^4\theta + K_3 \sin^6\theta + K_4 \sin^6\theta \cos 6\phi + \ldots\ldots\ldots\ldots\ldots\ldots\ldots (1.6)$$

If the last term is small compared with the preceeding term it will merely introduce a slight six fold undulation in the anisotropy energy surface in the region of the basal plane. A knowledge of the values of the anisotropy constants and their temperature variation is very important for the quantative and qualitative treatment of domain structure.

1.4.3 The Wall Energy

Bloch (1932) was the first to investigate the nature of the transition layer which separates adjacent domains magnetized in different directions. The change in the direction of magnetization from one domain to the next does not occur abruptly over one lattice spacing since this would involve an extremely high value of the exchange

energy. Instead the change will take place in a gradual way over many atomic planes. The exchange energy for a gradual change is less than that for an abrupt one by a factor $\frac{1}{N}$, where N is the number of equal steps over which the change occurs, also this may readily be shown by the application of equation (1.2). Therefore it can be said that the coupling energy of the boundary separating the two domains is inversely proportional to its thickness. This does not however mean that the case $N \rightarrow \infty$ would normally be reached when the domain wall could occupy the whole crystal. On the other hand, the rotation of the spins in the wall causes many to lie in directions different from the easy direction thus producing an increase in magnetocrystalline anisotropy energy and this will limit the width of the wall. An equilibrium spin arrangement will be reached when the sum of the exchange and anisotropy energy is a minimum and this may be shown to occur when the exchange energy is equal to the anisotropy energy. Therefore the domain wall must have a finite width. The rotation of the spin across the wall is in such a way that the magnetization always lies parallel to the plane of the wall, thus there is no divergence of the magnetization across the wall and no associated magnetostatic energy. The condition that there should be no magnetostatic energy associated with the wall in a crystal with one easy direction implies that the only walls which will form are 180° walls. If the wall makes an angle

with the initial position there will be a resulting magnetostatic energy. So the energy contribution to the domain wall energy of ferromagnetic crystals are anisotropy and exchange energy

$$\gamma = E_k + E_{ex}$$

A detailed calculation of wall energy and wall width have been given by Lilley (1950) Stoner (1950) and Chikazumi (1964). The above discussion is for bulk material while in a thin film the case is different. Below a certain critical thickness the Bloch wall is unfavourable and a Néel wall forms, Néel (1955). This type of wall has the rotation of the spin normal to the plane of the wall, that is the magnetization in the wall rotates from one domain to the next without leaving the plane of the film, but for thicker films the interaction between the strips of free poles formed at intersections of the wall with the specimen surface will contribute to the wall energy.

1.4.4

Magnetostatic Energy

Free poles on the surface of the ferromagnetic crystal make it necessary to consider the magnetostatic energy in the calculation of the size of magnetic domains. This energy is due to the coulomb interaction between magnetic free poles. That is, the magnetostatic energy is the energy of a magnetic vector in its own field when there is no external applied field. This energy is given by

$$E_m = -\frac{1}{2}\int \vec{I}\cdot\vec{H}\, dv \qquad \text{.....(1.7)}$$

where I is the magnetization and H is the field acting on the domain, the integration being over the total volume of the specimen. The energy is always proportional to the width of the domains.

Kittel (1949) produced an important evaluation of the magnetostatic energy of a crystal being divided into many domain sheets each magnetized in opposite directions. For a system of strips of alternate polarity and each of width D,

$$E_m = 0.852\ I^2 D$$

per unit area of the surface. If both sides of specimen are considered

$$E_m = 1.7\ I^2 D \qquad \text{.....(1.8)}$$

Williams Bozorth and Shockley (1949) and Kittel (1949) showed that the magnetization of the domains is not fixed on the surface along the easy direction of the crystal but may be rotated away from it giving an effective permeability μ^*. The free poles on the surface produce this effect and consequently the magnetostatic energy of the system will be changed. From the rotation of the magnetization will result two components, one parallel to the easy direction which will be assumed unchanged. The other component perpendicular to the easy direction is proportional to the demagnetizing field. The μ^* value has been calculated to be

$$\mu^* = 1 + K^* \qquad \text{.....(1.9)}$$

where parameter $k^* = \dfrac{2\pi I_s^2}{K}$

where I_s is the saturation magnetization and K an anisotropy constant. Fox and Tebble (1958, 1959) have shown that the energy associated with free poles at the surface of the specimen is reduced in a uniaxial crystal by a factor

$$2\left\{1 + (1 + K^*)^{\frac{1}{2}}\right\}^{-1} = 2\left\{1 + \sqrt{\mu^*}\right\}^{-1}$$

so the value of magnetostatic energy will be

$$E_m = 1.7\ I_s^2\ D\ \frac{2}{1 + \sqrt{\mu^*}} \qquad \text{.....(1.10)}$$

In material with high K and low I_s, $\mu_s^* = 1$ and the magnetization at the surface would not be deviated.

1.4.5 Magnetostriction and Magnetoelastic Energy

Becker et al (1939) developed the theory of magnetostrictive energy by minimising the total energy of the crystal and it was found to be proportional to $\lambda_s \sigma$. Where λ_s is magnetostriction coefficient, σ stress either applied or internal. Thus applying a stress σ to a crystal will produce a preferential direction of magnetization. The magnetoelastic anisotropy energy introduced may bring about a re-orientation of domains, for an isotropic specimen the energy could be represented by

$$E_\sigma = -\frac{3}{2}\ \lambda_s \sigma \cos^2 \alpha \qquad \text{.....(1.11)}$$

where α is the angle between the stress direction and the magnetization, for small α, the total anisotropy energy will be

$$K + \frac{3}{2}\ \lambda_s \sigma = K + K_\sigma \qquad \text{.....(1.12)}$$

That is the extra energy produced by an external factor may be added

to the magnetocrystalline anisotropy. The value of λs for cobalt is

$$\lambda s = - 50 \times 10^{-6}.$$

The magnetostrictive energy is dependent upon the orientation of the specimen, the temperature and also the applied field. It is found that generally the magnetostrictive energy decreases with increasing temperature.

1.5 Domain Structure

The domain structure in a ferromagnetic body is not a constant attribute of bulk material but is a function of dimensions, and the orientation of the boundary surface of the crystals as well as of the state of strain and of the magnetic field intensity. The most important factor is probably the demagnetizing field arising at the boundary of the specimen. The formation of domains reduces the magnetostatic energy associated with this field. Domain boundaries form and they lie in planes which correspond to minima in the boundary energy. In order to reduce the magnetostatic energy associated with a boundary there is generally continuity of the component of magnetization normal to the plane of the boundary. In a uniaxial crystal where the c-axis is the easy direction of magnetization boundary walls generally contain the c-axis. Possible domain configurations have been suggested by many workers. For uniaxial crystals these include the following.

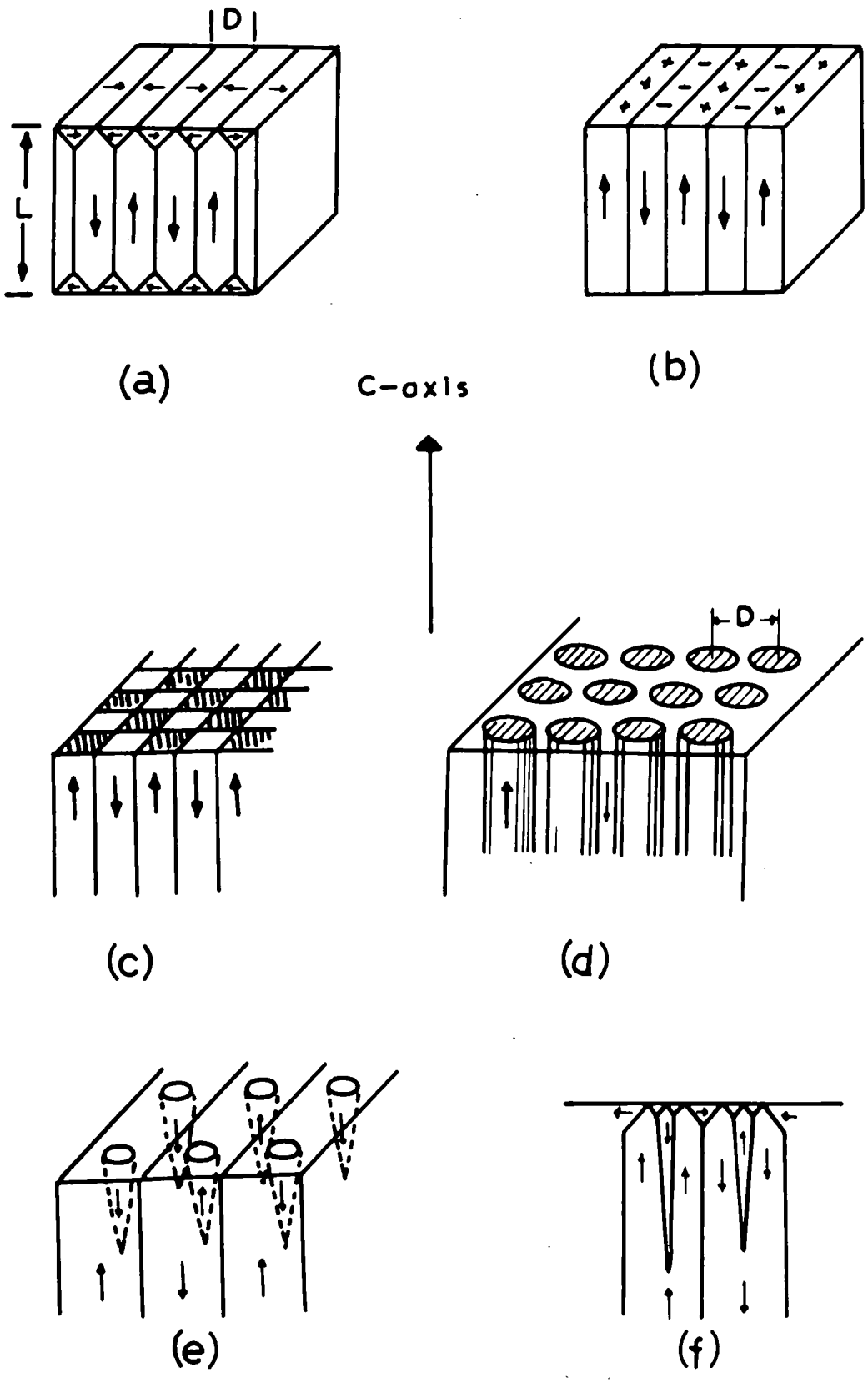

FIG. 1.3 Domain structure of uniaxial single crystal .

1.5.1 Landau and Lifshitz Model

A structure which is found when a large demagnetizing field arises as a consequence of the free pole on the basal plane. Landau and Lifshitz proposed the growth of closure structures in which the magnetization is directed along a hard direction and which will have a magnetocrystalline anisotropy energy which is proportional to their volume Fig. (1. 3a) , the extra magnetocrystalline energy per unit volume of specimen in the closure domains can be reduced by reducing the domain spacing and thus reducing the volume occupied by the closure domains, by this means the total area of the walls will increase and this means that it is not possible to reduce the free energy of the specimen indefinitely by this means. This structure gives a total energy per unit area

$$E = \frac{\gamma L}{D} + \frac{KD}{2} \qquad \text{.....(1.13)}$$

the minimum energy condition is

$$D = \sqrt{\frac{2\gamma L}{K}} \qquad \text{.....(1.14)}$$

which gives the minimum energy per unit area

$$E = \sqrt{2\gamma LK} \qquad \text{.....(1.15)}$$

1.5.2 Kittel Model

In material where the magnetocrystalline energy is very large compared to the magnetic energy. Closure domains do not exist since these secondary structures will have associated with them a large magnetocrystalline anisotropy energy and the structure will be of simple parallel 180° walls with no superficial domains fig. (1.3b). This has become known as the Kittel Model. The total energy is

$$E = \frac{\gamma L}{D} + 1.7\, I_s^2\, D \qquad \ldots\ldots\ldots\ldots\ldots\ldots (1.16)$$

Minimising this leads to

$$D = \sqrt{\frac{\gamma L}{1.7\, I_s^2}} \qquad \ldots\ldots\ldots\ldots\ldots\ldots (1.17)$$

and

$$E = 2I_s\sqrt{1.7\,\gamma L} \qquad \ldots\ldots\ldots\ldots\ldots\ldots (1.18)$$

while in the case of a chequer board Fig. (1.3c) Kittel (1949) gave

$$D = \sqrt{\frac{\gamma L}{.53\, I^2}} \qquad \ldots\ldots\ldots\ldots\ldots\ldots (1.19)$$

$$E = 2I_s\sqrt{.53\,\gamma L} \qquad \ldots\ldots\ldots\ldots\ldots\ldots (1.20)$$

for the circular pattern Fig. (1.3d)

$$D = \sqrt{\frac{\gamma L}{.374\, I^2}} \qquad \ldots\ldots\ldots\ldots\ldots\ldots (1.21)$$

$$E = 2I_s\sqrt{.374\,\gamma L} \qquad \ldots\ldots\ldots\ldots\ldots\ldots (1.22)$$

From this it is clear that the magnetostatic energy is proportional to the domain width.

1.5.3 Goodenough Model

The structures in Fig. (1.3b) will have a large demagnetizing field, so Goodenough (1956) proposed the structure shown in Fig. (1.3e) in which the magnetostatic energy decreases without the creation of closure structures and without increasing the wall energy appreciably. Lifshitz (1944) has also proposed a structure of a more complicated nature for a uniaxial crystal as shown in Fig. (1.3f). He also showed that under certain conditions this arrangement has lower energy than that of the simple closure structure. The calculationof magnetostatic energy for such a structure is very complicated, but Takata (1962), assuming that the region of reverse magnetization has a square base, calculated the magnetostatic energy for such a pattern and found that the minimum magnetostatic energy is 0.186 I_s^2 D in the case of two reverse domains one within the other magnetized in opposite directions (double reverse domains) and 0.285 I_s^2 D for single reverse domains.

1.5.4 Kaczer Model for Infinite uniaxial cylinder

Models for possible domain structures of a uniaxial infinite cylinder having an easy direction laid in the basal plane and no hexagonal anisotropy have been proposed by Kaczer (1962). Two possible structures were given; partially closed flux Fig. (1.4a), or the sub-division of the cylinder into disc-shaped domains (1.4b), parallel to the basal plane. The magnetization in each disc differs from the

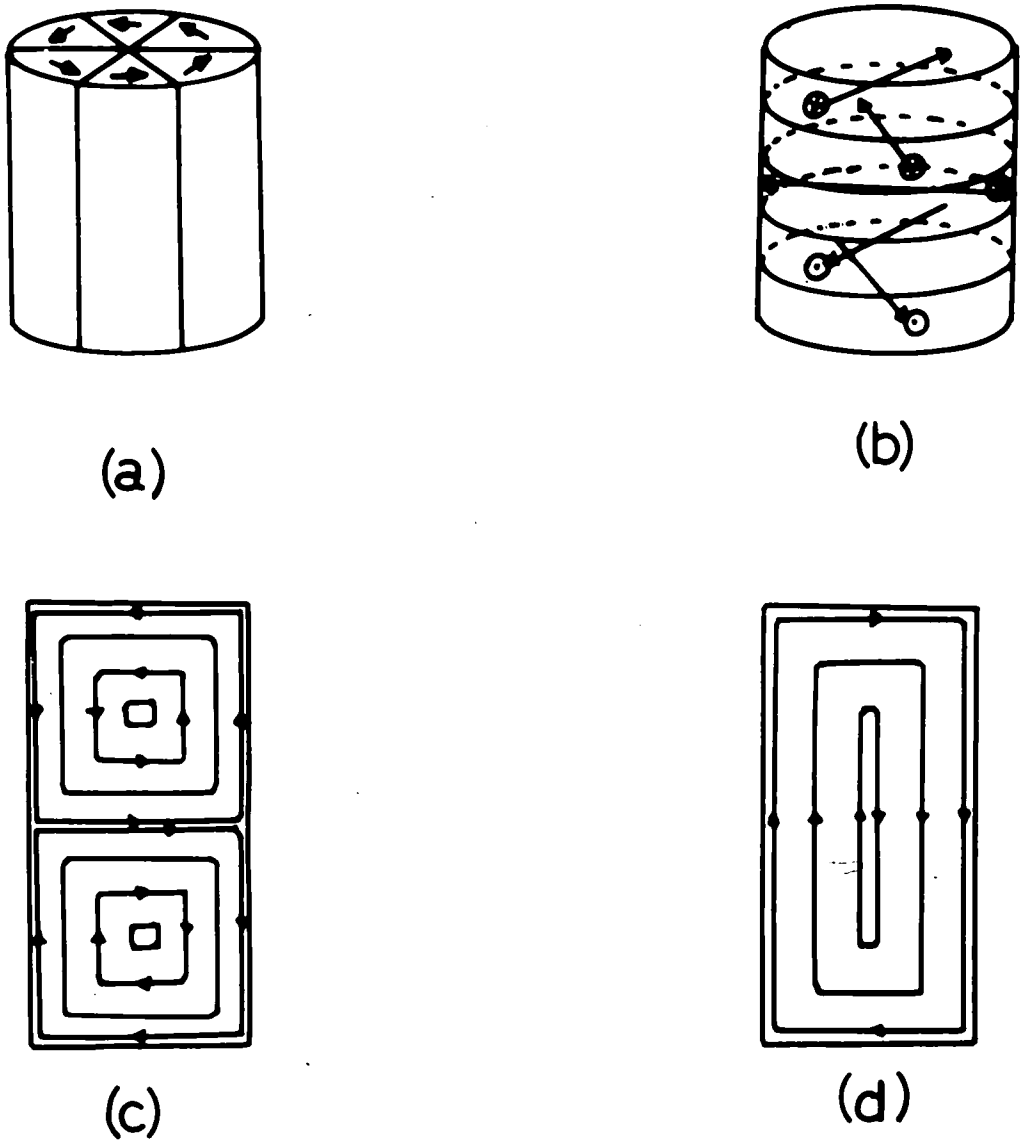

FIG 1.4

a&b Possible domain configurations for non-vanishing hexagonal anisotropy. (Kaczér)

c&d Theoretical possibilities for domain structures in the limit of zero anisotropy energy (Kittel)

neighbouring one by an angle $\frac{2\pi}{i}$ where i = 2, 3, 6. That is, the magnetization in each of these discs lies along one of the six-fold axes in the basal plane. The energy of the walls depends on the angle Φ_i between the direction of magnetization in neighbouring domains. It was found that the cylinder radius is the factor which decides which of these two types of structure will exist. For large radii the disc structure is formed while below a certain critical radius the partially closed flux configuration is more stable.

1.5.5 Domain Model for Vanishing E_k and E_σ.

In a special case where the anisotropy and the magnetostriction are both zero, Kittel proposed two possible domain structures Fig. (1.4c,d), each domain occupies a large part of the volume of the crystal. This case will be found when the Bloch wall thickness becomes comparable with crystal dimensions.

It may be concluded that the minimizing of the demagnetizing field of the specimen as a whole is satisfied by the division of the specimen into domains. The reduction of free energy brought about by this division is very large and of the order of $\frac{1}{2} N I_s^2$ where N here is the demagnetizing coefficient which depends upon the shape of the specimen. The value of N for different shaped specimens has been tabulated by Osborn (1945) and Brown (1962).

1.6 Domain Observation

The two most widely used techniques in observing and studying the magnetic domain structure in ferromagnetic bulk material are the Bitter technique and the Kerr magneto-optical effect. The Bitter technique simply involves placing a drop of magnetic colloid on a highly polished strain free surface. The small magnetic particles are then attracted to the regions where the stray field is strong. The stray fields are mostly present at the intersection of the Bloch wall with the surface so that observations of the surface through a microscope show up the domain boundaries in the surface as dark lines. The direction of magnetization in a given domain may be determined by means of a very fine scratch produced on the surface of the specimen. If the scratch is normal to the magnetization direction it gives rise to a stray local field and this will collect the magnetic particles. Should the particles be polarised by an applied or stray magnetic field they will be collected by some parts of the scratch and repelled by others. If, however, it is parallel to the magnetization the scratch will not attract the small particles in the colloid. The colloid technique gives a picture of domains in two dimensions. By choosing a proper surface with the smallest number of easy directions of magnetization it is possible to build up a model in three dimensions from the surface patterns. The powder technique has some limitations. The colloid may stain the surface if left on it for some time and this makes

it difficult to re-examine the pattern on this surface without further polishing. This limitation may be overcome by using a colloid suspension with celacol (sodium carboxy-methyl cellulose). Craik (1956) used this technique, allowing the film to dry on the surface and removing it from the specimen surface, the film could be examined either on an optical microscope or an electron microscope for high magnification. This method has a limitation of its own. If it is desired to study the wall movements it is impossible to use the strippable colloid technique. Another limitation of the colloid technique is that when materials with low anisotropy (which have a wide domain wall and hence low stray fields) are to be examined, the stray fields gradiant are too low to attract the colloid particles. The boiling and freezing points of the suspending medium impose yet another limitation.

Another method which is used widely is the Kerr magneto-optical effect technique. This makes use of the rotation of the plane of polarization of a plane polarized beam of light upon reflection from a ferromagnetic surface. This rotation is dependent upon the direction of magnetization on the surface, so that two domains magnetized in different directions produce rotations which differ in direction and magnitude, thus producing a contrast if the surface is viewed through suitably oriented analyser. We therefore see domains rather than domain boundaries as in the case of Bitter technique. There are again difficulties involved in using this technique, the differences in rotation

between two domains magnetized in different directions are very small. For a surface with an easy direction parallel to it the rotation is of the order of 5'. All the bulk specimens to be studied must be treated by electro-polishing, however small irregularities and the presence of inclusions will produce a large amount of surface noise. Fowler and Fryer (1954) used a photographic technique to eliminate this noise. They superimposed the positive of a photograph of the saturated specimen (where there is no domain structure present) upon a negative which includes the domain structure and a print was then made from the combined pair. Since crystals of the rare earth metals usually include a large amount of oxide and other impurities, this technique is difficult to apply to these materials at the present time. The bloming process first suggested by Kranz (1956) showed that when the specimen surface is coated with layers of transparent dielectric the Kerr rotation will increase and this will improve the contrast. This method of studying the domain structure is very useful in observing the domain wall movements and also there is no fundamental limitation to the temperature at which it may be employed. Material with low magneto-crystalline anisotropy may be studied by this technique.

Other techniques of investigating domain structures are available. The Faraday effect may be used with a very thin specimen, thin enough to allow the transmission of light through it. The specimen thickness should be about 10^{-5} cm for metal films, 10^{-4} cm for ferrites and 10^{-3} cm

for garnets. Hall et al. (1959) and Tebble (1965) have used Lorentz electron microscopy. This technique has the advantage of producing a high contrast. The specimen should be very thin to be studied by this method. Mayer (1967) used a mirror electron microscope. The electron beam is deflected at the surface of the ferromagnetic sample and interaction with the magnetic fields associated with the surface pole distribution causes a change in the trajectories of the electrons. As a result the pattern could be observed on a screen, the specimen surface acting as an electron optical mirror. Comprehensive surveys of methods of studying domain patterns are to be found in Carey and Isaac (1966), Craik and Tebble (1965), Suhl (1968) and Chikazumi (1964).

CHAPTER 2

EXPERIMENTAL TECHNIQUES

2.1 Specimens

2.1.1 Cobalt single crystal

A large piece of ingot was supplied by Professor L. F. Bates and was stated to have a high coercivity. A single crystal was cut from this ingot using a fine thread-like saw blade, the final shape of the crystal being rectangular with dimensions of 0.44 x 1.05 x 0.29 cm. The high coercivity might be due to inclusions present in the specimen. The large surface was a basal plane.

2.1.2 Gadolinium single crystals

A single crystal of Gadolinium of 99.9% purity and measuring 0.5x 3 x 2 mm with a large $\langle 11\bar{2}0 \rangle$ surface was obtained from Metals Research Limited. This percentage of purity is related to the presence of other rare earth metals and not the oxide content, in fact a large amount of the oxide impurity was present in the specimen. It was found to be distributed all over in a random manner. In an attempt to produce a specimen of lower oxide content a technique of solid state electrolysis as described by Spedding and Daane (1961) was used on a rod of Gadolinium metal. In the work of Spedding and Daane an electric current was passed through a rod of yttrium maintained at a temperature just below its melting point in vacuum. A large proportion of the foreign

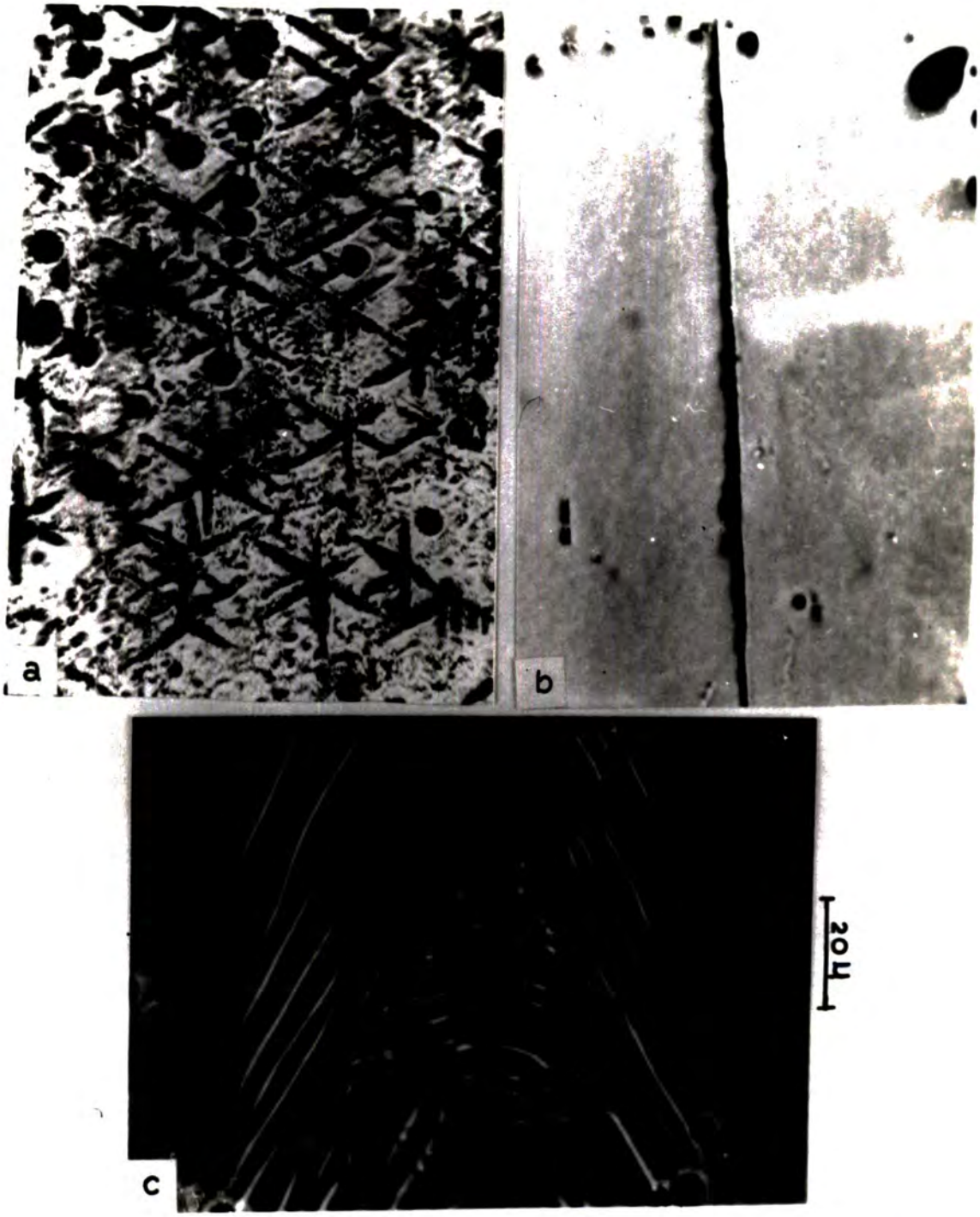

Fig. 2.1. (a,b) Gadolinium surface before and after electrolysis treatment.
c- surface structure produced on Gadolinium after mechanical polishing.

ions within a metal lattice migrated toward the anode which was water cooled. In the present work the technique was applied to Gadolinium by Metals Research Limited. This resulted in three samples of Gadolinium metal one of which was in excellent condition. Even in this however, the oxide and non metallic impurity had not completely moved toward the anode, but had aggregated within the metal as star shaped platelets with the c-axis normal to the plane. Although ideally a completely oxide-free specimen would have been preferable the presence of these platelets was found to be useful for observing the growth of daggers of reverse magnetization along inclusions as in the case of other ferromagnetic materials. Figure 2.1a and b show basal plane surfaces of two specimens before and after electrolysis treatment. The effect of the random spacing of these platelets, as will be seen later, is to separate the Gadolinium metal in to a set of films of different thicknesses. The specimen supplied was a single crystal disc of 4.91 mm diameter and 2.23 mm thickness. The surface of the disc was a basal plane and two more surfaces were cut at right angles to each other. This was done by mounting the specimen first and, after determining the direction of the main axes by means of an X-ray back reflection technique, grinding the specimen to the required orientation.

2.1.3 Terbium single crystal

A small specimen was cut from a large piece of ingot 99.9% purity

relative to the presence of other rare earth metals. After examination it was found that a large amount of inclusion was present, it was not possible to obtain any results on such a specimen. A further single crystal of Terbium was supplied by Metals Research Limited. This had been cut from a rod which had been purified by the method of solid state electrolysis, but here the impurities aggregated in a large mass and did not form platelets as in the case of Gadolinium. The specimen was in the form of a cube with dimensions of .257 x .302 x .242 cm. The large surface was a basal plane.

2.2 Preparation of the Specimens

Observation of domain structures requires a surface with a high polish and no strain. First the specimen was mounted, the material being carefully chosen since some mounting material could produce a high compression during solidification which in turn produces a strain in the sample especially for the rare earth metals which are comparatively soft. Mounting plastic powder N.H.P. 2031/19 mixed with liquid N.H.P. 1844 and added to it a few drops of hardening additive N.H.P. 123 was tried (this was supplied by North Hill Plastic Limited, London N.16). This mounting material produced a high temperature of about 335^{o}K resulting from the chemical interaction of the liquid with the powder. The mount will set in a few minutes forming a very solid block which is hard to break and thus permit removal of the specimen for the purpose of studying

the domain structure at low or high temperature. It was also found that this mount produces a strain in the specimen. This was very inconvenient in this work, so choosing another mounting was therefore necessary before further work takes place. A cold mount Ceemar Resin FR 262 mixed with a few drops of accelerator FR 252 and hardener FR 228, supplied by Ciba (A.R.L.) Limited, Duxford, Cambridge, gave excellent results, but one disadvantage of this mount is that it needs about 24 hours to set at a temperature of 290^{o}K. It is very easy to remove the specimen by cutting and breaking the edges of the mounting material. After the specimen has been set, a conventional method of mechanical polishing was carried out by using successively finer grades of emery paper (0/0, 2/0, 3/0, and 4/0) followed by diamond paste on a rotating wheel with grades 6, 3 and $\frac{1}{4}$ µm. Throughout the process dry kerosene was used as a lubricant. Between every stage the specimen was carefully washed with absolute alcohol to prevent the carrying on of particles of abrasive from the previous stage. In the case of Gadolinium and Terbium care must be taken during this process, a high pressure should not be used otherwise heavy scratches and surface structure like those shown in Figure 2.1c will be produced. At this stage the specimen surface was mirror like but had associated with it a high strain induced as a result of mechanical polishing. To remove the strain and the scratches and also the secondary effects which appeared on the surface of Gadolinium and Terbium and to get a work-free surface a

technique of electropolishing was used for Cobalt and a chemical polishing for Gadolinium and Terbium.

Cobalt was electrolytically polished in a solution consisting of 23% perchloric acid and 77% glcial acetic acid. A voltage of 24 volts D.C. was used between the specimen anode and stainless steel cathode. Care must be taken when using this cell, the solution must be surrounded by ice to keep the temperature of the solution under $300^{\circ}K$. The electrolyte was placed in a beaker equipped with a magnetic stirrer, this process resulted in a highly smooth and strain-free surface. In polishing Gadolinium and Terbium the technique of chemical polishing was adopted. In order to obtain a strain-free surface the specimen may either be annealed at temperatures of about $680^{\circ}K$ in a very high vacuum, better than 10^{-6} torr, or using a continuous flow of pure argon. The latter technique was not preferred since it was a very long process and since Gadolinium and Terbium are very active at high temperature. In the case of vacuum failure these metals will easily oxidize, therefore the technique of chemical polishing suggested by Roman (1965) was adopted, using a solution containing the following:-

20 ml. lactic acid

5 ml. phospheric acid

10 ml. acetic acid

15 ml. nitric acid

1 ml. sulphuric acid.

Water should not enter this solution during the preparation or in subsequent use. Polishing was done by using a cotton swab soaked in the solution and moved gently over the surface of the specimen. This was carried out for a few seconds after which the specimen was rinsed carefully with ethyl alcohol and dried in a stream of warm air. It was then examined under a microscope and the process repeated until a satisfactory surface was obtained. This solution could be stored for a long time. For safety it should be kept in an open container in a dust free atmosphere and at a temperature of about 290^{o}K. A very low temperature will crystalize the lactic acid and at a higher temperature reaction will take place and nitric acid will decompose from which nitric oxide will be liberated. At this stage the solution should not be used since it will damage the surface which will then need repolishing using emery paper to remove the defects on the surface.

2.3 Apparatus

The conventional method of studying domain structure on the surface of bulk specimens relies on the field inhomogeneity at the domain boundaries attracting small ferromagnetic particles, the boundaries are decorated by the small particles which may be observed by an optical microscope. In this case the domain walls rather than domains themselves will be observed, but by applying a small field perpendicular to the surface under examination the small particles will be polarized and these

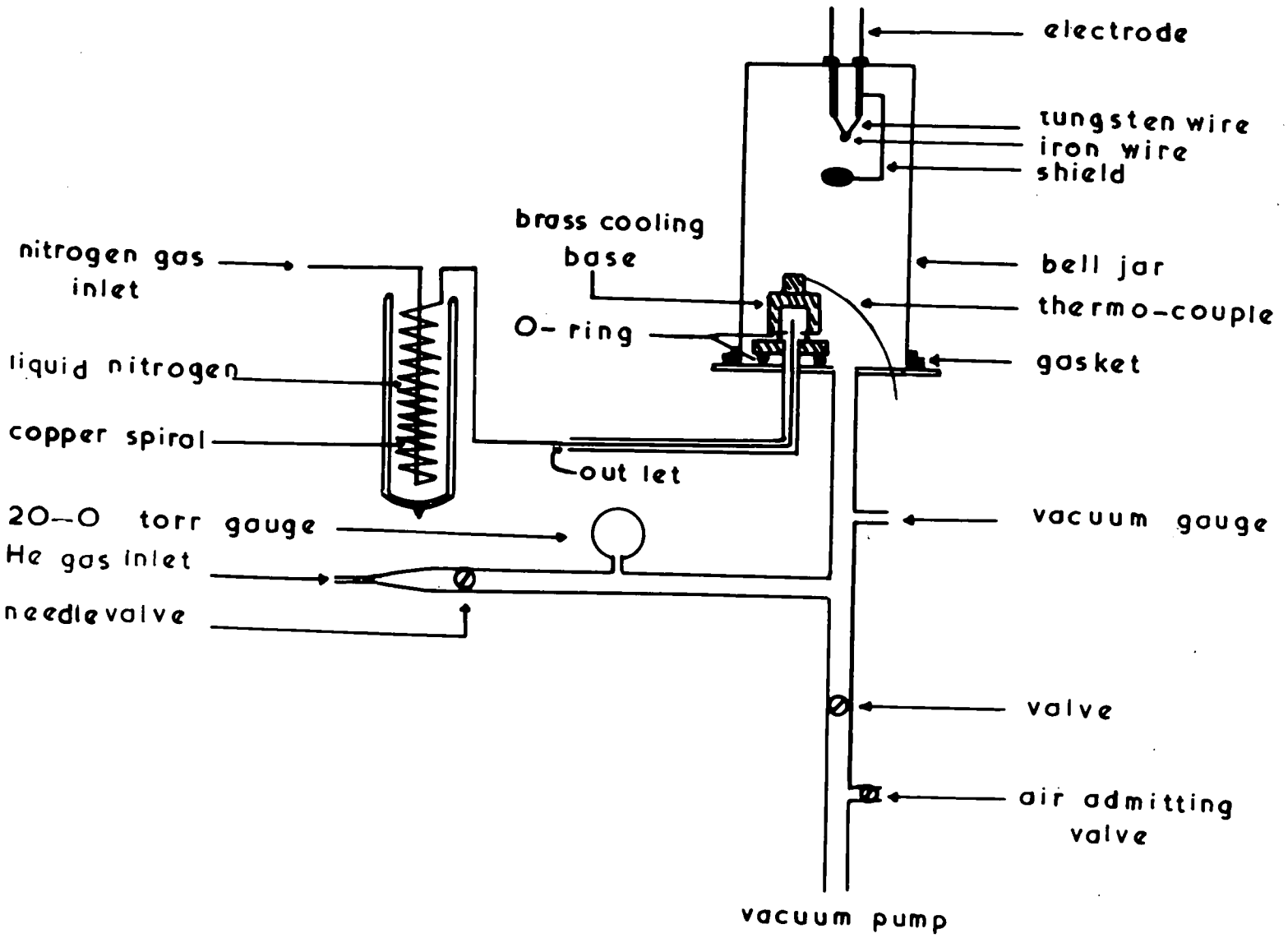

FIG. 2.2 The Evaporation Apparatus with the Cooling System

in turn will deposit preferentially on domains magnetized in directions such that the free surface has a suitable polarity. This technique originally due to F. Bitter, has been applied to the study of domains in a wide range of magnetic materials.

The Bitter technique cannot be applied at very high or very low temperatures. A dry colloid technique has been described by Hutchinson et al. (1965) and this has been applied in the present work. Small ferromagnetic particles are deposited on the surface in the presence of an inert gas at low pressure. The apparatus used for production of the small ferromagnetic particles is shown in Figure 2.2 and consists of a vacuum pump capable of producing 10^{-3} torr in a bell jar. Two vacuum-tight electrodes are attached to the top of the jar and these supply the power to the heating source for the purpose of evaporating iron or cobalt. The heating source is of tungsten wire of diameter 0.5 mm in the form of a "V" in order to minimize the area of contact between this and an iron wire of .02 mm diameter, and so reduce the alloying of the two metals. Iron was used throughout the experiment rather than cobalt wire since the latter easily alloys with the tungsten. The high current supply consists of a variable transformer connected to a large transformer of an input up to 240 volts and output of 130 amperes at 2 volts. It was found in this case that a current of 80 amperes and 1.5 volts gave the best results. The current was applied slowly to the heating source to ensure the complete melting of the iron wire forming a small bead which then slowly evaporated. The evaporation takes place

in Helium at a pressure of 0.2 torr; it is useful to flush the system with high purity helium before starting the evaporation of iron.

Within the bell jar the specimen was placed on a large brass block which has a cavity for cooling purposes, the block was of cylindrical shape with a diameter 5 cm and main axis of 6.5 cm. It was made large to maintain fairly constant temperature and cooled by nitrogen gas passing first through a copper spiral tube immersed in liquid nitrogen or ice. In order to insulate the cooling block from the rest of the apparatus it was placed on a formica disc. To maintain the vacuum within the system the formica disc has an "O" ring adjacent to each surface the one nearest to the brass block is smaller than that on the other side of the formica, this was necessary to prevent leakage to the vacuum system through the screw which attaches the formica to the brass block. The temperature was measured using a constantan copper thermo couple. A specific temperature was obtained by controlling the rate of flow of the cooled nitrogen gas. The iron particles produced in this way are about 200A° diameter, this being dependent upon the pressure of the helium gas at which the evaporation takes place, in this case the distance of the evaporation source to the specimen was 14 cm. It takes between two and five minutes for the iron particles to deposit on the surface of the specimen. A small shield was placed under the evaporation filament as this is necessary to prevent a direct deposit

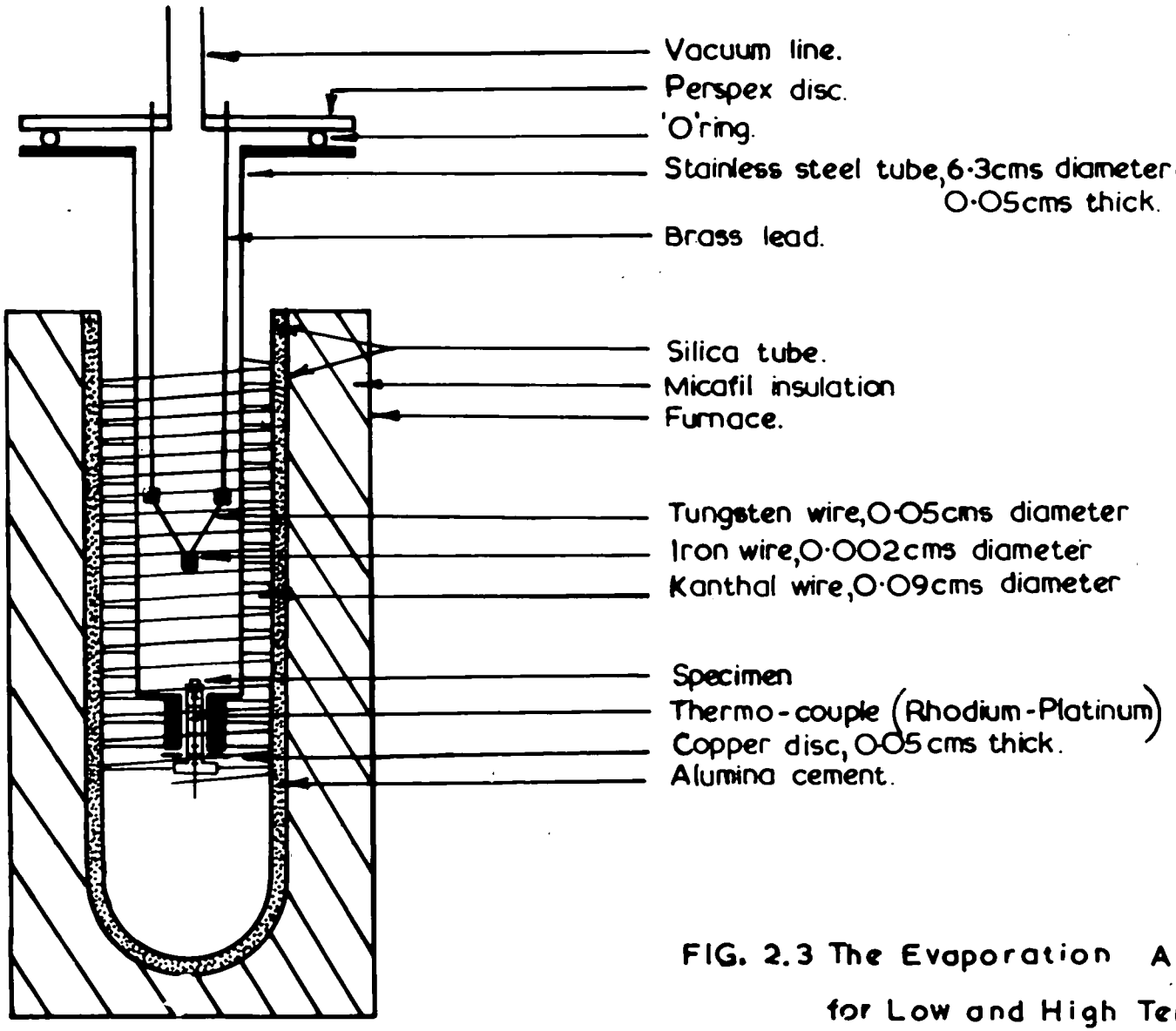

FIG. 2.3 The Evaporation Apparatus for Low and High Temperature.

of particles. In addition large particles of iron were sometimes emitted from the heater and the shield ensures that these cannot strike the specimen. The shield also serves to absorb the heat radiated from the filament and stops it from reaching the specimen.

At a very low or high temperature such as that used in the investigation on Cobalt, evaporation in a bell jar was not adequate since the temperature of the brass block will be much different from the surroundings inside the jar. This will set up convection currents which will exert a force on the iron particles. The force is proportional to the temperature gradient in the system. To overcome this difficulty the cooling block and the surroundings must be at very nearly the same temperature. Therefore another apparatus was designed. Details of this are shown in Figure 2.3. This consists of a 78 cm long stainless steel tube of diameter 6.3 cm and wall thickness 0.05 cm., sealed to a brass plate on which rests a perspex disc of thickness 1.3 cm and which, in turn, rests on an "O" ring. Through the perspex are two vacuum-tight electrodes joined to which are two brass leads of diameter .45 cm. The current was supplied through these to the filament. A copper tube was joined to the perspex disc and this was in turn joined to a vacuum system. The disc made of perspex was very useful since it is a transparent material which enables us to see through and to control the amount of evaporation taking place. The arrangement of the power supply and the heating filament is as described before. The specimen was placed on a

brass rod which was screwed into the end of the stainless steel tube. A thin copper washer of thickness 0.05 cm was used to ensure a tight vacuum seal. The distance between the filament and the specimen was 12 cm. For low temperatures the stainless steel tube was immersed in liquid nitrogen. For the study of the domain pattern at higher temperatures the stainless steel tube was placed vertically inside a furnace. This ensured an equilibrium temperature between all the objects inside the stainless steel tube. High temperatures were measured using a Rhodium-platinum thermo couple which was coupled to a Honeywell temperature control unit.

The furnace consists of two silica tubes the inner one of diameter 7.5 cm while the outer one was of diameter 12 cm. Kanthal wire of 0.09 cm diameter was wound around the silica tube to serve as a heating element. The gap between the two tubes was filled with alumina cement to form an insulating medium and to hold the heating wire firmly in its place. The outer tube is isolated from the surroundings by using Micafil insulation.

This technique is less limited in the range of temperature for which it is suitable, than the usual colloid technique and also gives satisfactory results even with an irregular surface (results could be obtained on five surfaces of a cube specimen at the same time). It has however the disadvantage that the specimen must be removed from the evaporation system and examined under the microscope. It is not possible to use the

technique for the study of detailed changes in domain structure with either magnetic field or temperature. Once the iron particles have settled on the specimen surface they are not subjected to any change either by rotation or displacement of the domain wall caused by temperature or external field variation. The small iron particles deposited on the specimen surface are easily removable by washing with ethyl alcohol. For most of the work done here domains were made visible by the use of a modified colloid unless it is specified that the results were obtained by the dry colloid method.

2.4 Colloid Preparation

Since it was difficult to follow the domain wall movement by using the technique described above it was decided that a suitable colloid should be developed. The magnetite should be suspended in a liquid which does not react with the rare earth metals and which does not freeze at reasonably low temperature. The colloid prepared by Bates and Spivey (1964) was useful, but it was very easily evaporated and it was found difficult to complete any set of experiments, before the colloid had dried. The magnetic colloid used in this case was prepared by the usual method of Elmore (1938) except that the magnetite was suspended in a secondary butyl alcohol and agitated in a bath by an ultrasonic tranducer for about 30 minutes. A stable finely dispersed colloid was produced. This did not evaporate so rapidly and did not stain the surface

very quickly. To use this colloid the specimen was mounted on a large brass block which could be cooled below room temperature by nitrogen gas that has been previously cooled by passing through a copper spiral immersed in ice or liquid nitrogen. The magnetic field was applied by means of small electromagnets either perpendicular or parallel to the surface under observation. The two electromagnets and the cooling block were designed to fit under the microscope. A Cook M4000 microscope was used to observe the patterns. The colloid was applied to the specimen surface and this was then covered by a microscope cover slide to retain the colloid on the specimen surface uniformly. A drop of secondary butyl alcohol was placed on top of the slide to prevent the formation of frost when the temperature was reduced. A small magnetic field of order of 150 Oe was needed to increase the contrast of the patterns with the specimen surface. It was found that the lowest temperature at which this colloid could be used was 230^{o}K; below this temperature the colloid does not freeze but the magnetic particles become very restricted in their movement and they will stick to the surface regardless of the effect of the stray field on the surface. It appears impossible to use the wet colloid technique at temperatures below 230^{o}K.

2.5 The Crystal Orientation

The X-ray laue back reflection method was used to determine the crystal orientation. Before mounting the specimen on the goniometer it was well etched to remove the strained layer. The process used in

producing a well etched cobalt surface was that of Jacquet (1935, 1936), this consists of electropolishing using an electrolyte of orthophosphoric acid (specific gravity 1.35). A voltage of 1.5 volts was maintained between the specimen as anode and a large cobalt cathode. In the case of Gadolinium and Terbium a chemical etching solution was used which consisted of:-

10 ml. phosphoric acid

10 ml. lactic acid

30 ml. nitric acid

20 ml. acetic acid.

After the solution had been applied by using a piece of cotton wool for a few minutes the specimen was rinsed with ethyl alcohol and dried in a stream of warm air. The specimen was then mounted on the goniometer and exposures were made using an X-ray tube with a cobalt anode. A large number of exposures were made and the orientation of the surface was determined to within $\pm \frac{1}{2}^{o}$. Many exposures were made with the X-ray beam incident at different points in the surface in order to make sure that the specimen was a single crystal. All the exposures showed clear spots arranged according to the surface orientation. It was found that covering the photographic plate by a thin sheet of aluminium of thickness .020 mm produced much better results especially for gadolinium and terbium. The background radiation is absorbed by the aluminium sheet leaving the spots which represent the parallel sets of planes in

the crystal. The spots on the photographic plates were transformed to a stereographic projection and then compared with the standard one given by Salkovitz (1951) for Cobalt. Although he gave inter-planer angles for magnesium which has the ratio of c/a = 1.6235 compared to that of Cobalt with c/a = 1.6320, the ratios are so close that the table could be used without any difficulty. The results for Gadolinium and Terbium were compared with those published by Koepke and Scott (1966). The results showed that the specimens each possessed three perpendicular surfaces with the following orientation:

Co	[0001]	, $< 2\bar{1}\bar{1}0 >$,	$<10\bar{1}0>$
Gd	[0001]	, $< 11\bar{2}0 >$,	$<10\bar{1}0>$
Tb	[0001]	, $< 11\bar{2}0 >$,	$<10\bar{1}0>$

2.6 Techniques Used in Present Work

Domain structures were observed using the dry and wet colloid techniques. A combination of these two methods was very satisfactory in giving a complete picture of the domain structure of the three metals. In addition the Kerr magneto-optical effect was used. In the case of rare earth metals, where the oxide inclusions are large in number, they render the surface irregular and the scattering of the incident light destroys the contrast between adjacent domains. In these circumstances the colloid technique will often still give results. The Kerr effect on Gadolinium was tried and it appeared

impossible to obtain any results in this instance because of the presence of the oxide inclusion and the difficulty in obtaining a very flat surface which is essential in using this method of investigation. For cobalt it was possible to observe the domain pattern as light and dark areas, the direction of rotation depending on the direction of magnetization in the reflecting surface. It was found that the light intensity for photography was very poor. A long exposure was required and special modifications were needed for to use at high and low temperatures. For these reasons the Kerr effect was not employed for any of the observation reported in this thesis.

2.7 Photographic technique

It was found that the domain structure of gadolinium and terbium crystals is on a very small scale compared to that of cobalt. To obtain a satisfactory picture with enough detail a high magnification was needed. The domain pattern was photographed using a small grain film of Ilford Pan F 35 mm., ASA 50, in a Pentax camera mounted on top of the microscope. The microscope had 16X eye piece and 40X objective, the magnification through the microscope was 1.5X. The camera was used with its lens removed and fixed to the microscope with a Pentax adapter. The specimen was placed on the cooling block when a wet colloid was used or put directly on the microscopic moving stage for examination when the dry colloid had been applied. The pattern was

observed using the eye piece extension or reflex viewer of the camera. It was found that low light intensity and longer exposure reduce the error in the exposure time. The domain patterns photographed were then developed using a fine grain developer, Paterson Acutol FX-14. This solution was diluted one to ten parts of water and the developing time was nine minutes at temperature 292°K. Best results were obtained by mixing one part to twenty parts of water and doubling the developing time. The film was then washed and then fixed in Kodak unifix, diluted one to three parts of water for six minutes. The prints were made in the usual way. Any measurements were made directly on the microscope moving stage which is attached to a micrometer.

CHAPTER 3

DOMAIN STRUCTURE OF COBALT SINGLE CRYSTAL

3.1 Previous work

Cobalt was one of the first metals upon which single crystal investigations on domains were carried out and has subsequently provided subject matter for many authors. The ease with which it was possible to study it was largely due to the metal having a high magnetocrystalline anisotropy and being easily available in single crystal form. The domain structure has been investigated at different plane orientations, under various conditions and using various techniques. Although the domain structure on the surface including the c-axis is one of the easiest to observe the complexity of the domain structure on the basal plane has aroused interest and stimulated further detailed study.

Bitter (1931) was the first to attempt to study the magnetic domains of cobalt on a specimen with a smooth surface. The specimen used on this occasion was unpolished and the results obtained therefore showed the well known maze pattern due to the strain involved on the surface. Elmore (1938) obtained a very successful pattern on an electro polished cobalt specimen, showing that the domain structure on prism planes consists mainly of domains parallel to the hexagonal axis, magnetized alternately in opposite directions. The pattern obtained on the basal plane showed a more complicated structure of a star shaped nature. This was shown to be due to a reversed magnetization, a large star representing

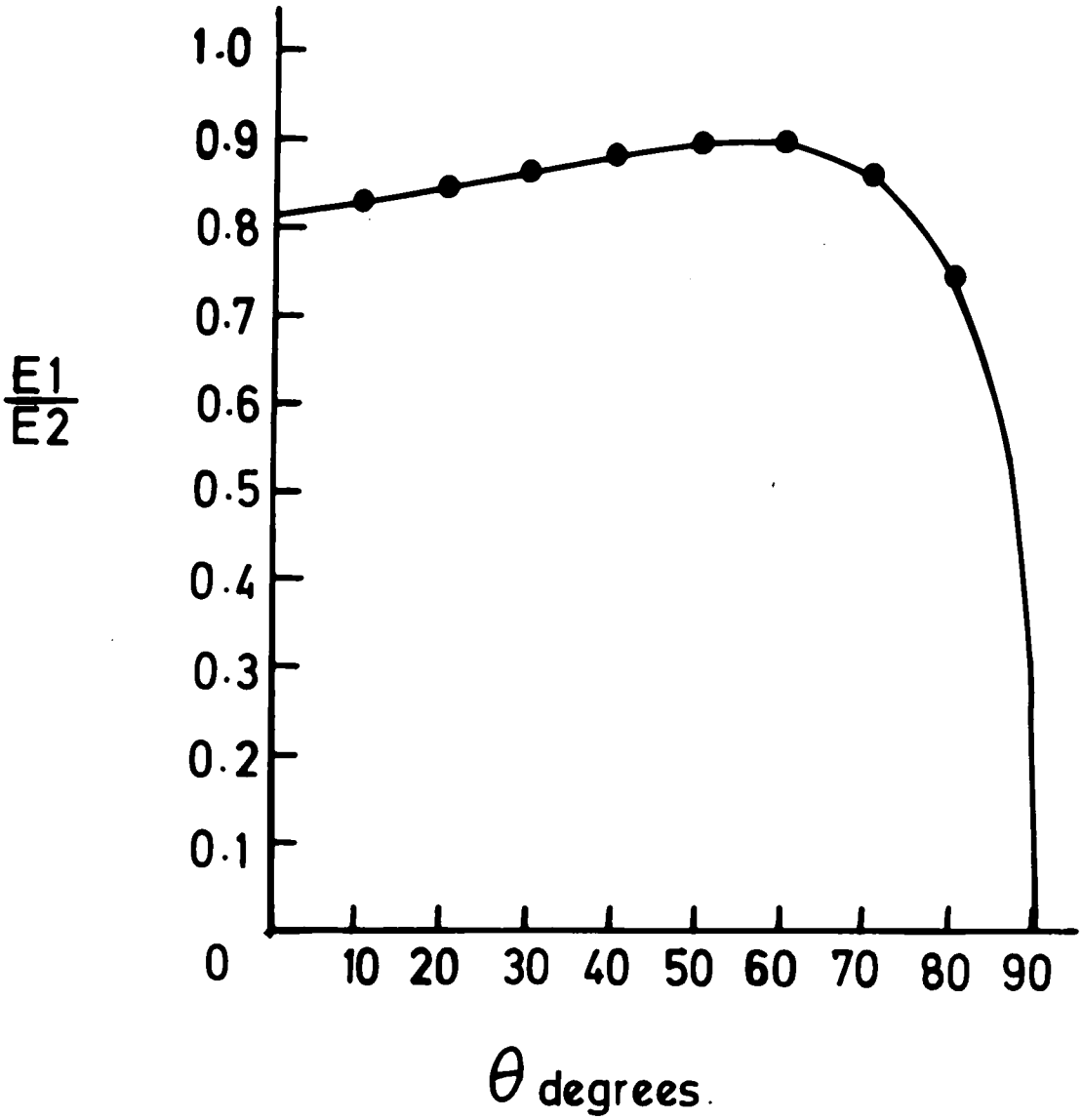

FIG. 3.1 ratio E1/E2 plotted against θ, at 290°k. (Hall, 1956)

a region of reverse magnetization extending deep into the crystal while a small one represents a region of reverse magnetization extending only a short distance within the specimen. When observed on a prism surface these regions produce a V-shaped line deposit. This model becomes known later as a Kittel type structure.

Landau and Lifshitz (1935) suggested that the star shaped region did not have magnetization perpendicular to the surface but possessed only that which was parallel to it, that is perpendicular to the c-axis (easy direction) thus leaving no free poles on the surface. This model is known as a Landau and Lifshitz type of structure.

The structure observed by Elmore (1938) has been confirmed in later work by Mee (1950), who applied a magnetic field in the prism plane surface at right angles to the direction of magnetization, and explained the disappearance of alternate domain boundaries which had been discussed by (Néel, 1944). André (1954), observed the pattern near a grain boundary dividing prism and basal plane, and Hall (1956) showed that the pattern formed on crystal planes, other than the basal and prism faces, had a basal structure with angles ranging from 0° (the basal plane) to about 54° away from the c-axis, while between 54° and 62° the pattern changes until it takes the usual 180° form. The energy for both the Kittel and the Landau and Lifshitz model has been calculated and compared, Fig. (3.1) shows these results at room temperature. It is clear that at all angles $E_1 < E_2$, where E_1 is the energy of the Kittel

model, E_2 is the energy of the system for Landau and Lifshitz model, θ is the angle between the c-axis and the normal to the plane of the observation. This shows that the structure on the basal plane should be essentially due to free poles. Fox and Tebble (1958) concluded from the work on a single crystal cobalt disc that the structure is one of Kittel type. Reverse daggers are formed when $\theta \leq 57^{\circ}$, when $\theta < 33^{\circ}$ the reduction in demagnetizing energy can only be brought about by rotation of the magnetization vector, but in both cases there is no formation of a closure structure. Gemmer (1942) by electron diffraction observed the stray field near a basal plane, which is of the order of 10^4 Oe., this field is detectable to about .01 mm above the surface. This could only be explained by the presence of a large free pole on the surface. Takata (1962) studied the domain pattern on the planes of wedge shaped cobalt crystals. He too considered the surface structure to be due to the free poles on the surface. The magnetastatic energy was calculated for co-planar parallel strips with alternate signs of free poles. For simplicity of calculation the author considered the base of the dagger as a square. It was demonstrated that the width of the domain strip decreases with a decrease in the thickness of the crystal. Wyslocki (1963) supported the theory of free poles on the surface and showed a clear colloid picture at the edge of the specimen where the reverse dagger was observed without the presence of a closure structure. Bates and Craik (1962) investigated the domain structure of cobalt using

an electron microscope, observing the pattern obtained by using a colloid which dries to form a thin film. They approached the matter differently from previous workers and supposed that the basal plane structure forms a continuous network which can not be divided into discrete rings. The structure remained unchanged when the field increased and then changed to one of reverse daggers at high fields. These results are believed to indicate that in the basal plane structure there are no domains with magnetization having a component normal to the plane. However, a field of some several thousand oersted will transform this into a free pole structure, thus the structure on a cobalt single crystal is thought to be of the Landau and Lifshitz type. Bates and Craik showed the pattern formation of a fine colloid structure around strained areas due to scratches, slip planes and twins. In spite of the fact that these were studied under high magnification the photograph showed poor contrast. An investigation of the dependence of domain width on specimen thickness was carried out on several crystals embedded in the parent one and showed the results $D \propto L^{\frac{1}{2}}$ where D is the domain width and L specimen thickness, Kaczer et al (1958) investigated the domain structure on cobalt whiskers. On the basal and prism plane of the whisker it was found that the structure is similar to that on bulk material. The pattern on the edge of the whisker showed dagger-like domains of reverse magnetization. The dependence of the domain width on the thickness of the specimen is closely represented by a two thirds power law, i.e. $D \propto L^{\frac{2}{3}}$ rather than $L^{\frac{1}{2}}$ as shown

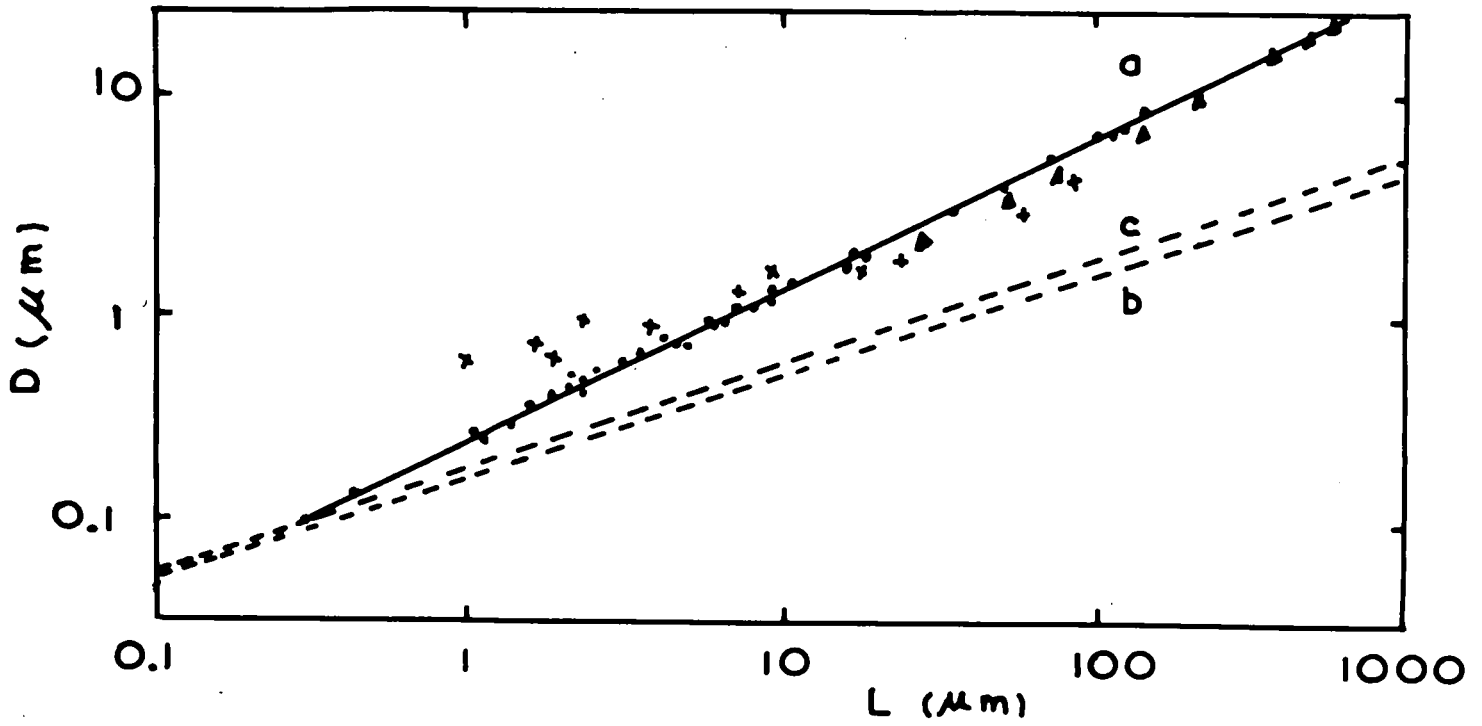

FIG. 3.2 Dependence of domain width D on thickness L of Cobalt crystal.

Experimental curves, a
- × Bates et al.
- ▲ Kandaurova et al.
- + Andrä.
- • Kaczér et al.

Theoretical curves,
- b Landau & Lifshitz.
- c Kittel.

by previous authors, this difference was explained as being due to different surface structure taken in consideration. However in a crystal of around several μ to tens of μ thick the surface structure is one of a mixed state, that is a region of free poles and closure structure. A model domain structure was suggested. Variation of domain width with crystal thickness showed that the experimental results deviated from the theory because of the influence of surface structures. These structures had an effect up to thicknesses of around 0.2 μm. Fig. (3.2) shows the variation of domain width with the thickness of the specimen.

Gemperle et al. (1963) investigated the honeycomb structure and found that it is meta stable and has higher energy than the usual plate structure. Wyslocki et al. (1965) studied the remanentdomain structures of a large single crystal. Two different types of regular stable domains were observed depending upon whether the creating field was parallel or perpendicular to the hexagonal crystal axis. In first case the structure was of a Kittel type, the basic domain appeared to have a rod-like shape with cross section showing regular hexagons. In the second case the domain structure consisted of a regular super-position of both the Kittel and the Landau and Lifshitz type. These results show differences from those obtained by Kaczer et al. (1961) (carried out on magneto plumlite) in two respects. In the first paper the creating field being necessary parallel to the hexagonal crystal axis while in the second paper it had to be perpendicular. The second difference is

that the honeycomb structure bears no relation to the hexagonal symmetry of the crystal lattice while the first author supposed it to be directly related to the crystal symmetry.

The recent interest in the domain structure of cobalt at elevated temperature is due to the fact that K_1 is strongly temperature dependent and induces uniaxial anisotropy at low temperatures and conical and planar at high temperatures.

Fowler and Fryer (1955) studied the pattern at high temperature by means of the longitudinal Kerr effect, results suggest a gradual widening of the domain wall as the transition temperature is approached. As the temperature raised above the transition region new domains formed. Andrä (1956) observed the pattern on the basal plane using a colloid suspension of magnetite in paraffin oil. At 653°K the domains on basal plane showed a preferred direction. Kaczer (1958) using a magnetic probe technique studied the structure variation in the temperature range from room temperature to 693°K. He observed that the domain width does not change up to 473°K but at 550°K a sudden change in the domain geometry takes place. He assumed the domain structure to be of Landau and Lifshitz type, but noticed that the domain width does not change with temperature as much as that shown in the formula given by Landau and Lifshitz.

Shur et al. (1964) studied the influence of the temperature on domain structure. In the range 290°K to 520°K, it was found that the equilibrium

domain width increases with rising temperature. Since the saturation magnetization I_s is constant in the investigated temperature range while the crystal anisotropy k_1 is reduced considerably it was assumed that the domain width should decrease because the value of the wall energy $\gamma \sim \sqrt{k}$ decreases sharply. This disagreement in their results was explained by the fact that with the decrease of the wall energy there occurs a sharp decrease of the magnetic pole density on the end faces of the crystal specimen. This only happens if the flux closure occurs on the surface of the specimen, indicating that there was a rotation of the magnetization vectors into the plane of the specimen. The rotation of the magnetization was revealed by using the polar Kerr effect technique which is only sensitive to the normal component of I_s. The considerable decrease in the contrast beginning at 470°K is evidence for the rotation of the magnetization vector. In this work it was shown that there was a considerable increase in the domain width at temperature 468°K and this is contradictory to the results obtained by Kaczer (1958), while observation by Fowler and Fryer (1955) show no change in the domain width from room temperature up to the transition region. Hubert (1968) using the Kerr-effect method, studied the structure change on a single crystal in the temperature range 293°K to 673°K on axial as well as basal planes. He also observed changes in the dimension of the domains near a stress region (twin lamellas). The structure was easily observable between temperatures of 470°K and 520°K, where the rotation of the easy

direction begins to deviate from the c-axis. Between 520°K and 610°K, it was difficult to observe the pattern, especially in a field free state. At a local stress the pattern is governed by the magnetostrictive self energy. The internal domain structure of these stressed regions can be altered by magnetic field. A very interesting investigation was carried out on thin Cobalt foil by Groundy et al. (1964) and Groundy (1965) using transmission electron microscope to observe magnetic domain structures in thin cobalt foil above room temperature. The change in domain pattern as the temperature increased was as predicted from the anisotropy measurement. They showed the rotation of the easy direction of magnetization and also the transition to a cubic phase at about 720°K where the formation of closure structure was observed.

3.2 The present work

So far the domain structure on the basal plane of cobalt has not been classified although there have been many predictions concerning the nature of it. The previous work gave no quantative measurement of the domain width with temperature. The present work was carried out with the following aims; to study the variation of domain width with temperature, to give some experimental evidence of the formation of domain structures at non-magnetic inclusions, and to find a relation between the dagger length ℓ and its base width d, to study the domain structure at liquid nitrogen temperature and to investigate the surface structure on the basal plane.

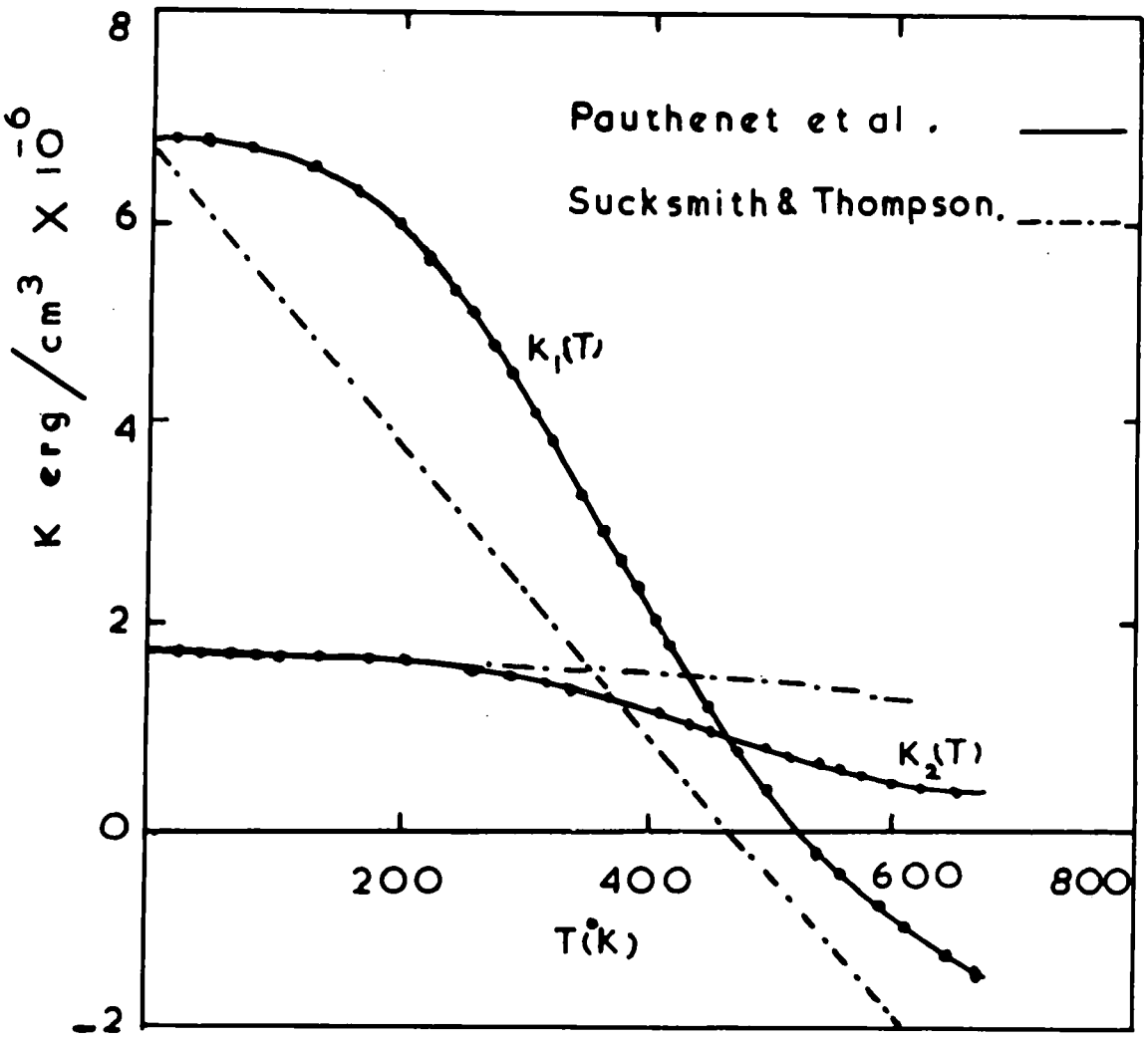

FIG. 3.3 Crystal anisotropy constants of Cobalt at various temperatures.

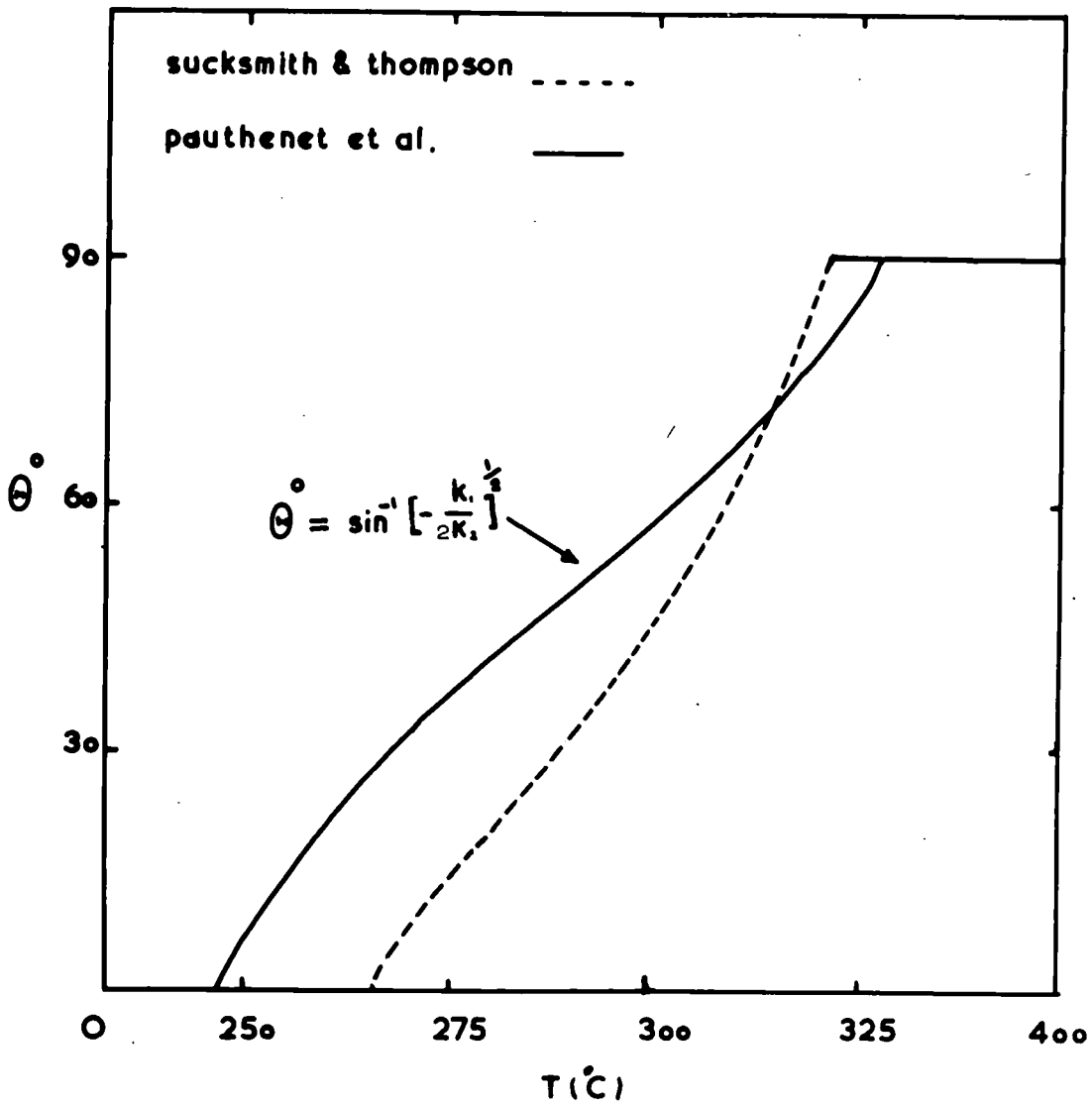

FIG.3.4 Easy direction in Cobalt as a function of temperature.

3.3 Variation of Domain width with temperature

Using the dry colloid technique described in the previous chapter the domain structure of a cobalt single crystal was studied with variation of temperature. Pauthenet et al. (1962) gave the anisotropy data shown in Fig. (3.3). The direction of easy magnetization rotates from the c-axis above 523°K to be on a cone above this temperature. The angle of this cone can be calculated by minimizing the anisotropy energy which leads to

$$\theta = \sin^{-1}\left\{-\frac{K_1}{2K_2}\right\}^{\frac{1}{2}} \qquad \text{.....(3.1)}$$

where θ is the angle between the direction of magnetization and the c-axis; relation (3.1) is valid only in the temperature range 523°K to 608°K. For each value of θ there will be a cone a generator of which is an easy direction of magnetization for that specific temperature. Fig. (3.4) shows the relation between the angle θ and temperature.

With the technique adopted the domain structure could be observed from liquid nitrogen temperature where the anisotropy is high according to Pauthenet et al. (1962) ($K_1 = 6.8520 \times 10^6$, $K_2 = 1.7130 \times 10^6$ erg/cm^3) to about 475°K (where $K_1 = .7138 \times 10^6$, $K_2 = .8565 \times 10^6$ erg/cm^3). Above this temperature the contrast was very poor and useful patterns could not be obtained. This unfortunately meant that it was not possible to investigate the interesting region above 523°K where the easy direction lies on a cone making an angle with the c-axis. However above 523°K the

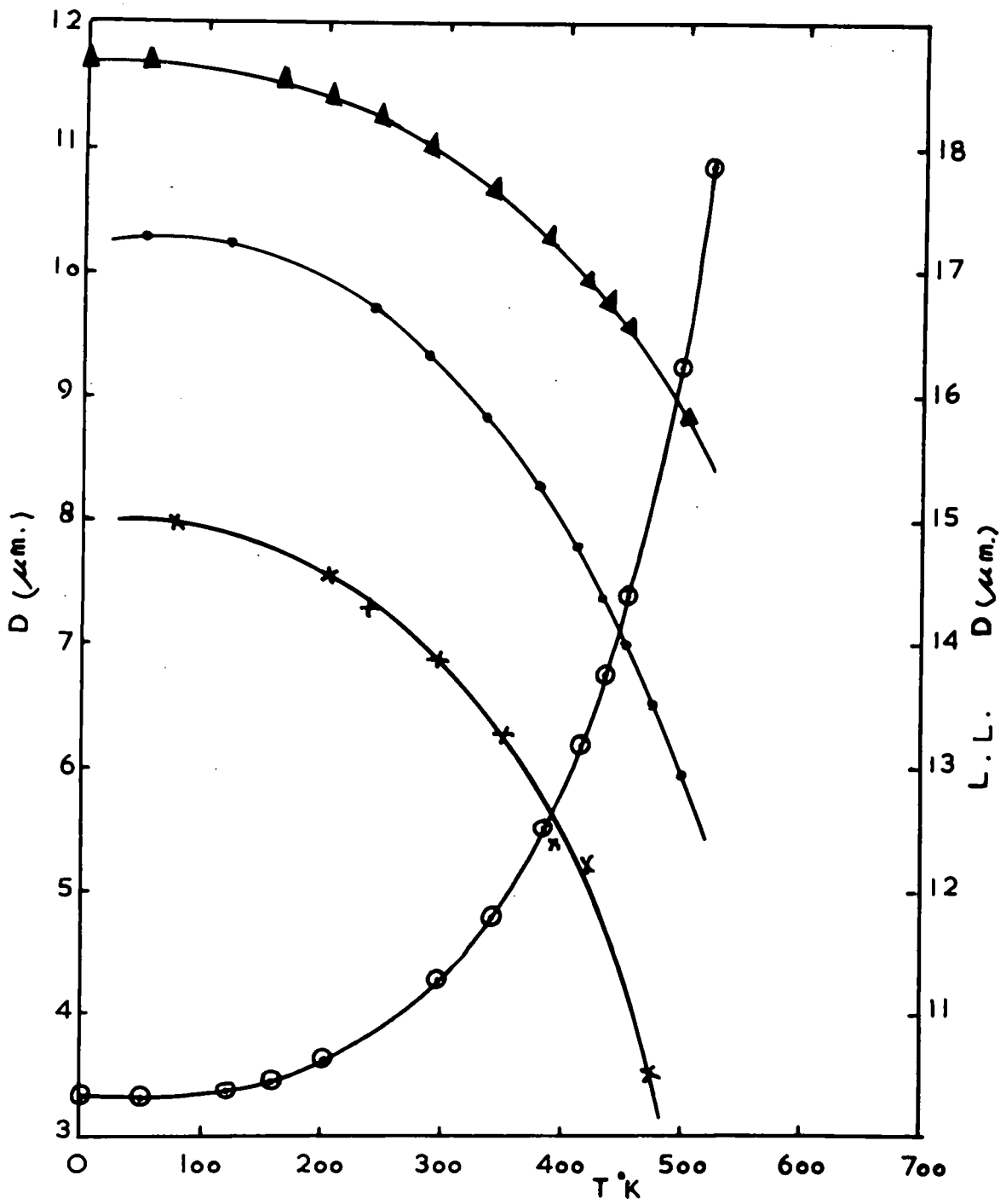

FIG. 3.5 Temperature dependence of domain width D

Theoretical curves

- ● Kittel $D = \sqrt{\frac{\gamma L}{1{\cdot}7\, I_s^2}}$
- ▲ Kittel $D = \sqrt{\frac{\gamma L(1+\sqrt{11})}{3{\cdot}4\, I_s^2}}$
- ⊙ Landau & Lifshitz $D = \sqrt{\frac{2\gamma L}{K}}$

Experimental curve ×

pattern may be so complex that domain width could not be measured.

At each temperature the average domain width, of all domains involved in the crystal, which extended from edge to edge, was measured and the results compared with the theoretical ones for models assuming two different types of surface structure. The theoretical calculations of domain width was made on the assumption that the saturation magnetization I_s was considered to be constant, 1442 e.m.u./cm^3. within the experimental range of temperature since the change in I_s with temperature is very small compared with the change of anisotropy. Bloch wall energy was calculated from the formula used by Kaczer (1963)

$$\gamma = 2\sqrt{AK_1}\left(1 + \frac{1+X}{\sqrt{X}} \text{ arc sin } \sqrt{\frac{X}{1+X}}\right) \ldots\ldots\ldots (3.2)$$

where $X = \frac{K_2}{K_1}$. A is the exchange constant, the value being obtained from Tannewald and Weber (1961). In this paper A was given as temperature dependent between room and helium temperature. The difference between these is very small and also the uncertainty in the measurement was ± 5.5%. So A was considered in this work as temperature independent. The value used was $A = 1.30 \times 10^{-6}$ erg/cm. Fig. (3.5) shows a comparison of the experimental and theoretical variation of the domain width with temperatures. The results indicate that the minimum domain width which corresponds to the maximum domain wall width is reached at the transition point 523°K. As the temperature was raised the domain wall thickness increased and the stray field decreased considerably (as shown in fig. 3.6 (a,b) until a point was reached at which the domain pattern could not be

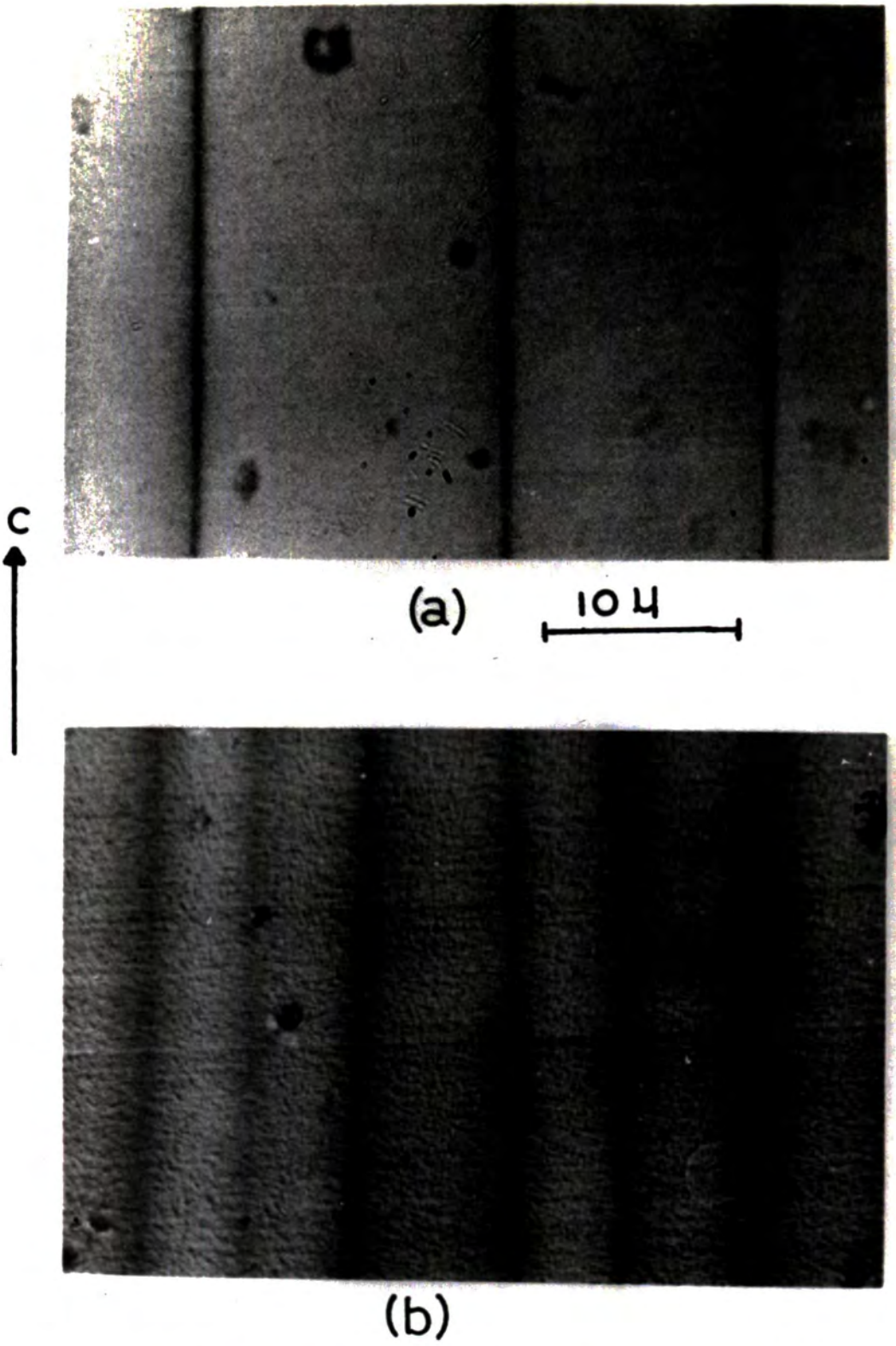

Fig.3.6. Domain Structure of Cobalt Single Crystal at,
a- 77°K.
b- 375°K.

observed by this technique. It is clear that the domain width decreases with the rise of temperature in agreement with the theory proposed by Kittel, though the spacing calculated using the Kittel theory is higher than that observed and inclusion of a μ^* correction makes the difference even greater. The general form of the curve however in a good agreement and completely at variance with the Landau and Lifshitz model. Fig. 3.6a was taken at liquid nitrogen temperature while 3.6b was taken in a different region of the speciman at 375°K. The increase in the width of the Bloch wall agrees with theoretical expectations since the wall width $\delta \sim K^{-\frac{1}{2}}$. It was difficult to draw any conclusion from the variation of domain structure on the basal plane with changing temperature. A decrease in the contrast took place as the temperature was raised and started from about 400°K.

3.4 Domain structure at non-magnetic inclusion

There is good experimental evidence of domain nucleation at inclusions in cubic crystals with many directions of easy magnetization. For a uniaxial material there is no experimental evidence for the existence of reverse spikes based on inclusions. Goodenough (1954) considered the conditions which bring about a reverse domain at a non-magnetic inclusion. For polycrystalline materials the most likely source of nucleation energy is the surface density of free poles at the grain boundaries. For single crystals the reverse domains would nucleate

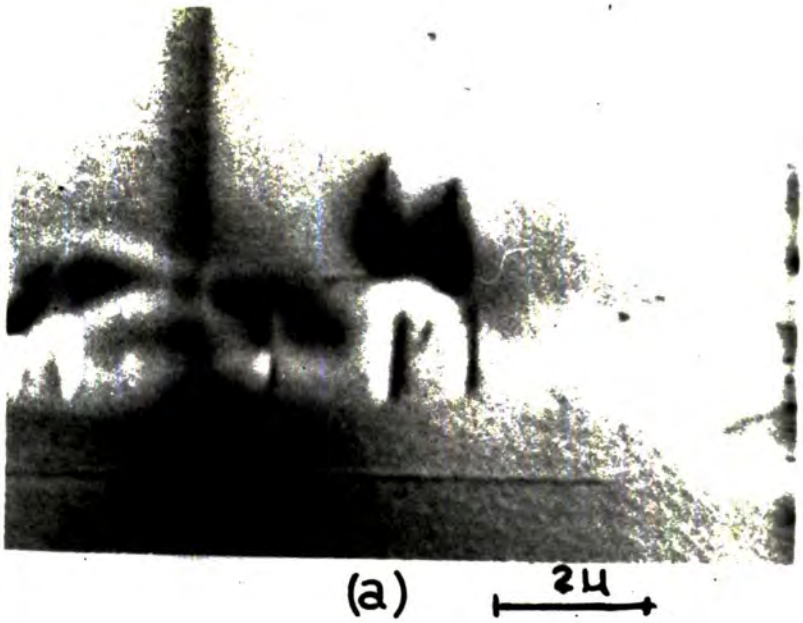

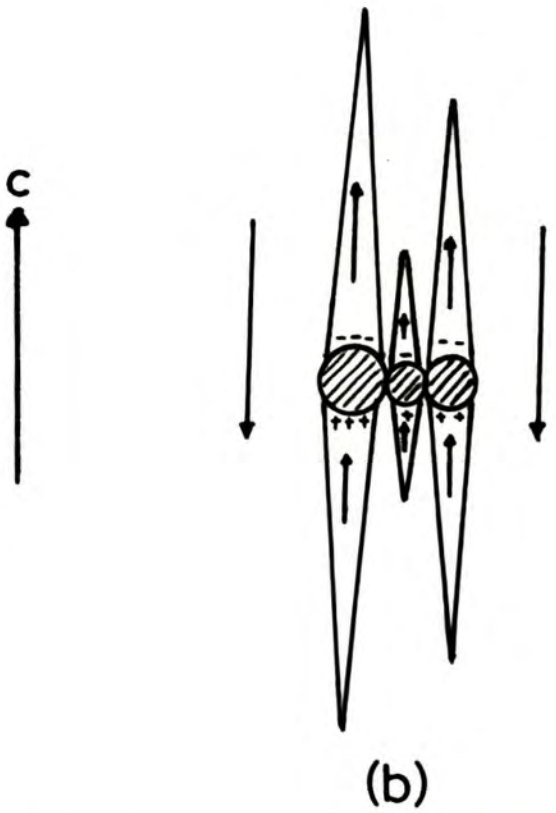

Fig. 3.7. a- Daggers of Reverse Magnetization at non-Magnetic Inclusion.

b- Interpretation of a.

primarily at non-magnetic inclusions. Carey and Isaac (1964) examined the conditions under which the reverse spikes will form around a non-magnetic inclusion in a uniaxial material. They based their calculation on the assumption that the total energy associated with an inclusion in the material may be reduced by the formation of domains of reverse magnetization. Both previous papers suggested that the formation of domains of reverse magnetization depend upon the size of the inclusion and the external applied magnetic field. Using the dry colloid technique it has been possible to observe daggers of a non-magnetic inclusion. Fig. 3.7b suggests an interpretation of fig. 3.7a which was obtained at 77°K, without an external applied field. Use was made of the formula derived by Carey and Isaac. For a zero applied field,

$$\frac{\left(\frac{\ell}{d}\right)^2}{\mathrm{Ln}\left(\frac{4\ell}{d}\right) - 2} = \frac{4\sqrt{2}\, R\, I^2}{3\gamma} \qquad \ldots\ldots\ldots\ldots\ldots\ldots (3.3)$$

where ℓ is the length of the reverse spike, d its base diameter, R the radius of the inclusion at which the dagger developed, γ the wall energy, the value of which at 77°K is 12.9 erg/cm^2 obtained from fig. (3.16) and I_s the saturation magnetization. It was assumed that $d = \sqrt{2}\, R$. The value of ℓ and d were measured directly from the specimen surface and it was found that $\ell = 1.4$ μm and $d = 0.42$ μm. Substituting this value in 3.3 we obtained $R = 0.17$ μm. This value is smaller than the critical diameter given by Carey and Isaac, where they showed that it is energetically

unfavourable for reverse spikes to form in zero field at spherical inclusions of a radius smaller than 7.5 μm. It is important to note that the relation 3.3 was obtained on the assumption that the formation of reverse daggers reduces the magnetostatic energy of an inclusion by one half. However the difference in the experimental result and that calculated from 3.3 may be due to the fact that the theoretical value may need some correction since the inclusions involved as shown in fig. 3.7a are not perfect spheres. They are also so close to each other that the value of the demagnetizing factor N may change from that for a perfect isolated sphere. As could be seen from the photograph these domains of reverse magnetization appear in pairs at the surface of the inclusion. This is obvious since different polarities appear at opposite sides of the inclusion. This may be seen clearly from the deposit of iron particles which appear in the two regions. The lower region shows no deposit while the upper one shows dark regions. This is due to the formation of free poles of opposite polarity. The wall of the spike can be seen to have a region with a heavy deposit of iron particles and one without any deposit. This may be due to the different polarities which appear on either side of the dagger resulting from the rotation of spin in the dagger wall as the magnetization changes direction through the wall from the main domain to the inside of the dagger. As a result of this a normal component will arise which will emerge at one side and enter at the other side of the dagger. The emerging component in the upper dagger appears on the opposite side in the lower dagger (presuming that emerging component

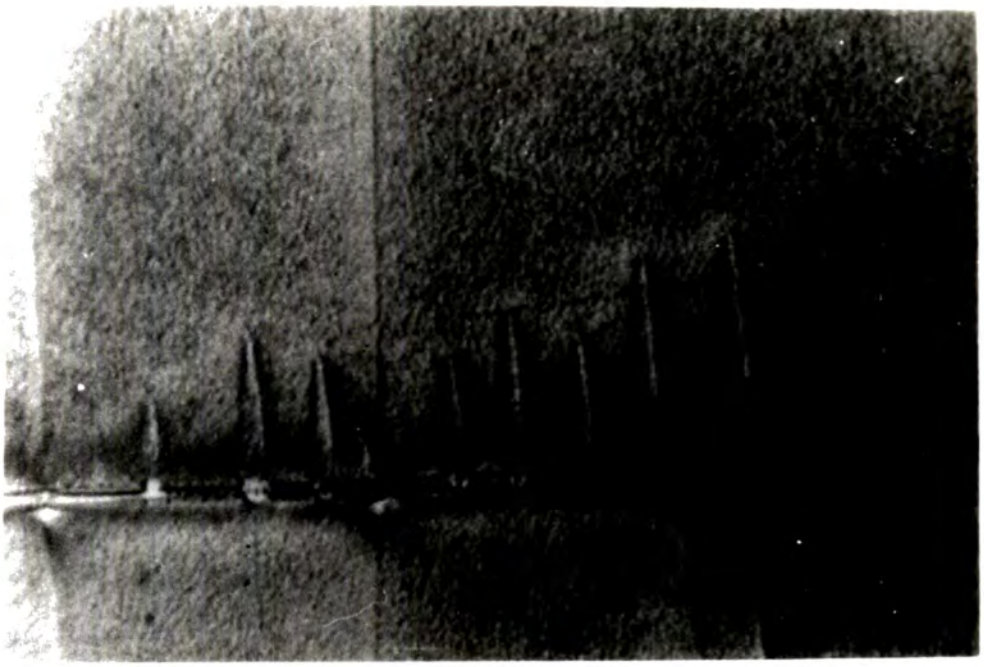

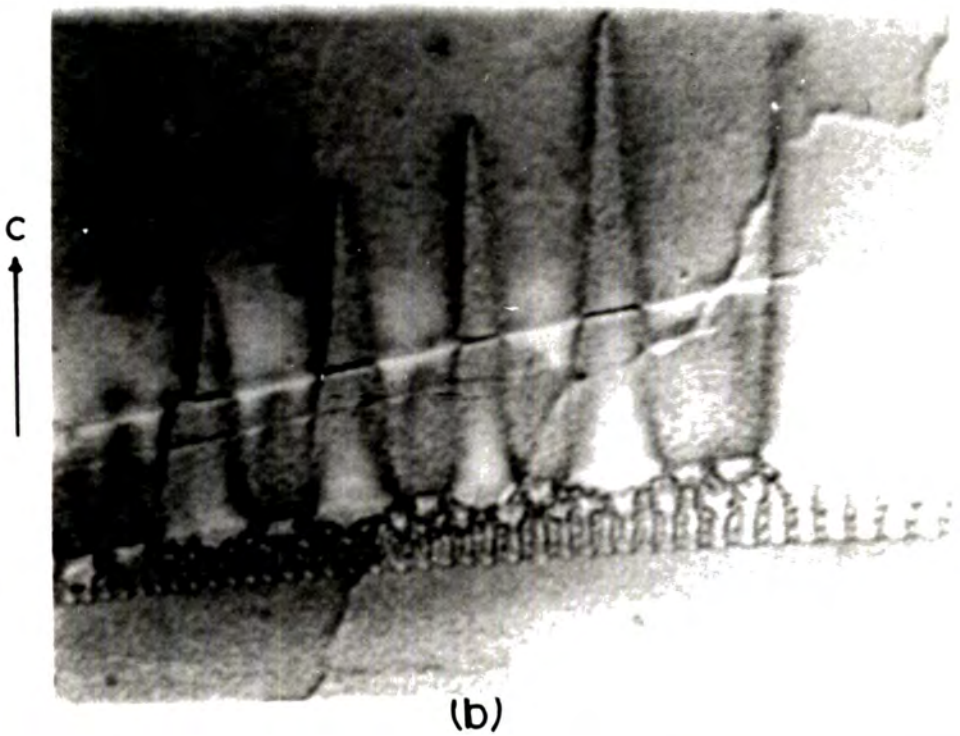

Fig. 3.10. a- Development of Different Types of Reverse Daggers Probably at Lamella Precipitate.
b- Domain Pattern Showing the Effect of Scratch.

collects the colloid due to the polarisation of the colloid by the stray field). This occurs because of the different polarity of the free poles which develop on the surface of the upper and lower dagger. The same applies to daggers which develop at twin bands. Surface scratches can also be valuable in indicating magnetization direction, Williams et al. (1949). In fig. 3.10b there is a segment of twin band, around which a dagger development has taken place. A fine scratch was left from the mechanical polishing and this cut the daggers through the middle. It can be seen clearly that around the scratch (inside the daggers), there is a heavy deposit of colloid, while in the main domain there is complete rejection of the particles. Since the scratch lies very nearly perpendicular to the magnetization in both the main domain and in the daggers it will develop strong regions of free pole on its sides. If the colloid particles are polarised by the stray field so that they are aligned in the same sense as the magnetization in the daggers they will be preferentially attracted to region of the scratch lying inside daggers and repelled by the remainder of the scratch.

3.5 Domain structure at liquid nitrogen temperature

Since the anisotropy is uniaxial at this temperature no change in the domain structure of cobalt at 77^{o}K was expected, however there are two important factors directly involved with the domain structure which had an effect. Firstly the anisotropy energy was considerably greater than that at room temperature and secondly a twin structure will form readily

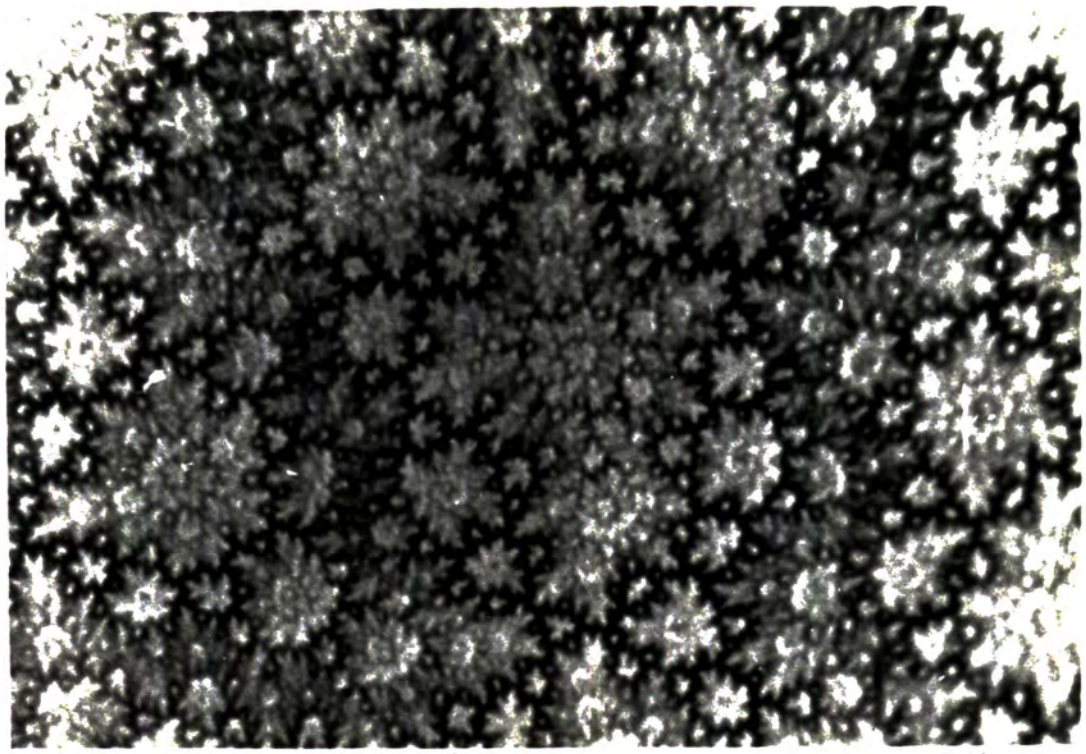

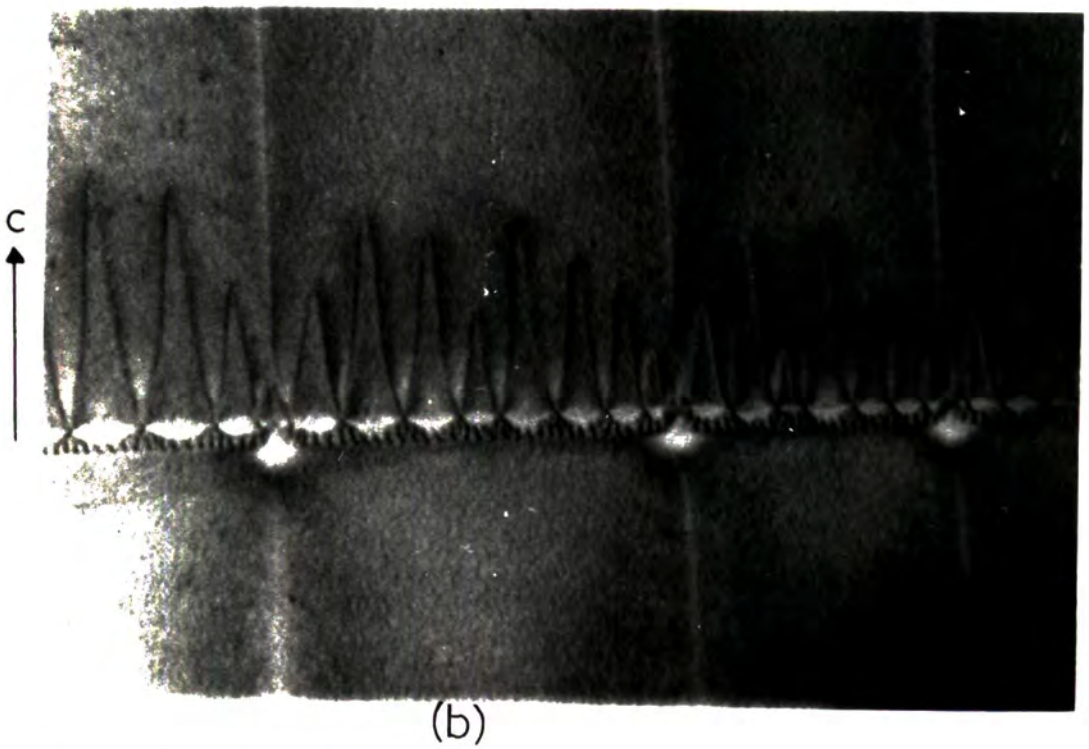

Fig. 3.8. Domain Pattern observed at 77 K on:
a- Basal Plane.
b- $\langle 1\bar{1}20 \rangle$ surface.

when the specimen is cooled to this temperature. The structure remains when the specimen is warmed to room temperature. Hall (1957) reported a $\langle 10\bar{1}2 \rangle$ composition plane of deformation twins in a large grained cobalt specimen which has been compressed in a vice. Davis et al. (1962) observed twins laid on the planes of $\langle 11\bar{2}1 \rangle$ orientation produced by cooling to 77°K. Fig. 3.8(a,b) shows the domain pattern obtained on the basal plane and on the surface $\langle 10\bar{1}0 \rangle$ at 77°K with no external applied field. Patterns on both surfaces were similar to those of early workers at room temperature, but here the definition of the pattern is improved considerably, this was due to the increase in the value of anisotropy constant. Fig. 3.9(a-f) show a domain pattern formed at a twin band. Two types of twin were observed, normal lenticular twins fig. 3.9 (e,f) and also some very narrow twins like the one shown in fig. 3.9 (a,b), these were of composition planes $\langle 11\bar{2}1 \rangle$. At the twin band daggers of reverse magnetization developed with other daggers inside or beside each other as shown in the arrangement of fig. 3.9(a,b). The domain structure inside the twin band is of the same nature as that observed on the basal plane and this is the case since the twinning produces a reorientation of the lattice, the c-axis of the twin being almost at right angles to the c-axis of the parent crystal. The nature of the reverse spikes grown on a twin band is usually of the same nature as those which appear at a grain boundary. A different type of structure is sometimes observed an example of which is seen in fig. 3.10a. It is possible that this structure develops at lamellar precipitates of oxide,

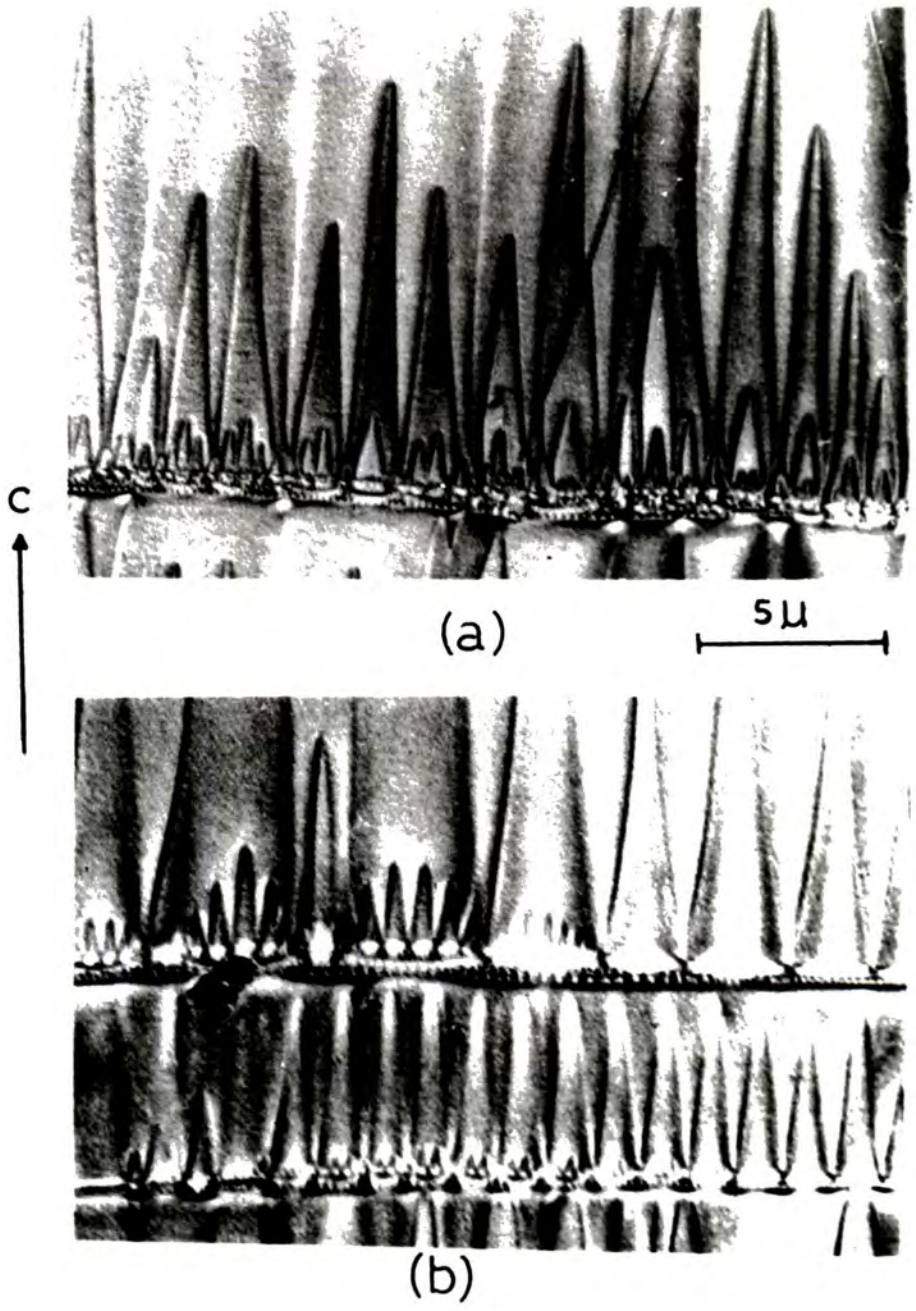

Fig. 3.9. (a-b) Domain of Reverse Magnetization at Twin Band, at 77°K.

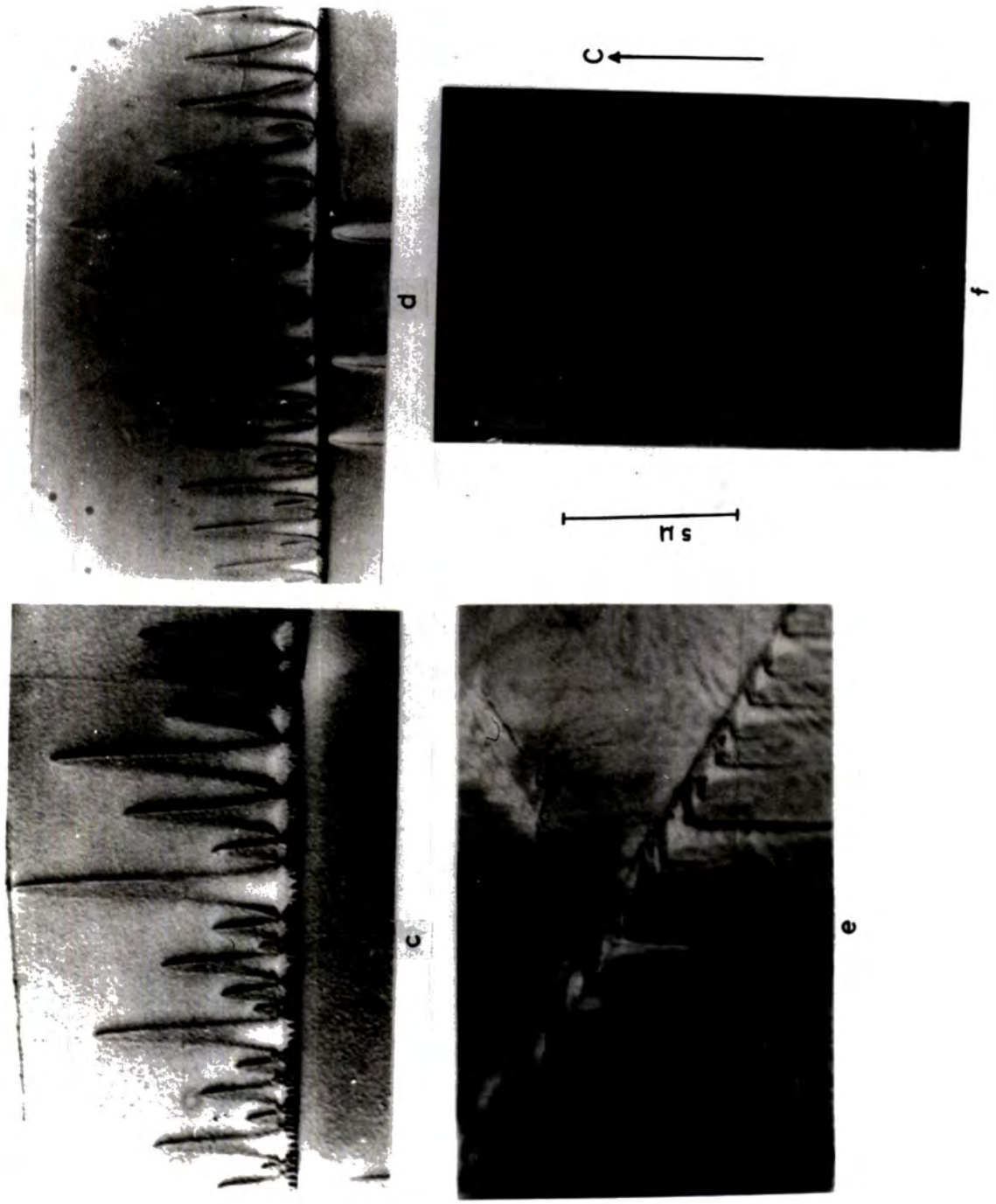

Fig.3.9. (c-f) Structure of Reverse Daggers at Twin Band, at 77°K.

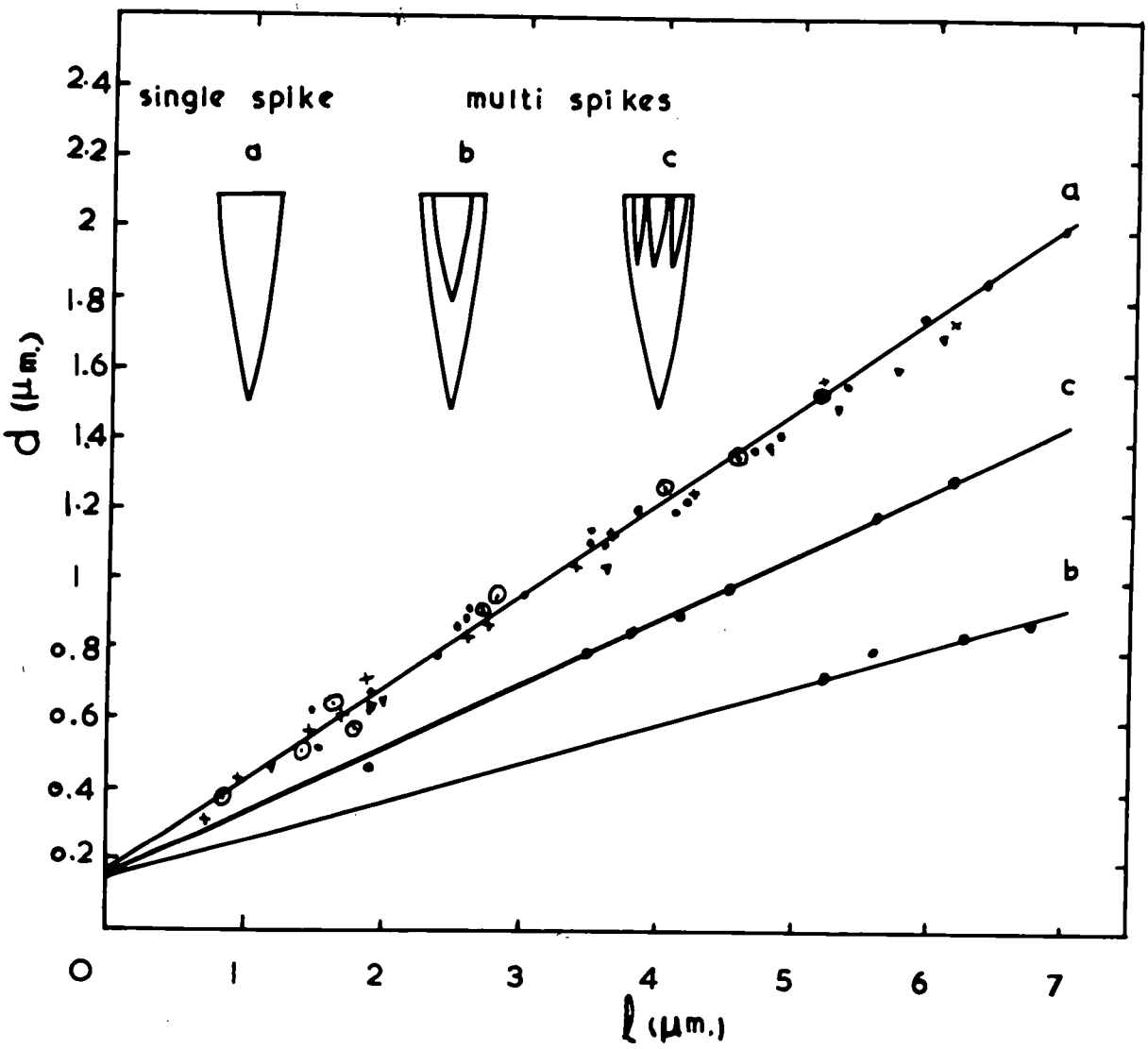

FIG.3.12 Variation of the length "l" of the dagger of reverse magnetization with its base diameter "d"

the difference being explained by the fact that the oxide layer is large enough (in this case) to be considered as a serious discontinuity in the lattice.

It is generally true that within the boundaries of a domain the magnetization is uniform, that is the spins are strictly parallel to the easy direction. However this alignment could be disturbed by free poles on the surface or imperfections in the crystal lattice. Nuclei of the daggers of reverse magnetization appear in all places where there are strong localized demagnetizing field resulting from free poles. The length of these depends upon the orientation of the grain boundary and the state of strain in the region at which the daggers grow. It was found for a particular type of structure that there was a simple empirical relation between the dagger length ℓ and the diameter of its base d. This is plotted in fig. 3.12. The points on the graph (a) were obtained from different regions on the surface. A set of these which is indicated by dots on (a), is obtained from fig. (3.8b) and (3.9) while those on (b and c) were obtained from fig. (3.9(a,b)). It may be concluded that ℓ and d are in a direct proportion in both single and multi-dagger development. However in multi-dagger development the slope is of a different value and thus the dagger has a smaller base than a single dagger of the same length. From this graph it can be seen that at a certain value of d, ℓ is zero. This means that for values of d less than this, creation of reverse daggers is not possible. Thus reduction in the magnetostatic energy at this critical radius could

only take place either by the rotation of the magnetization near to the surface or by development of regions in which there is magnetization perpendicular to the c-axis, that is the formation of closure structure of a very small size. From fig. 3.12 it can be seen that if closure regions exist they will be of diameter less than .18 μm, though the strain and orientation of the region where these daggers grow has a direct effect on the relation of ℓ and d. For all types of daggers ℓ and d represent the length and the base width of the main dagger.

3.6 Variation of the exchange constant A with temperature

Tannenwald (1961) used spin wave resonance to measure the exchange constant A and its temperature dependence. The results obtained at room temperature, 77°K and 4°K were 1.3, 1.42, and 1.43 erg/cm x 10^{-6}. Another method which may be used to determine A uses the observed domain spacing and was described by Kaczer et al. (1962). From the relationship given by Kittel (including the μ^* correction)

$$D = \sqrt{\frac{2\sqrt{AK}\,(1+\sqrt{\mu^*})L}{1.71\ I_s^{\,2}}} \qquad \text{.....(3.4)}$$

If values without a subscript indicate room temperature values and the subscript t indicates a value at some other temperature then

$$\frac{A_t}{A} = \frac{K}{K_t}\left(\frac{I_{st}}{I_s}\cdot\frac{D_t}{D}\right)^4 \cdot \left(\frac{L}{L_t}\cdot\frac{(1+\sqrt{\mu^*})}{(1+\sqrt{\mu_t^*})}\right)^2 \qquad \text{.....(3.5)}$$

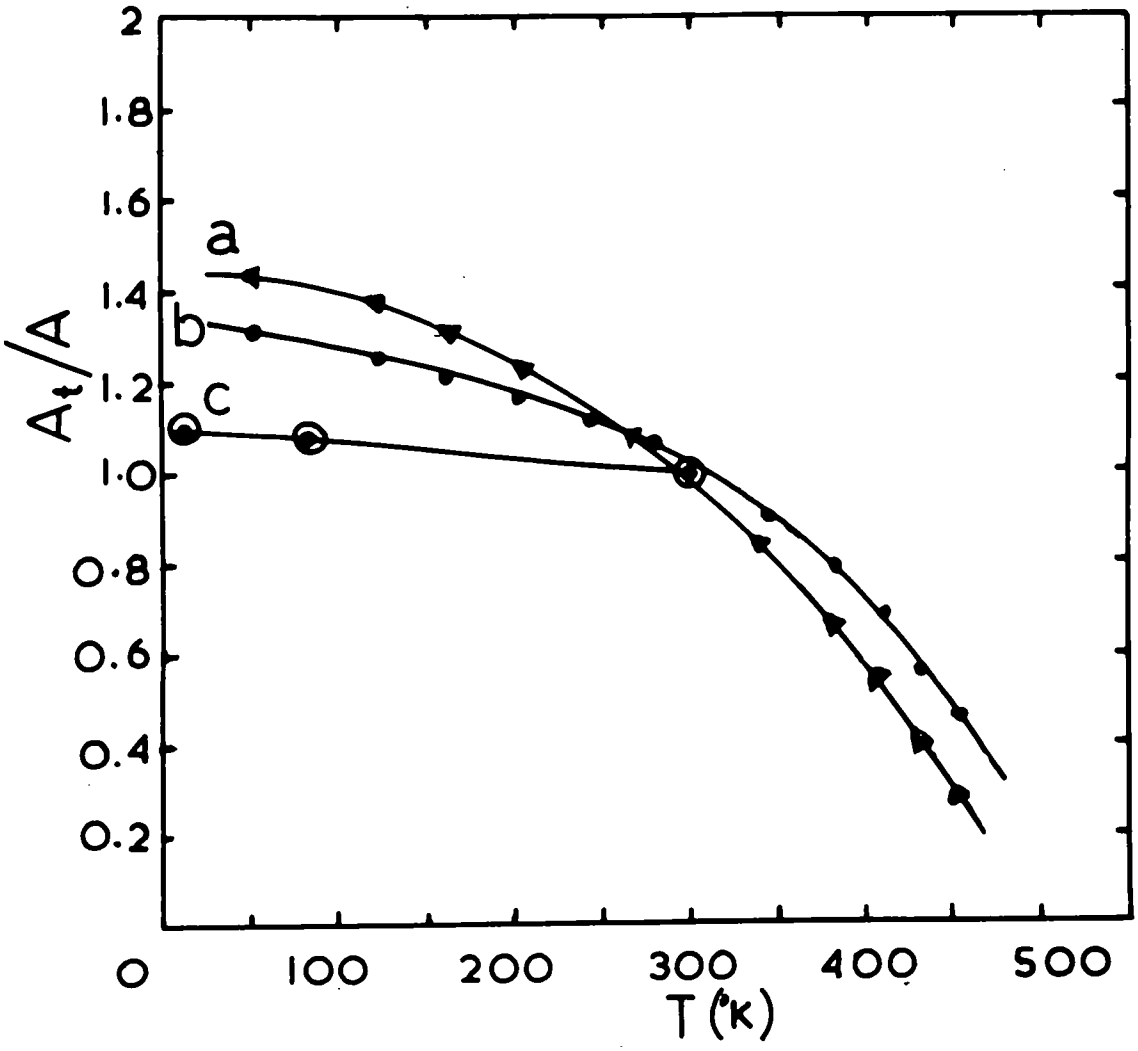

FIG. 3.13 Temperature dependence of the exchange constant in Cobalt.

a–With μ^* correction.

b–Without μ^* correction.

c–S.W.R. (Tannenwald 1959)

The difference between L and L_t is very small. The ratio is very nearly equal to unity. Also the value $\frac{I_{st}}{I_s}$ is always very close to unity in the limit of the experiment. The results are plotted in fig. 3.13. It is clear that the value of A is decreasing with increase of temperature and this is in agreement with the results obtained by Tannewald. Any difference between (a,b) and that of (c) shown in fig. 3.13 may be due to the formula used in our calculation of A. Since it was assumed that the surface structure is one of free poles type, but in fact there may be some region of closure structure which in turn contributes to the total energy and this will give a different relation from that given in equation 3.5. Thus the domain structure could be related to the intrinsic properties of the crystal and this is one way in which the domain study could be of great interest and value.

3.7 Interpretation of surface structure observed on the basal plane of cobalt single crystal

Many different interpretations have been given for the structure on the basal plane of cobalt single crystal and an outline of these has been given earlier. An attempt was made on a $\langle 10\bar{1}0 \rangle$ surface to observe the possibility of any closure structure existing on the edge of the specimen near the basal plane. The pattern in fig. (3.11a) demonstrates clearly the absence of any secondary structure near the surface. There is no closure structure with magnetization in a direction different from

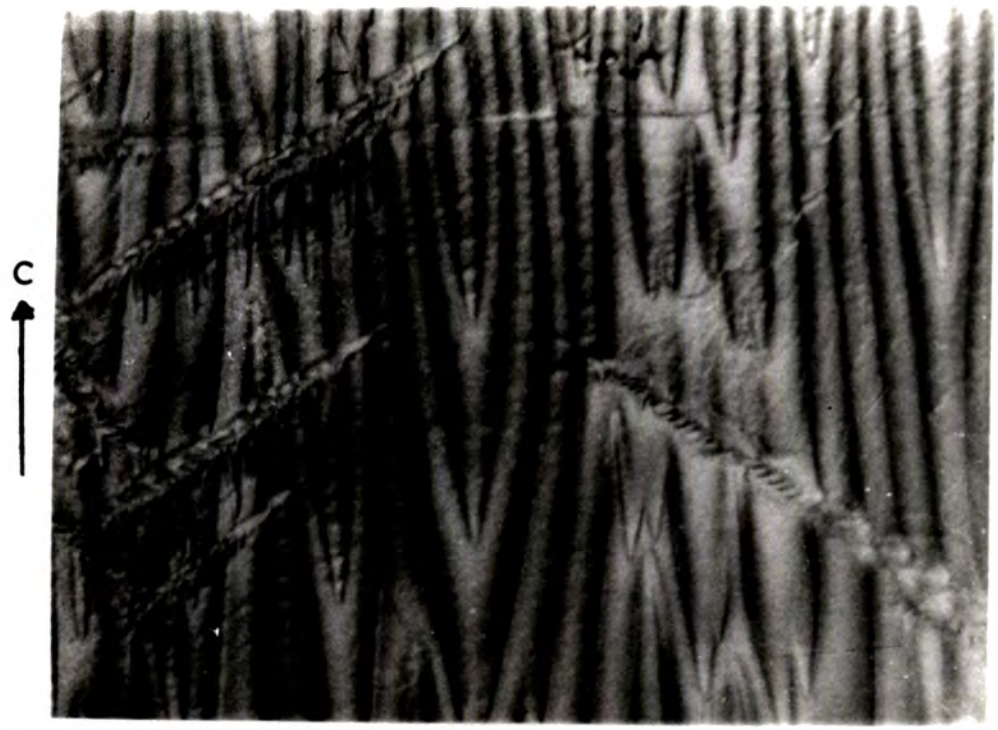

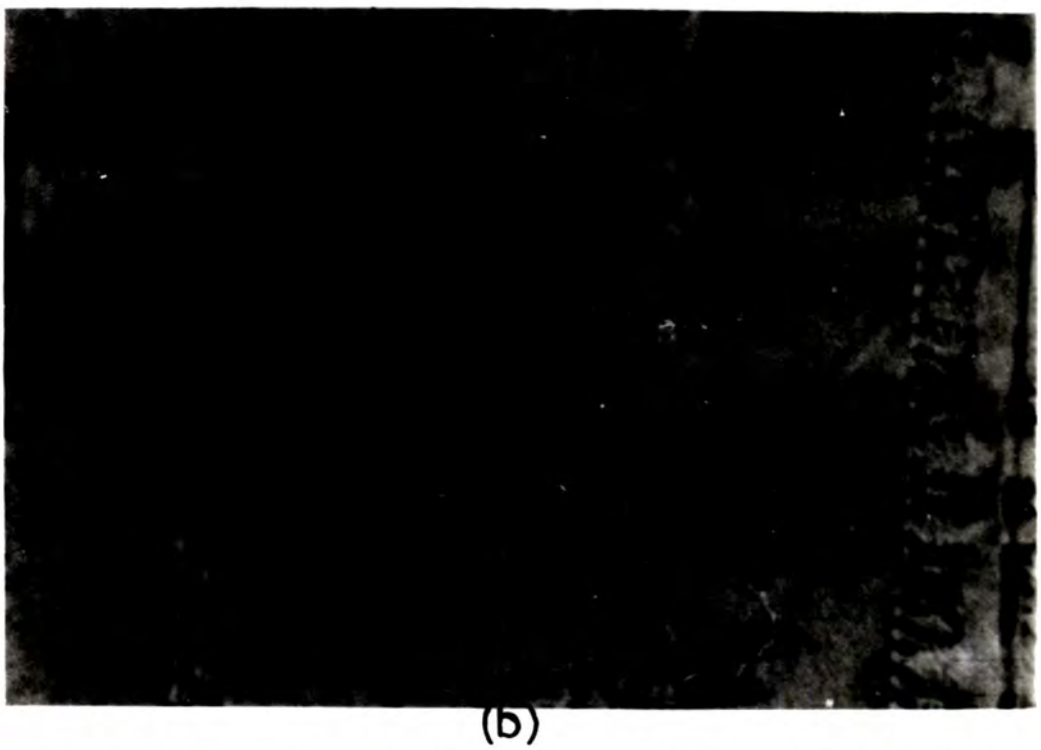

Fig. 3.11. a- Domain Structure at the Edge of $\langle 10\bar{1}0 \rangle$ Surface.

b- Pattern on Basal Plane with Small Grain Shows the Growth of the Reverse Daggers at the Grain Boundary.

that of the c-axis. The wall is straight and meets the basal plane at 90°. The dagger of reverse magnetization observed is of a simple type, the base including no closure structure. Wyslocki (1963) obtained the same results at room temperature. On the basal plane the structure behaviour under an applied field of 300 Oe. in different directions, shows no sign of a secondary structure which changes direction with the applied field as in the case of the gadolinium single crystal see Chapter 5. Fig. 3.11b shows a region on a basal plane surface which includes a number of small grains with the c-axis lying in the surface.

At the grain boundaries the daggers of reverse magnetization grown as a result of the discontinuity of the magnetization, and the consequent development of free poles in order to reduce the magnetostatic energy. The bases of these spikes are simple with no indication of closure structure. The variation of domain width with temperature is determined by the type of the basal plane structure. From 3.5 it can be seen that the experimental results are in agreement with those of Kittel model.

Kittel (1949) showed that the free energy density E_{FP} for a surface free pole structure is given by equation 1.15. If closure domains are formed giving complete flux closure the free energy density E_{CL} is given by equation 1.12.

so

$$P = \frac{E_{CL}}{E_{FP}} = \left(\frac{K}{3.4\ I_s^2}\right)^{\frac{1}{2}} \qquad \text{.....(3.6)}$$

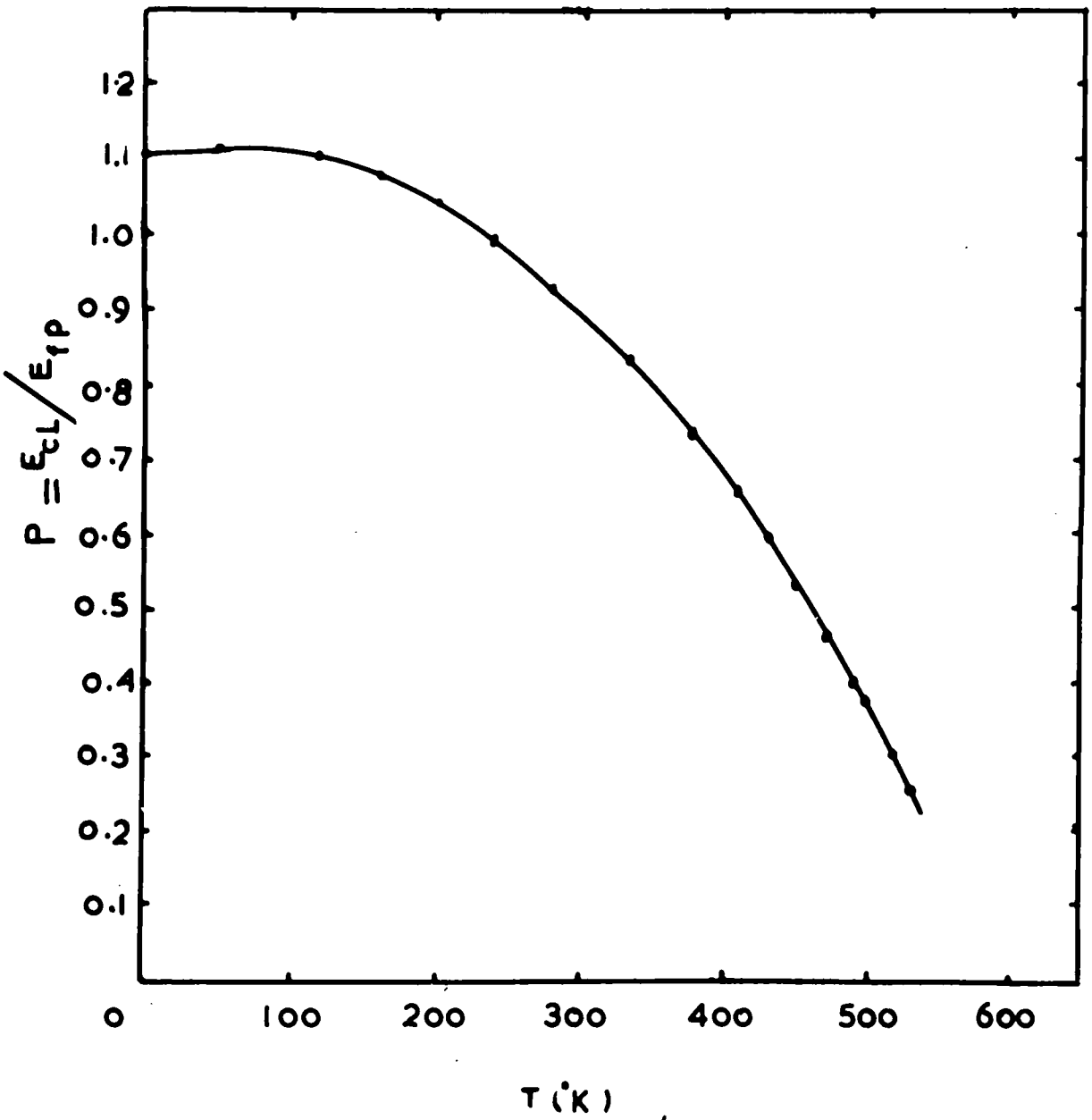

FIG. 3.14 Variation of $P = E_{cL} / E_{fp}$ with temperature

where K is the difference between the magnetocrystalline anisotropy energy for magnetization along the c-axis and basal plane. For cobalt $K = K_1 + K_2$ is a good approximation.

This ratio will determine whether free poles or closure domain structures will be energetically most favourable. If $P \gg 1$ a surface free pole structure would be expected to form while for $P \ll 1$ one would expect development of closure domain structures in which the magnetization is perpendicular to the c-axis. The ratio P was plotted against T and the results are shown in fig. 3.14. It appears that the maximum value of P is ~ 1.1 at absolute zero, where one expects the pattern to be due to free poles. The gradual change of P may introduce a change in the surface structure. If a closure structure develops this would be most likely at higher temperatures where P is becoming appreciably less than unity since K_1 is reduced considerably from that at room temperature, the reduction in the contrast as the temperature was increased was due to considerable widening of the domain wall as the transition temperature was approached and not as a result of the rotation of magnetization from c-axis into the plane of the specimen as suggested by Shur (1964).

However the lowest value of P is about 0.25 at 523°K where the easy direction of magnetization begins to deviate from the c-axis. From the transition temperature down to room temperature the value of P is small enough for a partial closure structure to develop. This development would not involve a considerable increase in the magnetocrystalline

anisotropy energy since the value of K decreases with temperature. Moreover the regions of transverse magnetization might be very small and might not act as a complete flux closure, but as a partial one. The reduction in the magnetostatic energy must be higher than the increase in the magnetocrystalline anisotropy energy in order to encourage the development of such minute partial closure regions. The difficulty in observing these at the edge of the specimen could be explained by their quenching at the surface due to unevenness or the presence of strain at the edge of the specimen.

3.8 Evaluation of energies which determine domain structure in Co

Wall boundary energy Suppose that all the boundaries involved in a cobalt crystal are of 180° type, in this case the calculation is fairly straight forward. Energy of the wall per unit area of the surface

$$E_W = \frac{\gamma L}{D} \quad , \qquad \ldots\ldots\ldots\ldots\ldots\ldots\ldots\ldots\ldots\ldots (3.7)$$

The magnetostatic energy per unit area taking account of both sides of the specimen

$$E_m = 1.7\ I_s^{\,2}\ D \qquad \ldots\ldots\ldots\ldots\ldots\ldots\ldots\ldots (3.8)$$

total energy

$$E_{FP} = E_W + E_m = \frac{\gamma L}{D} + 1.7\ I_s^{\,2}\ D \qquad \ldots\ldots\ldots (3.9)$$

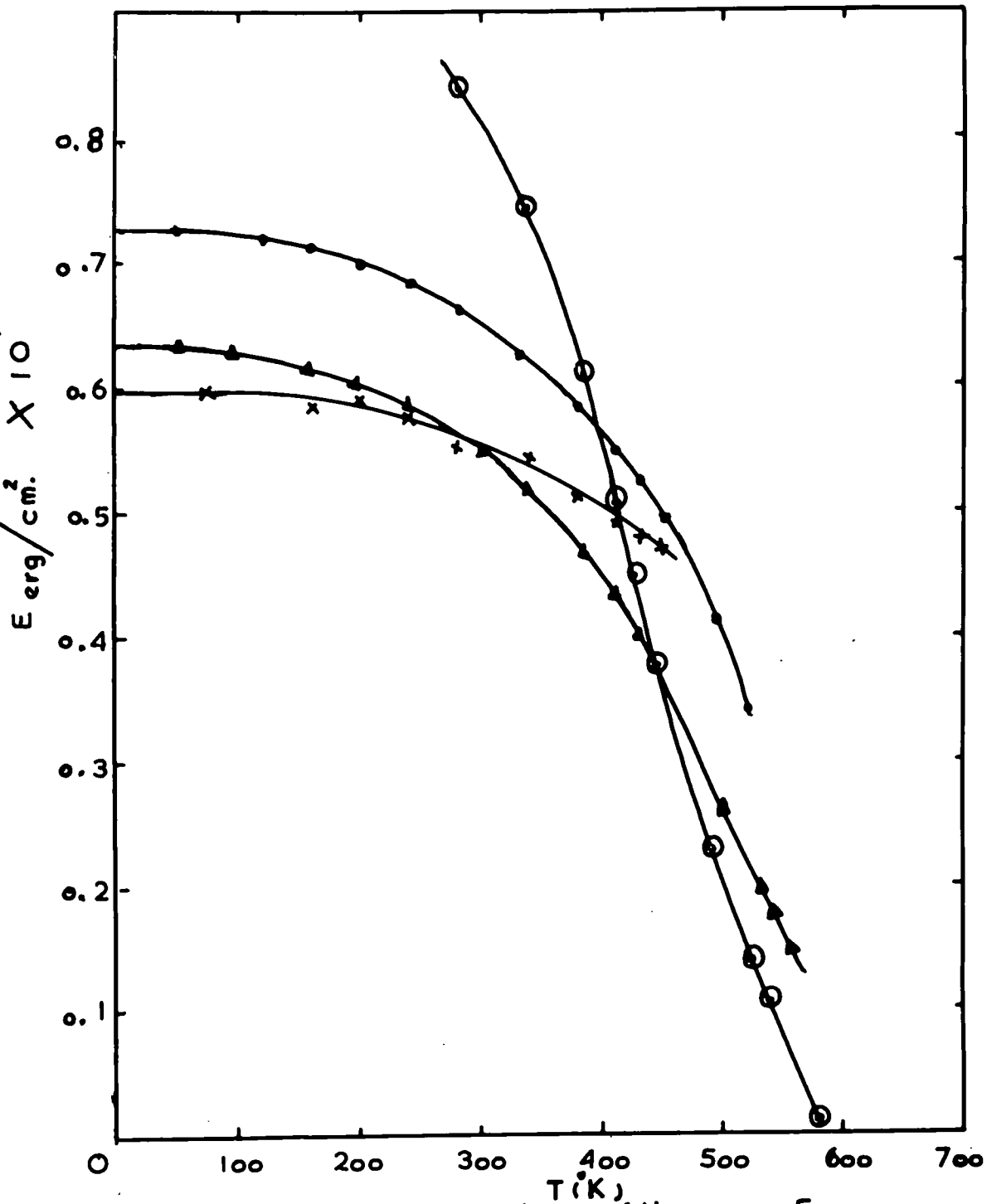

FIG. 3.15 Temperature dependence of the energy E.

Theoretical curves
- ● Kittel $E = 2I_s\sqrt{1.7YL}$
- ▲ Kittel $E = 2.62 I_s \sqrt{\frac{2YL}{1+\sqrt{\mu}}}$
- ⊙ Landau & Lifshitz $\sqrt{2YLK}$

Experimental curve ×

minimization, gives for the domain width, equation 1.14 and for energy density equation 1.15.

Williams, Bozorth, and Shockley (1949) and Kittel (1949) gave a correction to the magnetostatic energy. This results from the rotation of magnetisation vector on the specimen surface, it is applied by multiplying the calculated demagnetized energy by a factor $\frac{2}{1+\sqrt{\mu^*}}$, μ^*(permeability)=1 if it is parallel to the easy direction. The new form for the energy is

$$E_{FP} = \frac{\gamma L}{D} + \frac{2}{1+\sqrt{\mu^*}} \; 1.7 \; I^2 \; D \quad \ldots\ldots\ldots (3.10)$$

so

$$D = \sqrt{\frac{\gamma(1+\sqrt{\mu^*})L}{3.4\, I_s^2}} \quad \ldots\ldots\ldots\ldots\ldots\ldots (3.11)$$

and

$$E_{FP} = 2.61 \; I_s \sqrt{\frac{2\gamma L}{1+\sqrt{\mu^*}}} \quad \ldots\ldots\ldots\ldots\ldots (3.12)$$

μ^* is a temperature dependent since

$$\mu^* = 1 + \frac{2\pi I_s^2}{K} \quad \ldots\ldots\ldots\ldots\ldots\ldots (3.13)$$

Because of the considerable variation in the spacing of the domains an average spacing for all those which appeared was taken. This value was reasonably comparable to the spacing that would occur in the true equilibrium state used in estimating the energy. The results were plotted, the experimental ones for the Kittel model (with and without μ^* correction) and for the Landau and Lifshitz model. The energy calculated

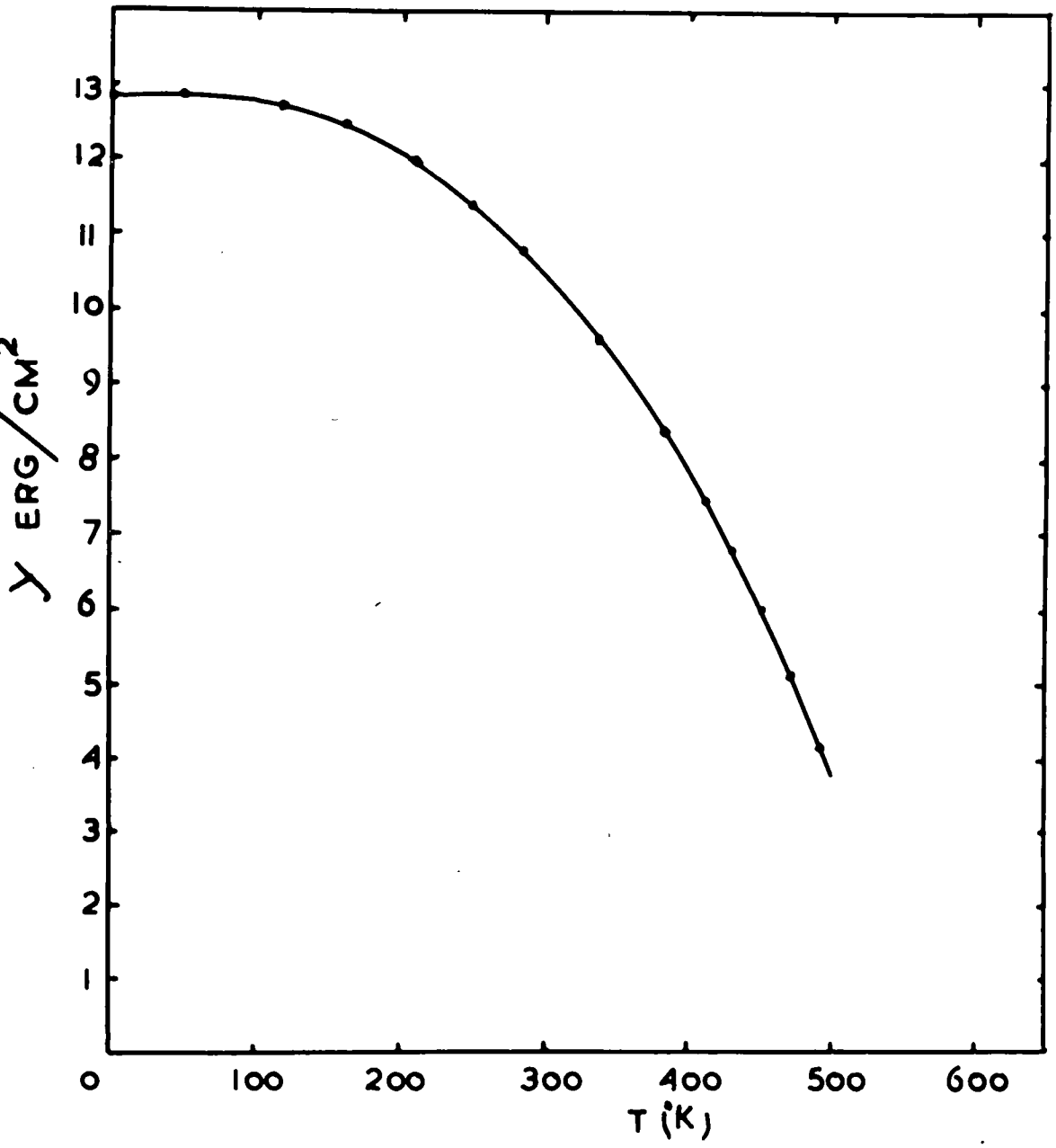

FIG. 3.16 Temperature dependence of domain wall energy of Cobalt single crystal.

from Landau and Lifshitz model is higher than that of the Kittel one. Fig. (3.15) shows the experimental and theoretical results, the best agreement shown with the Kittel model including μ^* correction. Both experimental and theoretical calculations give the value for energy density at room temperature of about $.61 \times 10^4$ erg/cm^2. This value depends upon the calculated value of the wall energy γ, γ being given the following value (at room temperature)

γ erg/cm^2	Ref.
8.20	Stoner (1950)
13.7	Fox (1956)
11.0	Williams, Bozorth, (1949) & Shockley
10.50	Calculated in this thesis

The value of γ as a function of temperature is shown in fig. (3.16).

The differences in these values resulted from the uncertainties in the measured value of the exchange interaction constant A.

CHAPTER 4

RARE EARTH METALS

4.1 Introduction

The interest in and consequent study of the rare earths is of a scientific rather than an industrial nature. Although the rare earths are interesting they are also expensive and difficult to prepare in a pure state. An additional deterent to industrial engineering interest is that magnetic ordering occurs in all cases below room temperature. Thus the industrial applications of the rare earths as magnetic materials are somewhat limited. The increasing interest, from a scientific point of view, in the rare earths may be accounted for by certain properties, high spontaneous magnetization in the heavy rare earths and an interesting variety of types of magnetic ordering including the existence of anti-ferromagnetism in some of these metals. In addition it would be expected that particularly interesting domain structure would result from the various form of anisotropy involved. The series includes the elements from Cerium with atomic number 58 to Lutetium 71 and often Scandium 21 Yttrium 39 and Lanthanum 57 are considered as members of the series. Because all the members of the rare earths have similar external electronic structure they exhibit almost identical chemical properties and are therefore arranged outside the regular array of the periodic table. The detailed investigation of the properties of the rare earths has been relatively recent, most work being done during the last 10 years. The successful preparation of single crystals at Ames, Iowa, by Spedding and

his co-workers has enabled more detailed experiments and thus increased our understanding enormously, Spedding et al (1947, 1954(a,b), 1957, 1961). Neutron diffraction experiments on single crystals performed at Oak Ridge by Wilkinson et al (1961 (a,b), 1962), Cable et al.(1961, 1964), Koehler et al. (1961 (a,b), 1962 (a,b), 1963, 1965) and Moon et al. (1964) have also made it possible to understand the essential nature of the rare earth magnetic structures.

4.2 Electronic structure

Generally, each of the rare earth metals exhibits an effective moment in the paramagnetic state which is almost identical to that of the corresponding tripositive ion. The electronic structure is

$$(4f)^n\ (5s)^2\ (5p)^6\ (5d)^1\ (6s)^2$$

where n increases from 0 to 14 as the atomic number increases, so the outer electron shells which determine the chemical and certain physical properties of the metals are the same for all the rare earths. This causes difficulty in separating the metals from one another. The (5s)(5p) shells serve as a screen for the 4f electrons while the valence electrons $(5d)^1(6s)^2$ are easily removed to become conduction electrons. At each lattice site there is left a highly localized moment due to unpaired electrons in the 4f shell, this moment is quite well given by the application of Hund's rules Hund (1925). So the localized magnetic

electrons carrying the major part of the bulk magnetic moment are different from the itinerant conduction electrons which contribute little magnetic moment, these electrons are important in connection with the magnetic properties. primarily as a coupling mechanism between localized 4f electrons, this is discussed in some detail by Cooper (1968) and Chikazumi (1964). This is only applicable to the heavy rare earths since the light groups are basically more complex. Thus the variation of the behaviour of the strongly coupled 4f shell electrons will determine the large difference between the elements of the rare earth group. The magnetic moments will arise from the electrons in this incomplete 4f shell. The number of the electrons in the 4f shell generally increases by one from one element to the next. This statement is not quite correct since the 4f shell prefers to be empty, half filled or completely filled, 0, 7 or 14 electrons. Therefore Ce and Tb (with 1 and 8, 4f electrons) have the same tendency to promote one 4f electron into the outer shell. While Eu and Yb (with 6 and 13, 4f electrons) tend to extract an extra 4f electron from the outer shell in order to reach the stable structure. This extra 4f electron which is related to the conduction electrons will contribute to the change in some of the properties of the metals. On the basis of the total electron spin in the 4f shell, it is possible to divide the rare earth metals into two sub-groups; the Cerium sub-group(light) which extends from

Cerium to Gadolinium, in which the seven vacant states with spin up are successively filled. (Lanthanum may be included although it may not be considered a rare earth metal because it does not have 4f electrons). The second sub-group is the Yttrium (heavy), from Terbium to Lutetium which corresponds to the successive filling of - $\frac{1}{2}$ spin states. Evan though this division is used, Europium, Gadolinium and Terbium may be included in either group depending on the properties considered. The variation between the two sub-groups is due to the effect of the differences in the dimensions of the atoms. The atomic radius of the light rare earths decreases slightly from about 1.8 A^{o} to about 1.42 A^{o} as the atomic number increases from 57 for La to 71 for Lu. The exceptions are Ytterbium and Europium which behave as divalent ions in a metallic phase. The wave function of the 4f electrons is considered to be concentrated towards the nucleus by the strong coulomb attraction of the effective nuclear charge. The heavier the nucleus the larger its positive charge and the stronger the attraction of the electrons. This causes theshell to be pulled in, thus the atoms of the heavy rare earth metals have a smaller metallic radius. The heavy metals crystallize in a normal hexagonal close packed (hcp) form, at room temperature and below. The one exception is Ytterbium which crystallizes in face centred cubic (fcc) and has two conduction electrons with a closed 4f shell. This changes to a body centred cubic (bcc) phase at high temperature. The hexagonal structure is constructed by stacking

TABLE 4.1

Element	Modification	Atomic No.	Mol. wt.	Density gm/cm^3	Crystal Form	Lattice parameter a.A^o	Lattice parameter C.A^o	Transition point C^o	M.pt. ^oC	Atomic Radius A^o
Scandium Sc		21	44.96	2.992	h.c.p.	3.3090	5.2733	$\alpha \rightarrow \beta$ 1335	1539	1.655
Yttrium Y	α - Y	39	88.92	4.478	h.c.p.	3.6474	5.7306	$\alpha \rightarrow \beta$	150	1.778
	β - Y				bcc	4.11				
Lanthanum La	α - La	57	138.92	6.174	h.c.p.	3.770	12.159	$\alpha \rightarrow \beta$ 310	920	1.885
	β - La				fcc	5.304		$\beta \rightarrow \alpha$ 220		
	γ - La				bcc	4.26		$\beta \rightarrow \gamma$ 864		
Cerium Ce	α - Ce	58	140.13	6.771	fcc	4.85		$\alpha \rightarrow \gamma$ 113	795	1.825
	β - Ce				hcp	3.68	11.92	$\gamma \rightarrow \alpha$ 178		
	γ - Ce				fcc	5.1612		$\beta \rightarrow \gamma$ 100		
	δ - Ce				bcc	4.11		$\gamma \rightarrow \beta$ 10		
								$\gamma \rightarrow \delta$ 725		
Proseodymium Pr	α - Pr	59	140.92	6.782	hcp	3.6725	11.8354	$\alpha \rightarrow \beta$ 792	935	1.836
	β - Pr				bcc	4.13				
Neodymium Nd	α - Nd	60	144.27	6.96	hcp	3.6579	11.7992	$\alpha \rightarrow \beta$ 862	1024	1.829
	β - Nd				bcc	4.13				
Promethium Pm		61	152	5.259					1035	
Samarium Sm	α - Sm	62	150.35	7.536	rhombohdral	8.966	$\alpha = 23^o 13'$	$\alpha \rightarrow \beta$ 917	1072	1.811
	β - Sm				bcc	4.07				
Europium Eu		63	152	5.259	bcc	4.582			826	1.994
Gadolinium Gd	α - Gd	64	157.26	7.895	hcp	3.636	5.7826	$\alpha \rightarrow \beta$ 1264	1312	1.810
	β - Gd				bcc	4.06				
Terbium Tb	α - Tb	65	158.93	8.272	hcp	3.601	5.6936	$\alpha \rightarrow \beta$ 1326	1364	1.801
Dysprosium Dy		66	162.51	8.536	hcp	3.5903	5.6475		1407	1.795
Holmium Ho		67	164.94	8.803	hcp	3.5773	5.6158		1461	1.789
Erbium Er		68	167.27	9.051	hcp	3.5588	5.5874		1497	1.779
Thulium Tm		69	168.94	9.332	hcp	3.5375	5.5546		1545	1.769
Ytterbium Yb	α - Yb	70	173.04	6.977	fcc	5.4862		$\alpha \rightarrow \beta$ 798	824	1.940
	β - Yb				bcc	4.45				
Lutetium Lu		71	174.99	9.842	hcp	3.5031	5.5509		1652	1.752

two hexagonal layers A and B. However, the hcp structure found in the light group is constructed by stacking three hexagonal layers A, B and C, in order ABAC with the repetition interval along the c-axis twice as large as in the normal structure while for Samarium the construction is even more complicated. Details of crystal structures are given in Table 4.1.

The ratio c/a for the heavy series varies between 1.57 and 1.59 which is slightly different from the ideal value of 1.633. This is also true for Yttrium and Lutetium which respectively have unfilled and fully filled 4f shells, while for the light series c/a ranges from 1.61 to 1.62 and is closer to the ideal value. More complicated structures exist for Lanthanum, Praesodymium and Neodymium (the c/a ratio is 3.2) and Samarium with a crystal structure in which c/a is 7.2. The resulting difference in the ratio c/a between the members of the rare earth is due to the difference in the stacking sequence, Gschneidner (1961).

4.3 Magnetic Properties

The characteristic magnetic properties of the rare earths differ from those of the ferromagnets of the iron group. One of the most interesting properties is the fact that five of them (Tb, Dy, Er, Ho and Tm) show antiferromagnetism over a certain range of temperatures and the ordering is found to be spiral or helicodal. Magnetic measurements on the heavy groups are difficult since they all have extremely high

magnetocrystalline anisotropy and fields of up to 70 Koe. may not be sufficient to saturate polycrystalline samples. The measurement of the spontaneous magnetization I_s near the Curie temperature was not easy to carry out due to the fact that these materials have a complex magnetic structure above the Curie point and could be changed to a ferromagnetic by the application of a field of a few thousand oersted. Moreover, the arrangement of the magnetic moments in the ferromagnetic region is not a simple parallel alignment in most cases except for Gadolinium which possesses a normal ferromagnetic structure. Magnetization measurements have been carried out by many workers and a list of references is given at the end of this chapter.

As mentioned above the magnetic electrons in ferromagnetic rare earth metals arise from the incomplete 4f shell and the magnetic moment of this series is determined by the number of 4f electrons which increases regularly from 0 for La to 14 for Lu. The electrons in this shell are like those in the 3d shell of the transition metals, except that in rare earth metals the unfilled 4f shell is screened from the crystal field by the 5s and 5p closed shell electrons. This makes the crystalline field less effective than the LS coupling. The 4f shell with orbital quantum $\ell = 3$ has seven orbitals, the magnetic quantum numbers of which are - 3, - 2, - 1, 0 1, 2, and 3, these are filled with fourteen electrons (according to the Pauli principle each orbit can have two electrons) half with spin up and half with spin down. The value of the

TABLE 4.2

Element	4f Electron for 3^+ Ion	Magnetic susceptibility at 25°C x 10^{-6} emu/mole	Electronic state of 3^+ ion S	L	J	g factor	Saturation Magnetic moment in Bohr Magnetons gJ	T_n °K	T_c °K
Sc		8.08							
Y		191							
La	0	101	0	0	0	0	0	none	none
Ce	1	2430	$\frac{1}{2}$	3	$2\frac{1}{2}$	0.857	2.14	12.5	none
Pr	2	5320	1	5	4	0.800	3.20	25	none
Nd	3	5650	$1\frac{1}{2}$	6	$4\frac{1}{2}$	0.727	3.27	7.5	none
Pm	4	-----	2	6	4	0.600	2.40	unknown	none
Sm	5	1275	$2\frac{1}{2}$	5	$2\frac{1}{2}$	0.286	0.72	14.8	none
Eu	6	33100	3	3	0	-----	0.0	90	none
Gd	7	356000	$3\frac{1}{2}$	0	$3\frac{1}{2}$	2.00	7.0	none	289
Tb	8	193000	3	3	6	1.5	9.0	229	222
Dy	9	99800	$2\frac{1}{2}$	5	$7\frac{1}{2}$	1.333	10.0	178.5	85
Ho	10	70200	2	6	8	1.25	10.0	132	20
Er	11	44100	$1\frac{1}{2}$	6	$7\frac{1}{2}$	1.2	9.0	84	20
Tm	12	26200	1	5	6	1.167	7.0	56	22
Yb	13	71	$\frac{1}{2}$	3	$3\frac{1}{2}$	1.143	4.0	none	----
Lu	14	17.9	0	0	0	-----	0	none	----

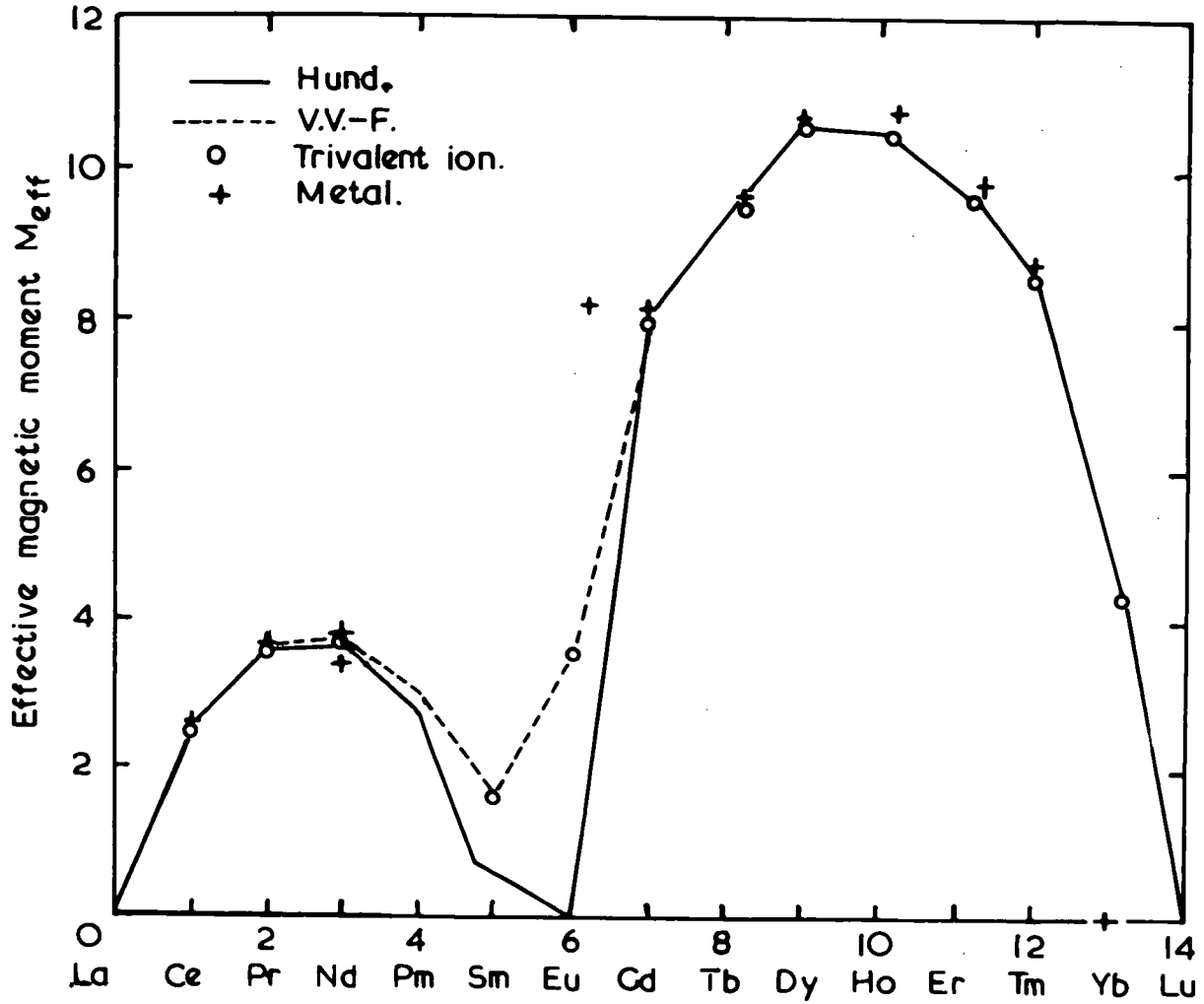

FIG. 4.1.

THE DEPENDENCE OF THE ATOMIC MAGNETIC MOMENT ON THE NUMBER OF ELECTRONS IN THE 4F SHELL.

total angular momentum J shown in Table 4.2 is calculated by J = L - S for a shell less than half full ($n \leq 7$) and J = L + S for more than half filled shell ($n \geq 7$). The effective magnetic moment could be calculated by

$$M_{eff} = g\sqrt{J(J+1)}\ \mu_\beta$$

where μ_β is the Bohr magneton $= \frac{eh}{4\pi mc}$, and g is the Landé splitting factor.

$$g = 1 + \frac{J(J+1) + S(S+1) - L(L+1)}{2J(J+1)}$$

The experimental values of M_{eff} and those obtained by theoretical considerations are plotted in Figure 4.1. Excellent agreement is observed except for Samarium and Europium. With these two, the values of L and S are such that when they are anti-parallel the value of L-S is small and the energy difference between the states of an ion for the two lowest values of J is small because it is proportional to the difference in the value of J(J+1). Even though the difference in energy between the states with highest and with the lowest value of J is large the two separate values for M_{eff} which was calculated by Van Vleck (1932) for Sm and Eu differ in the values assumed for the screening coefficients, representing the effect of the electrons surrounding the nucleus in reducing the action of the nuclear charge upon the 4f electrons which are used in calculating the separation term between the ground and the first excited state.

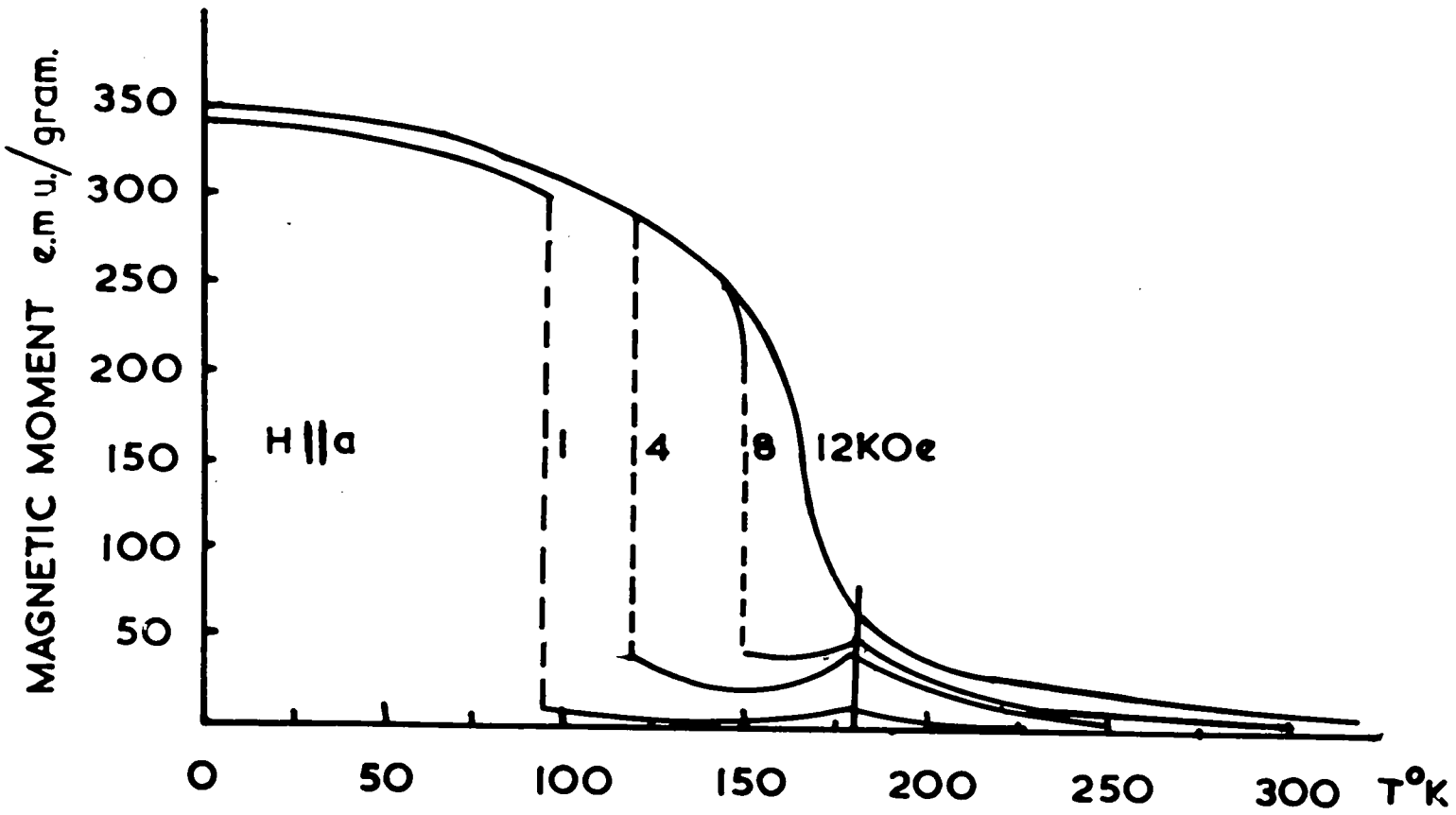

FIG. 4.2. MAGNETIC FIELD AND TEMPERATURE DEPENDENCE OF THE MAGNETIZATION OF DYSPROSIUM.

The Curie temperature of the elements which exhibit ferromagnetism decreases with increasing atomic number. At a certain temperature above the Curie point these elements become antiferromagnetic. The transisition is clearly observed in the magnetization and neutron diffraction experiments. In the paramagnetic region the magnetization increases with the decrease of the temperature as in most paramagnetic materials, the increase in temperature is proportional to inverse of the susceptibility. As the temperature decreases the magnetization reaches a maximum and then decreases and the structure will become antiferromagnetic at the Néel point. With a further decrease in temperature the Curie point is reached and the system becomes ferromagnetic. Below this point the spontaneous magnetization increases rapidly with decreasing temperature. From Figure (4.2) it can be seen that the Néel point depends upon the magnitude of the external applied field. In the case of Dysprosium for example in a field of order of 12 Koe. or larger there will be no anti-ferromagnetic region and the transition from paramagnetism to ferromagnetism will take place at the Néel point, that is Néel and Curie points will occur at the same temperature.

4.4 Magnetic structure

The magnetic structure of the rare earth metals has been very fully investigated, the most rewarding method is the neutron diffraction

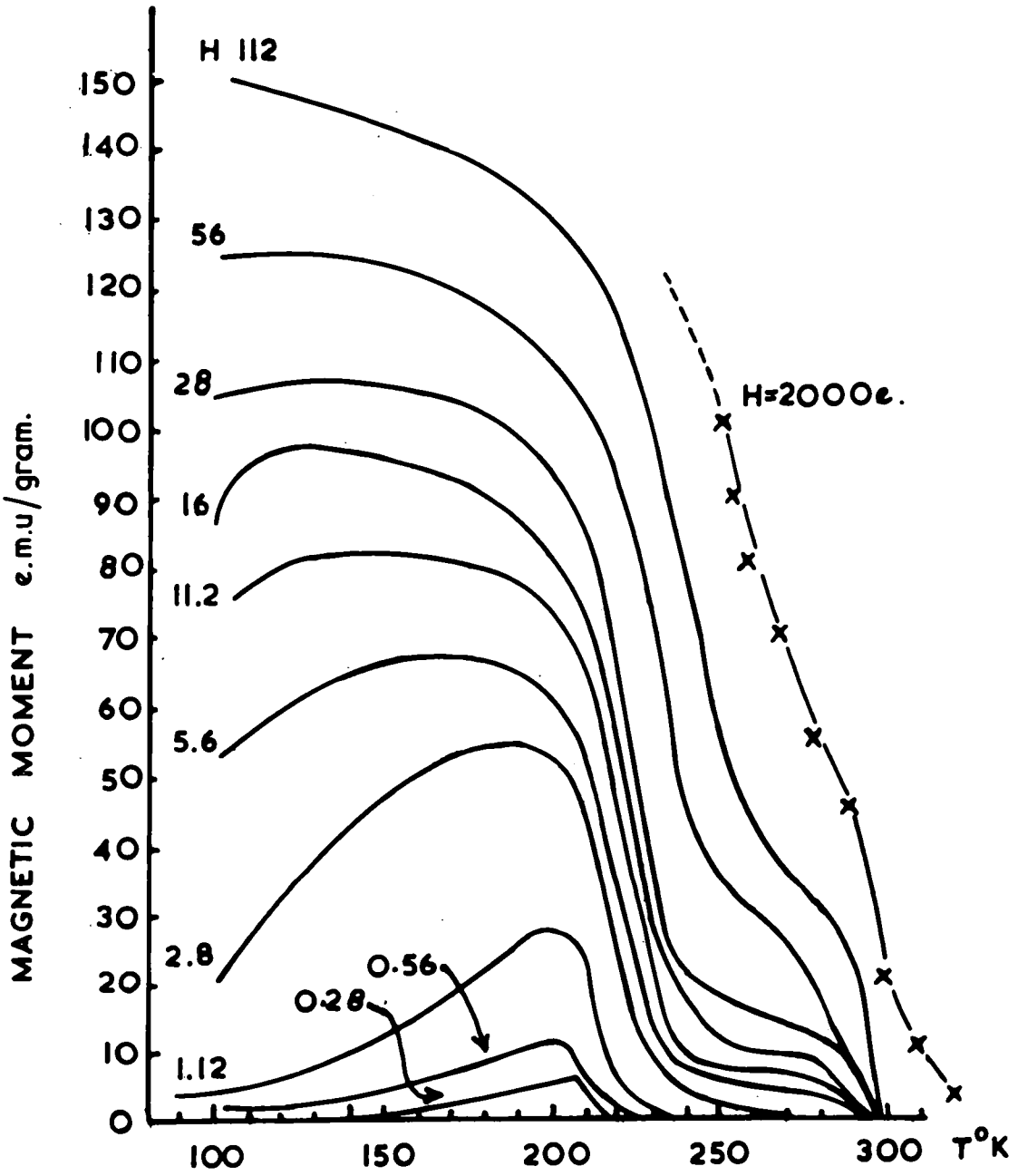

FIG. 4.3. MAGNETIC FIELD AND TEMPERATURE DEPENDENCE OF THE MAGNETIZATION OF GADOLINIUM.

technique, although, with a few exceptions, there is agreement with other methods of investigation (single crystal magnetization measurements susceptibility measurements and specific heat data) Gadolinium was originally regarded as normal ferromagnetic over its entire ordering range, e.g. Legvold (1953) and Elliott (1953), but measurements by Belov (1961, 1962) indicated that in a weak field of the order of a few oersted magnetization anomalies appear in the region 210 ÷ 250°K as shown in fig. 4.3. This suggests that antiferromagnetism exists in Gd with a Néel point of 290°K and a Curie point at about 210°K. Neutron diffraction data, Will et al. (1964) and Cable et al. (1968) confirms the ferromagnetic structure and the variation of the easy direction with temperature, the ferromagnetic moment is aligned along the c-axis below 289°K, and changes to a cone of easy magnetization below 242°K. Those results rule out the suggestion that Gd may be antiferromagnetic. It is possible that the anomaly which appeared in the measurements of Belov et al. is due to the considerable decrease of the anisotropy energy in the region 210 - 250°K. For Terbium the helical magnetic structure occurs in the temperature range 229°K to 220°K. All the spins are entirely within the basal plane, but there is a rotation of about 20° from one layer to the next resulting in a helical arrangement along the [0001] direction. In this temperature range the antiferromagnetism may be changed to ferromagnetism by

application of a field greater than 800 Oe. parallel to the basal plane. Similarly Dysprosium exhibits a helical magnetic structure in the temperature range from 179 to 85°K. The rotation of the moment from one layer to the next varies from about 42°K at 179°K to about 26°K at 87°K. Below 85°K Dysprosium is ferromagnetic with an easy direction of magnetization along [11$\bar{2}$0]. A field of few hundred oersted near 90°K increasing to 10 Koe at 160°K parallel to [0001] is needed to change the antiferromagnetic to a ferromagnetic structure. Almost the same behaviour as that of Tb and Dy is found in Holmium, its helical structure occurs from about 132°K to 20°K. In this temperature range, the turn angle decreases linearly from 51° at the Néel temperature to 30° at 20°K; below 20°K there exists a small ferromagnetic component parallel to the c-axis and another component remains in the helical arrangement in the basal plane with an angle of 30° between the moments in adjacent layers. The field required to transfer the metal from antiferromagnetic to ferromagnetic is about 3 Koe at 33°K, rising to 30 Koe at 100°K. The investigation of Erbium by neutron diffraction showed different results from those shown above. Between 84 and 52°K the structure is of sinusoidal type with moment parallel to the [0001] direction the period of modulation is seven atomic layers, the magnitude changes with direction along the c-axis, while there is no ordering of the moments perpendicular to the c-axis. Between 54°K and 20°K the components in the basal plane began to order in a helical arrangement

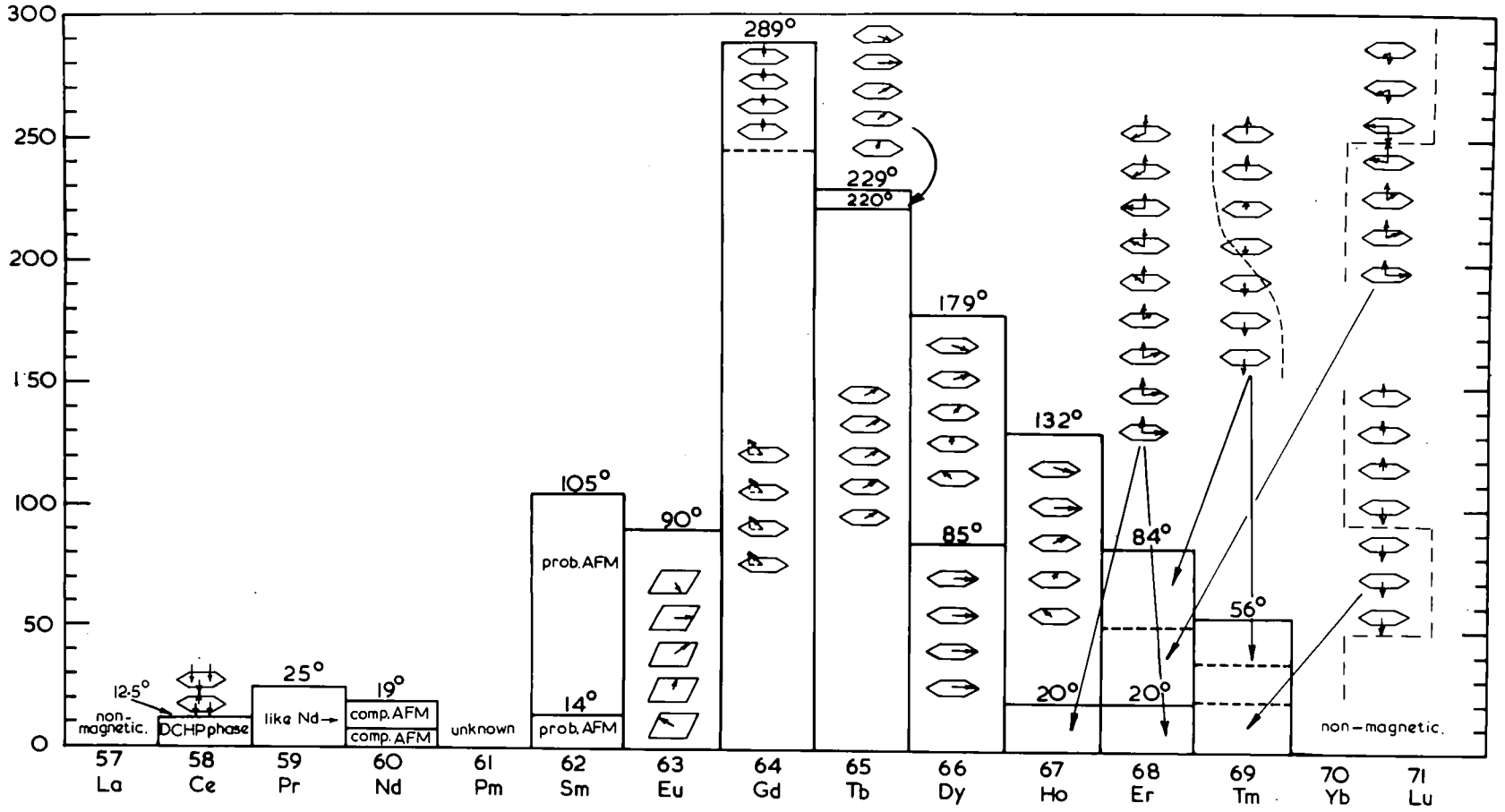

Fig. 4.4. MAGNETIC CONFIGURATION OF RARE EARTHS IN ZERO FIELDS.

and the parallel components tend to form a type of anti-phase domain structure in which several layers with moments pointing up are followed by an equal number with moments pointing down forming a square wave. Below $20^{\circ}K$ ferromagnetic ordering occurs along the [0001] axis, but with part of the total moment remaining helically ordered in the (0001) plane with an angle of 43.3° between the moments of adjacent layers. Thus the magnetization lies along a cone with semi angle 28.5° from the c-axis. In Thulium from about 56 to $40^{\circ}K$ there is a linear spin-wave magnetic structure. Ordering of the moments is found only in the direction [0001] and varies sinusoidally with a period of seven atomic layers. At $4.2^{\circ}K$ Thulium shows an anti-phase domain type structure arranged in alternate groups of four and three pointing up and down along the c-axis. The periodicity of seven is preserved in Thulium between 20 to $40^{\circ}K$ and the anti-phase domain structure changes gradually to the cycloidal one.

The above discussion is summarized in Fig. (4.4).

MAGNETIZATION OF RARE EARTHS

REFERENCES

Gadolinium

Belov, K.P., and Ped'ko, A.V., Soviet Phys. Jetp., 15, 62, (1962)

Behrendt, D.R., Legvold, S., and Spedding, F.H., Phys. Rev., 106, 723, (1957).

Elliott, J.F., Legvold, S., and Spedding, F.H., Phys. Rev., 91, 28, (1953).

Griffel, M. Skochdopole, R.E., and Spedding, F.H., Phys. Rev., 93, 657, (1954).

Henry, W.E., J. App. Phys., 29, 524, (1958).

Nigh, H.N., Legvold, S., and Spedding, F.H., Phys. Rev., 132, 1092, (1963).

Terbium

Henry, W.E., J. App. Phys., 30, 99S, (1959)

Hegland, D.E., Legvold, S., and Soedding, F.H., Phys. Rev., 131, 158, (1963).

Leipfinger, H., Z. Phys., 150, 415, (1958).

Thoburn, W.C., Legvold, S., and Spedding, F.H., Phys. Rev., 112, 56, (1958).

Dysprosium

Belov, K.P., Levitin, R.Z., Nikitin, S.A., and Ped'ko, A.V., Sov. Phys., Jetp, 13, 1096, (1961).

Behrendt, D.R., Legvold, S., and Spedding, F.H., Phys. Rev., 109, 1544, (1958).

Legvold, S., "Rare Earth Research. II"., E. V. Klebe, Editor MacMillan p. 142, (1961).

Leipfinger, H., Z. Phys., 150, 415, (1958).

Holmium

Henry, W. E., Bull. Amer. Phys. Soc., 4, 176, (1959).

Legvold, S., "Rare Earth Research II" E. V. Klebe, Editor Macmillan, p. 142 (1961).

Leipfinger, H., Z. Phys. 150, 415 (1958).

Rhodes, B.C., Legvold, S., and Spedding, F.H., Phys. Rev., 109, 1547, (1958).

Strandburg, D.L., Legvold, S., and Spedding, F.H., Phys. Rev., 127, 2046, (1962).

Erbium

Elliott, J.F., Legvold, S., and Spedding, F.H., Phys. Rev., 100, 1595, (1955).

Green, R.W., Legvold, S., and Spedding, F.H., Phys. Rev., 122, 827, (1961).

Legvold, S., "Rare Earth Research II", E. V. Klebe, Editor Macmillan, p. 142, (1961).

Skochdopole, R.E., Griffel, M., and Spedding, F.H., J. Chem. Phys., 25, 75, (1956).

Thulium

Leipfinger, H., Z. Phys., 150, 415, (1958).

Rhodes, B.C., Legvold, S., and Spedding, F.H., Phys. Rev., 109, 1547, (1958).

Davies, D.D., and Bozorth, R.M., Phys. Rev., 118, 1543, (1960).

CHAPTER 5

THE DOMAIN STRUCTURE OF GADOLINIUM SINGLE CRYSTALS

5.1 Previous Work

Rare earth metals are one of the most difficult group of metals to study so far as domains are concerned. This, as has been mentioned previously, is due to the high impurity normally involved in the metal. Little work has been done in this field except for that of Birss et al. (1963) and Bates et al. (1964), both using the Bitter technique with a modified colloid. Birss et al. observed needle-shaped domains running parallel to the c-axis at a temperature of about 268°K while Bates et al. observed a variety of structures at temperatures in the range 180°K to 210°K. These observations did not yield enough detailed information to enable the complete domain structure to be elucidated, that is, to decide the internal domain structure and whether surface poles were present or complete or partial flux continuity achieved by closure domains. Both authors suggested that the poor results were due to the low anisotropy and also the spontaneous magnetization being low compared with that of cobalt. It is, however, more likely that the poor resolution they obtained was due to the strong influence of the presence of oxide inclusions on the domain structure and perhaps also to the residual strain resulting from these inclusions.

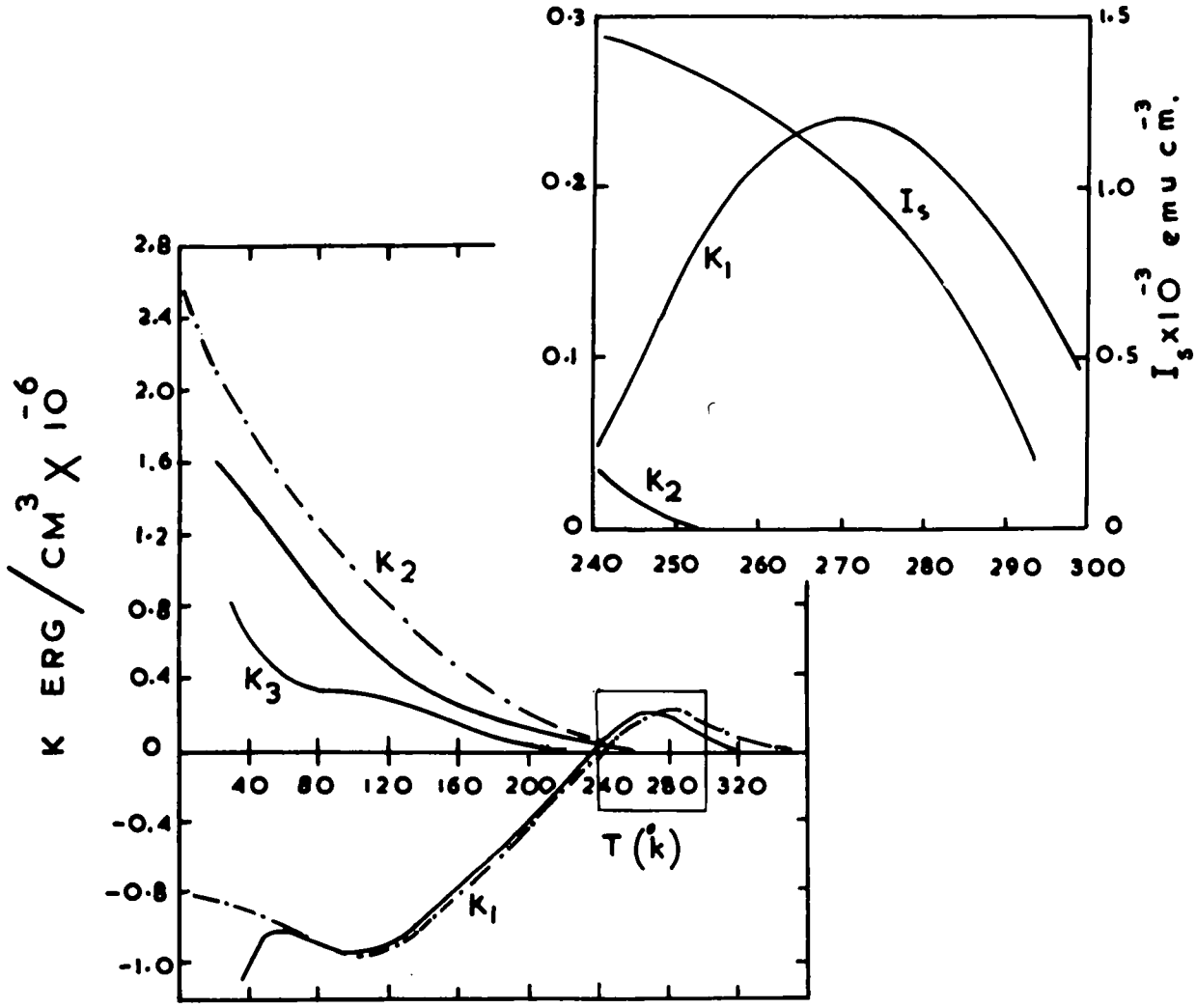

FIG. 5.1 Temperature Variation of the Anisotropy Constants of Gadolinium.

——— Corner et al.

—.—.— Graham.

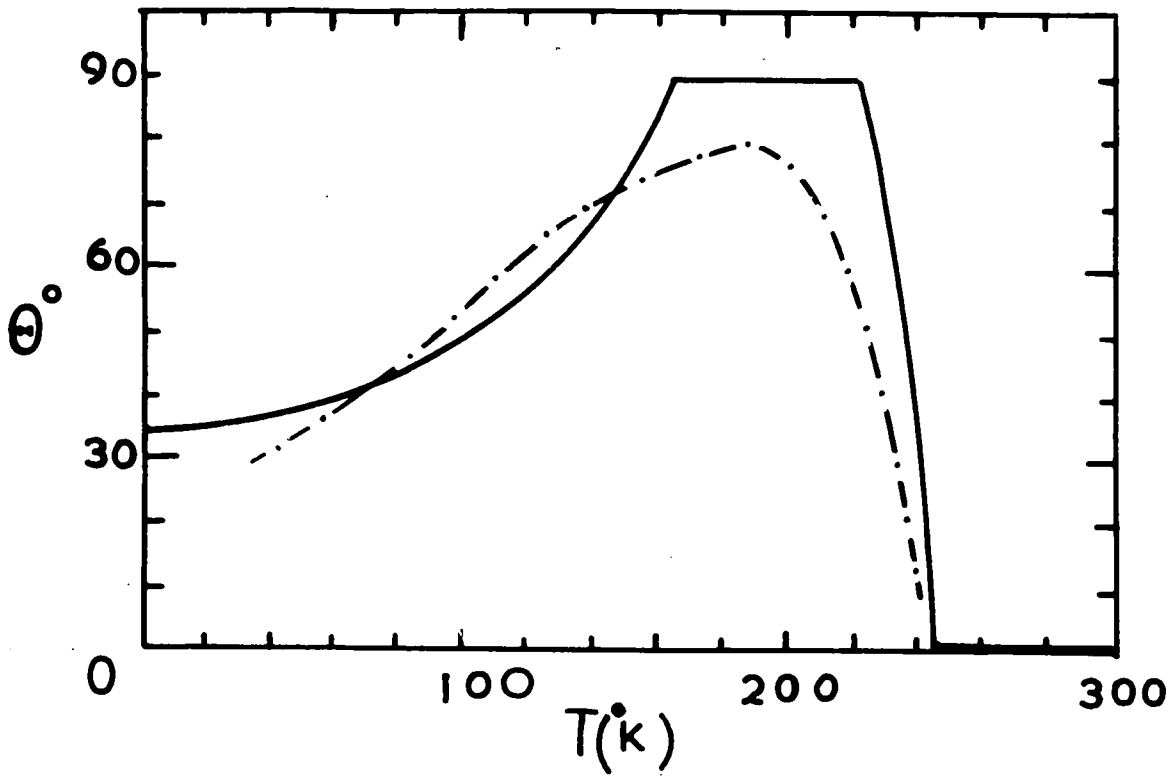

FIG. 5.2 Easy direction in Gadolinium as a function of temperature.

_ . _ . _ Corner et al.

——— Graham.

5.2 Present work

Gadolinium is essentially different from the other ferromagnetic rare earths in that it exhibits normal ferromagnetism over its entire ordering range. Torque measurements of the anisotropy constants of gadolinium have been made by Corner et al. (1962) and Graham (1962). Corner et al. included the constant K_3 to describe the torque curves obtained, where Graham used only K_1 and K_2. The variation of the anisotropy constant with temperature along with the value of magnetization are shown in Fig. 5.1. The easy direction is the c-axis between Curie temperature 290°K and 240°K. Below 240°K the easy direction lies on a cone about the c-axis. The angle θ between the easy direction and the c-axis reaches the maximum value of 70° at 220°K, where at 37.5°K the direction of easy magnetization lies at an angle of 30°. However, Graham reports that the easy direction is in the basal plane below 225°K these results being shown in Fig. 5.2. The measurements of Corner et al. were confirmed by Nigh (1963) and by the neutron diffraction measurements of Cable et al. (1968).

The basal plane magnetocrystalline anisotropy constant K_4 has been determined by Darby et al. (1964) and Graham (1967). This was found to be very small and of the order of 10^3 erg/cm^3 and has a maximum value of about 2.6×10^3 erg/cm^3 at 4.2°K. This constant contributes to the anisotropy energy below 160°K. Measurements have been made with strain

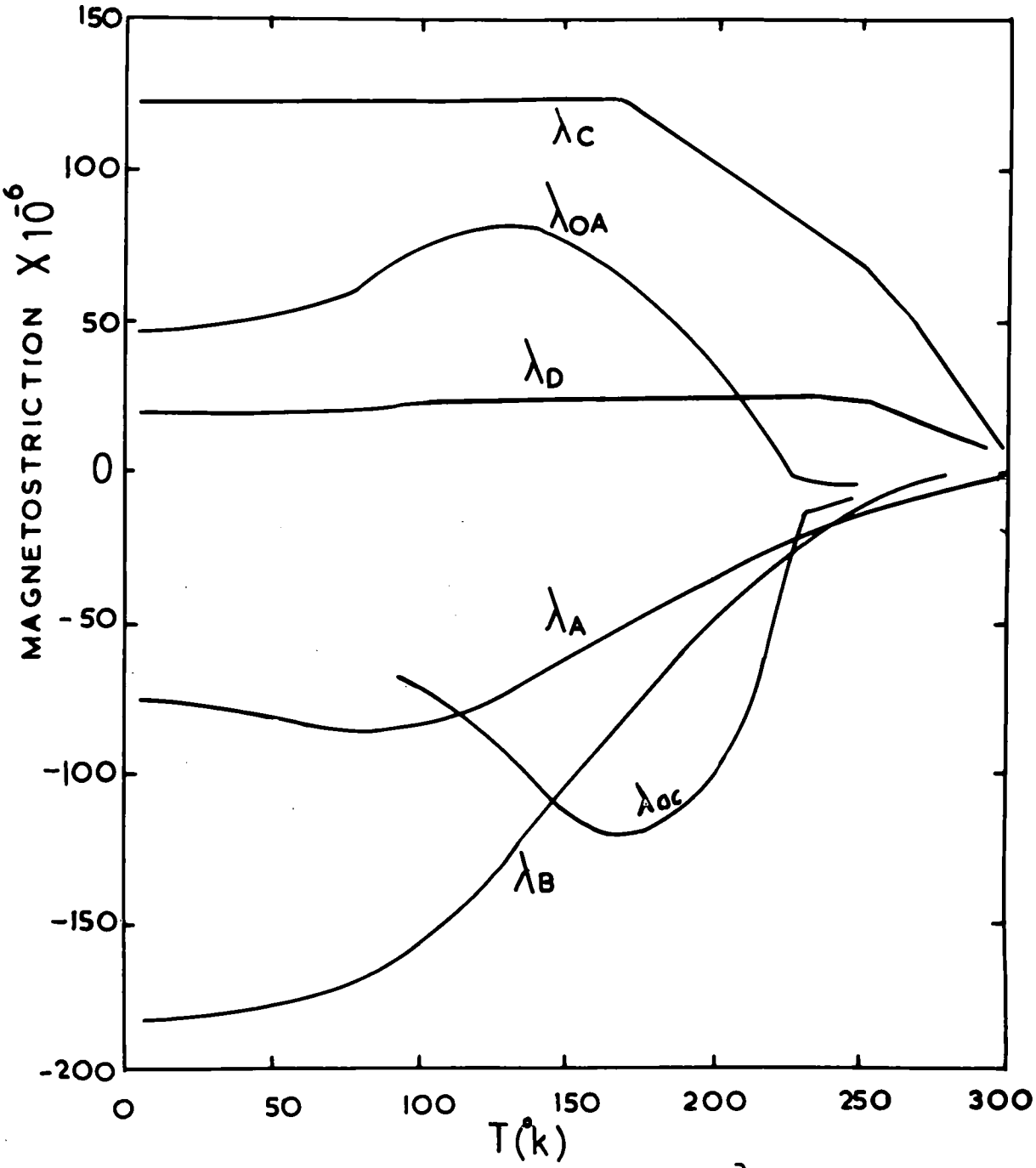

FIG. 5·3 Magnetostriction constants of Gd; λ_{OC} is the magneto striction parallel to C, and λ_{OA} to a, resulting from magnetization from zero to saturation parallel to C. (Bozorth et al.)

gauges of the magnetostriction of single crystals of gadolinium. Bozorth et al. (1962). The four constants necessary for a description of a hexagonal crystal have been evaluated over the temperature range of $4^{o}K$ to above the Curie point. Using fields up to 30 Koe the results are shown in Fig. 5.3, where λ_{OC} and λ_{OA} are the deformations parallel and perpendicular to c-axis when the unmagnetized crystal was magnetized to saturation.

The present work will provide experimental evidence of the internal magnetic domain structure as well as the nature of the superficial domains at a surface perpendicular to the c-axis. Also the results of a study of the effect of magnetic field as well as variations of temperature are presented. The variation of the structure with the thickness of the specimen has been investigated.

The investigation of domain structure on gadolinium began on a small sample in which a large amount of oxide inclusion was present. The sample was first mounted in the mounting plastic N.H.P. 2031/19 as mentioned in Chapter two, after polishing evaporation of dry colloid took place at temperature of $274^{o}K$. Fig. 5.4a shows a strain pattern which is produced as a result of the mounting plastic, with no indication of domain structure. Since the chemical polishing revealed the underlying oxide inclusions and since these were present in a large quantity it was decided to anneal the specimen in vacuum at a temperature of $680^{o}K$ for 5 hours to relieve the strain and then a very slight

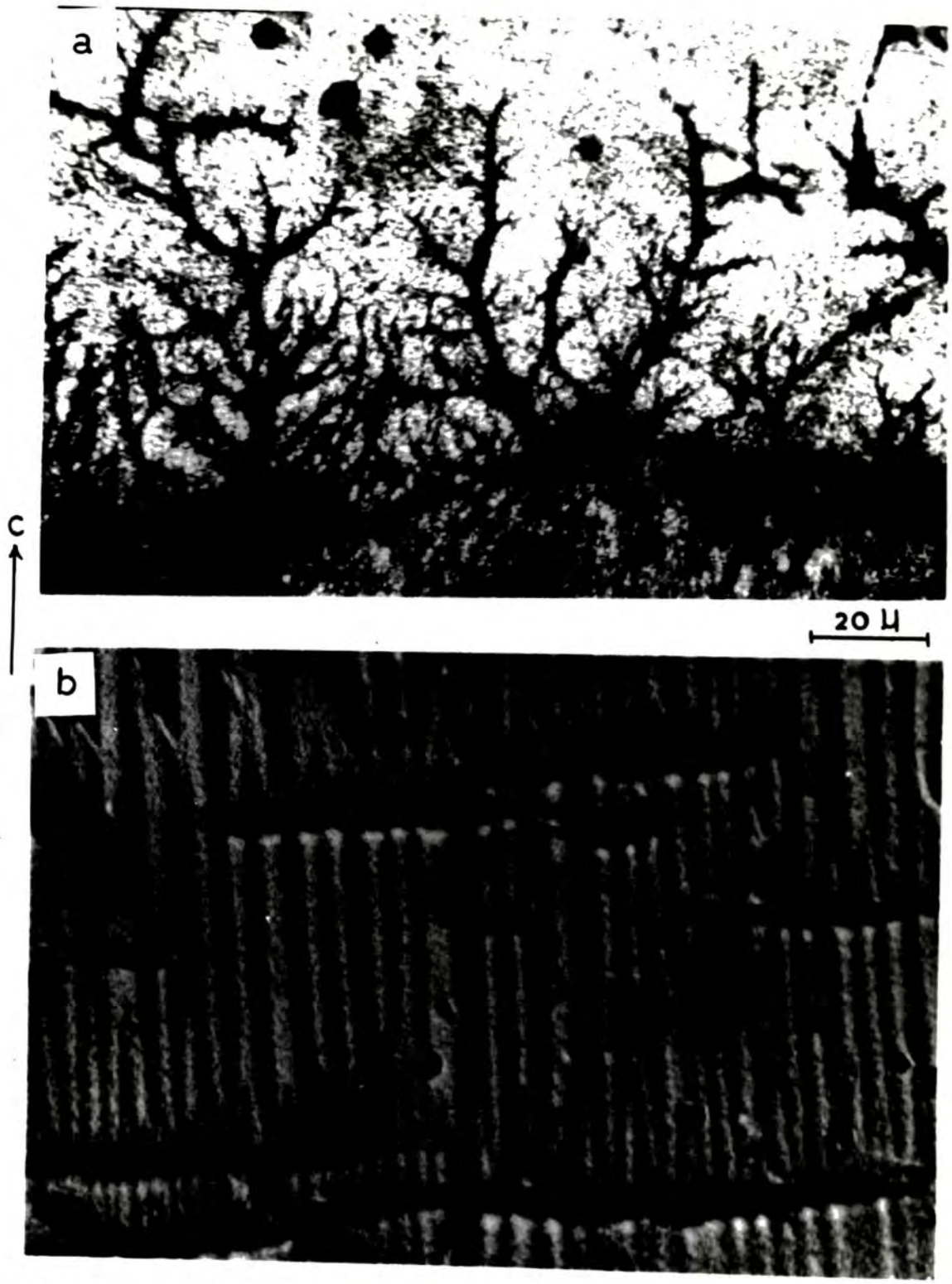

Fig. 5.4. a- Strain Pattern found on Gadolinium Single Crystal.

b- Domain Pattern on the same surface at 274°K.
(magnetic field of 300 Oe. applied normal to the surface)

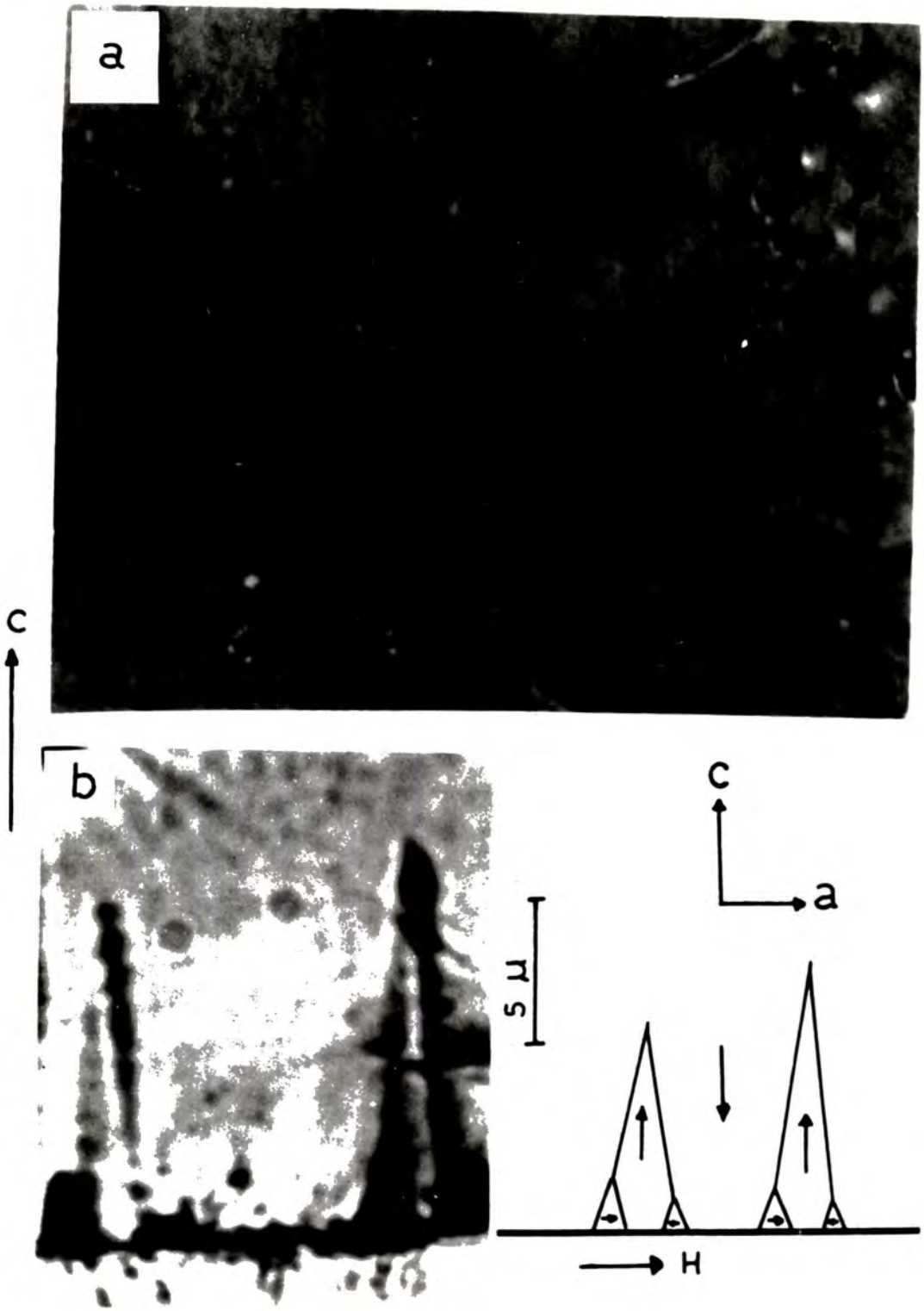

Fig. 5.5. a- 180 Domain on $\langle 10\bar{1}0 \rangle$ surface (300 Oe. applied along c-axis).

b- Daggers of Reverse Magnetization on $\langle 10\bar{1}0 \rangle$ surface (300 Oe. applied along a-axis).

chemical polish was given to remove the minute scratches. A typical domain pattern was obtained at 274°K with a field of 300 Oe. applied normal to the surface as shown in Fig. 5.4b. This reveals the strong influence of the inclusions on the domain structure and it was decided that no further useful work could be carried out on this sample.

Work was therefore started on the sample which was previously treated by solid state electrolysis. This was done in order to eliminate or at least to allow oxide contained to be aggregated together into large inclusions leaving clear areas for the purpose of domain study.

5.3 Domain structure on a surface containing the C-axis at 274°K.

Observations were made at 274°K where the anisotropy constant k_1 has very nearly its maximum value 2.4 x 10^6 erg/cm^3, the easy direction being along the c-axis. In addition the magnetization attained a value of about 950 e.m.u. per cm^3. Clear domain patterns have been observed on all prepared surfaces at this temperature. There is no difference between the patterns observed on $\langle 11\bar{2}0\rangle$ and $\langle 10\bar{1}0\rangle$ surfaces. This is not surprising since the material is very nearly isotropic in the basal plane ($k_4 = 0$) at this temperature. A typical structure is shown in Fig. 5.5(a,b) on a $\langle 10\bar{1}0\rangle$ surface. Here the pattern shown consists of 180° parallel walls and the spacing was greatly different at different regions on the surface. This resulted from the plates of

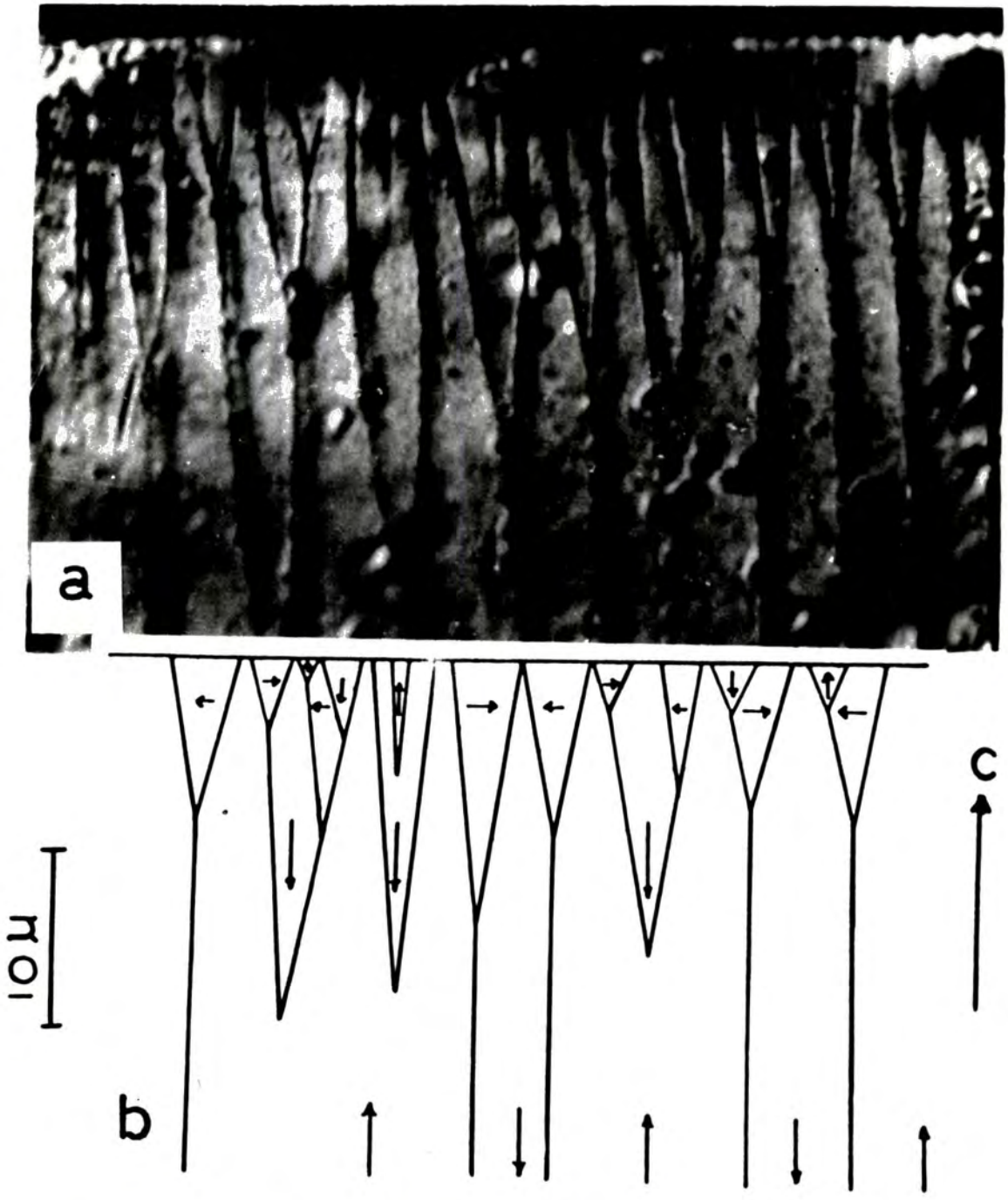

Fig. 5.6. a- Domain structure on $\langle 11\bar{2}0 \rangle$ surface near edge of the specimen at 274°K. (magnetic field of 300 Oe. applied along c-axis).

b- Interpretation of a.

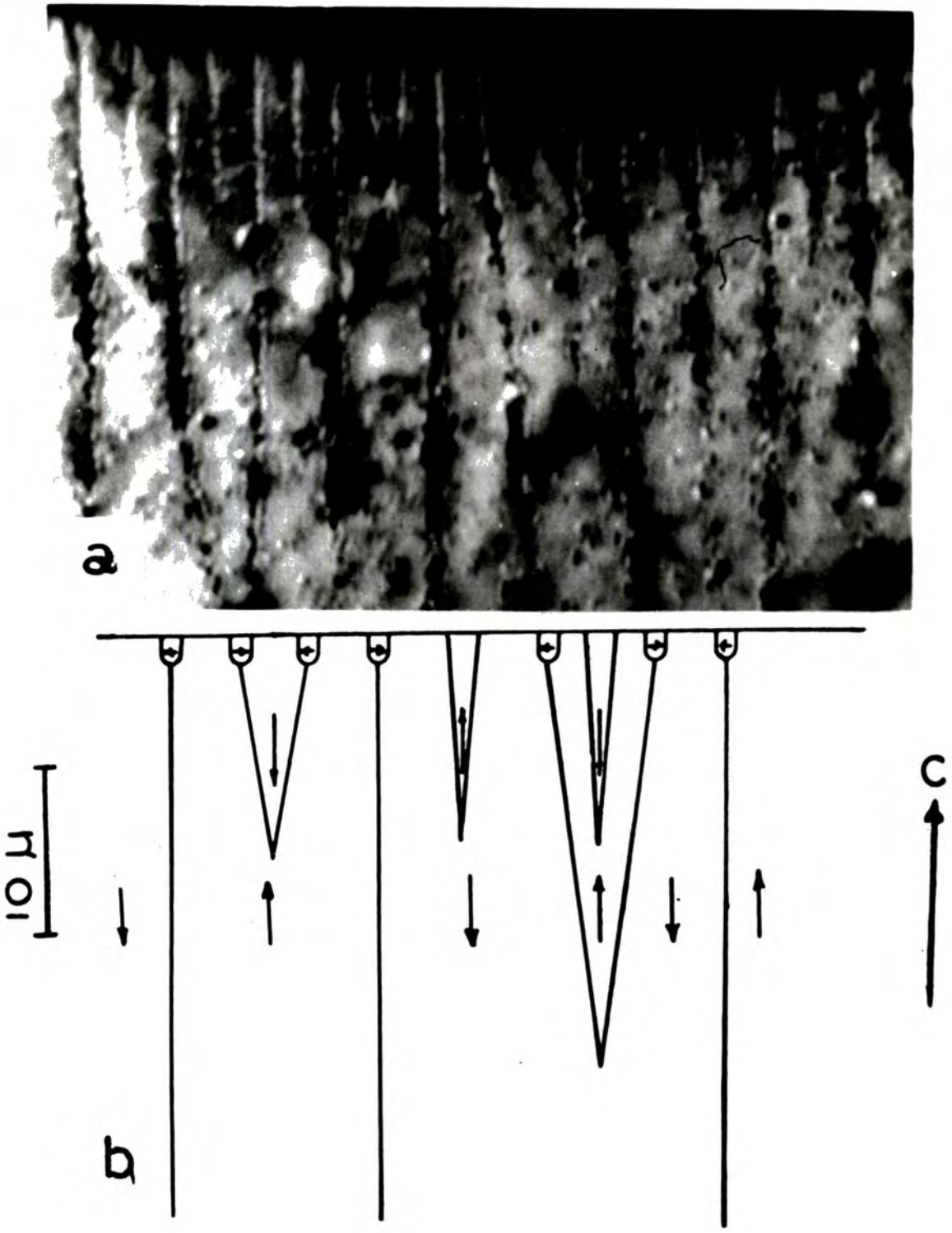

Fig. 5.7. a- Domain structure on $\langle 11\bar{2}0 \rangle$ surface near edge of the specimen at 274 °K. (magnetic field of 300 Oe. applied along c-axis).

b- Interpretation of a.

oxide which are distributed randomly in the body of the specimen with the c-axis normal to the plane of the oxide. Fig. 5.6a and 5.7a are near the edge of a $\langle 11\bar{2}0 \rangle$ surface. In Fig. 5.6a the formation of closure structures may be clearly seen, but these do not give complete flux closure and still there are areas of free poles on the basal plane surface. Reverse daggers are also evident. Fig. 5.6b gives a suggested interpretation of 5.6a. A less complicated structure obtained at another point near the edge of a $\langle 11\bar{2}0 \rangle$ surface is seen in Fig. 5.7 along with a suggested interpretation. Here it is again evident that the minimization of energy involves the formation of both reverse daggers and closure domains, but there are still free poles on the basal plane surface. Since similar patterns are observed on the two perpendicular surfaces it would not be expected that the 180° boundaries between the main domains would be constrained to lie in any particular crystallographic plane so long as it contained the c-axis.

5.4 Domain structure on Basal Plane Surface at $274^{\circ}K$

As may be expected of any uniaxial ferromagnetic material the pattern observed on the basal plane surface is very complex, and that there is no preferred direction of wall alignment thus confirming the isotropy of magnetic properties in the basal plane at this temperature. This structure changes in a consistent fashion in going to thin layers. With a decrease of the specimen thickness the domain structure is simplified as will be discussed later.

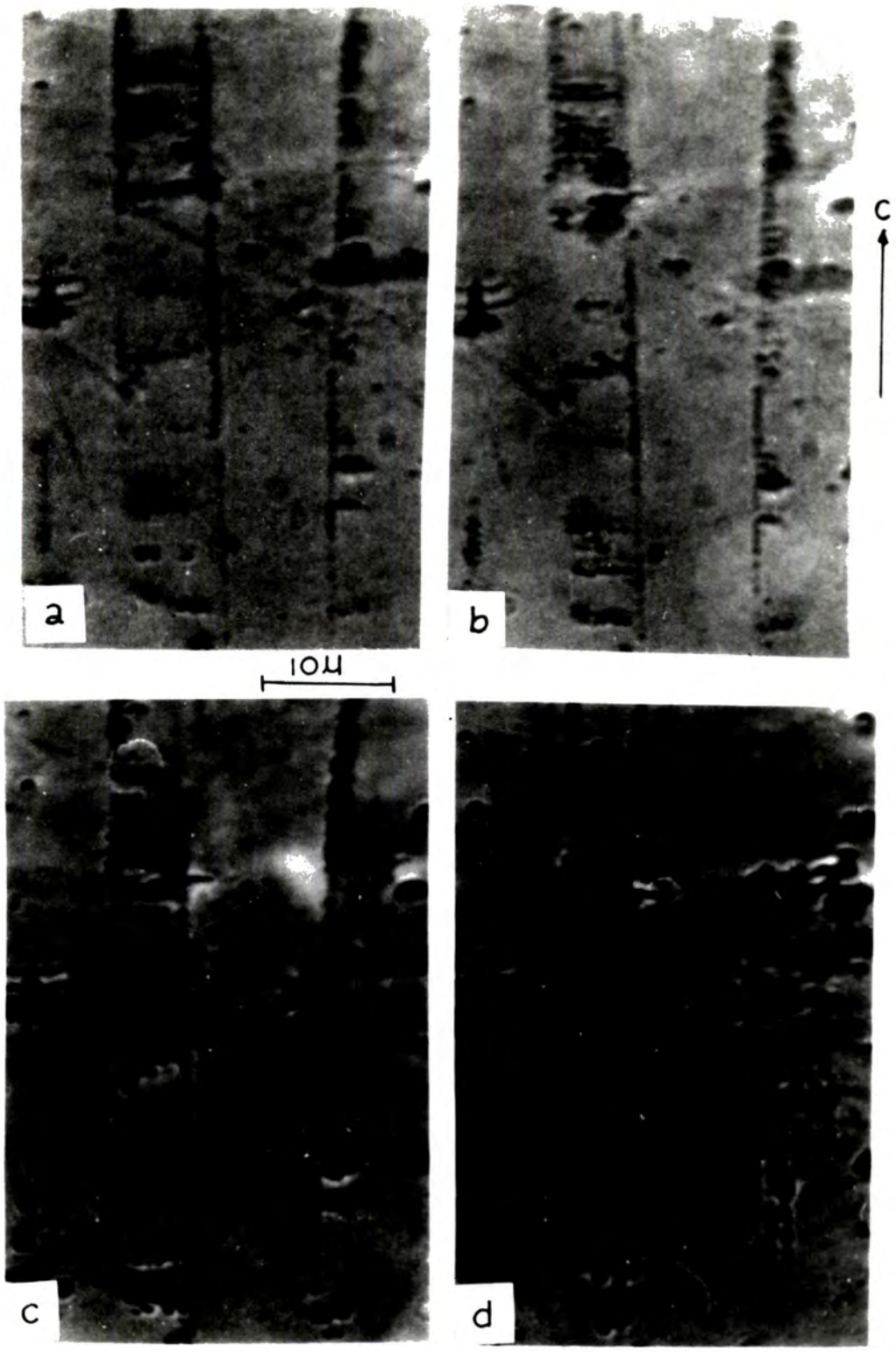

Fig.5.8. (a-d) Domain Structure on $\langle 11\bar{2}0 \rangle$ surface. Magnetic field applied along c-axis.

a- 120 Oe., b- 220 Oe., c- 300 Oe., d-560 Oe.

All the patterns shown at 274°K have been obtained by the modified colloid using secondary butyl alcohol.

5.5 The behaviour of patterns under the effect of magnetic field

5.5.1 Applied field parallel to the surface under observation

Application of a small magnetic field usually causes the movement of Bloch walls so that favourably oriented domains grow in volume. At higher fields regions of inverse magnetized domains or entire domains of such type suddenly collapse. This is observed on a $\langle 11\bar{2}0 \rangle$ surface when a magnetic field is applied along the c-axis as shown in Fig. 5.8 (a-d), the walls remains straight and parallel during this movement except near impurities which pin the movement of the walls. The change in width of the domains continues until a second stage is reached where the walls are seen to collapse and disappear. On reducing the field the walls gradually reappear. It can be seen that as the field increases deposits of colloid appear on alternate domains in addition to the deposit along the walls. This may be due to the applied magnetic field not being accurately parallel to the surface but having a small normal component which polarises the colloid. If the domain magnetization is also not quite parallel to the surface the colloid will then deposit preferentially on alternate domains where the surface polarity is appropriate. The application of magnetic fields of up to 1400 Oe along the b-axis in the basal plane, are shown in fig. 5.9(a-d).

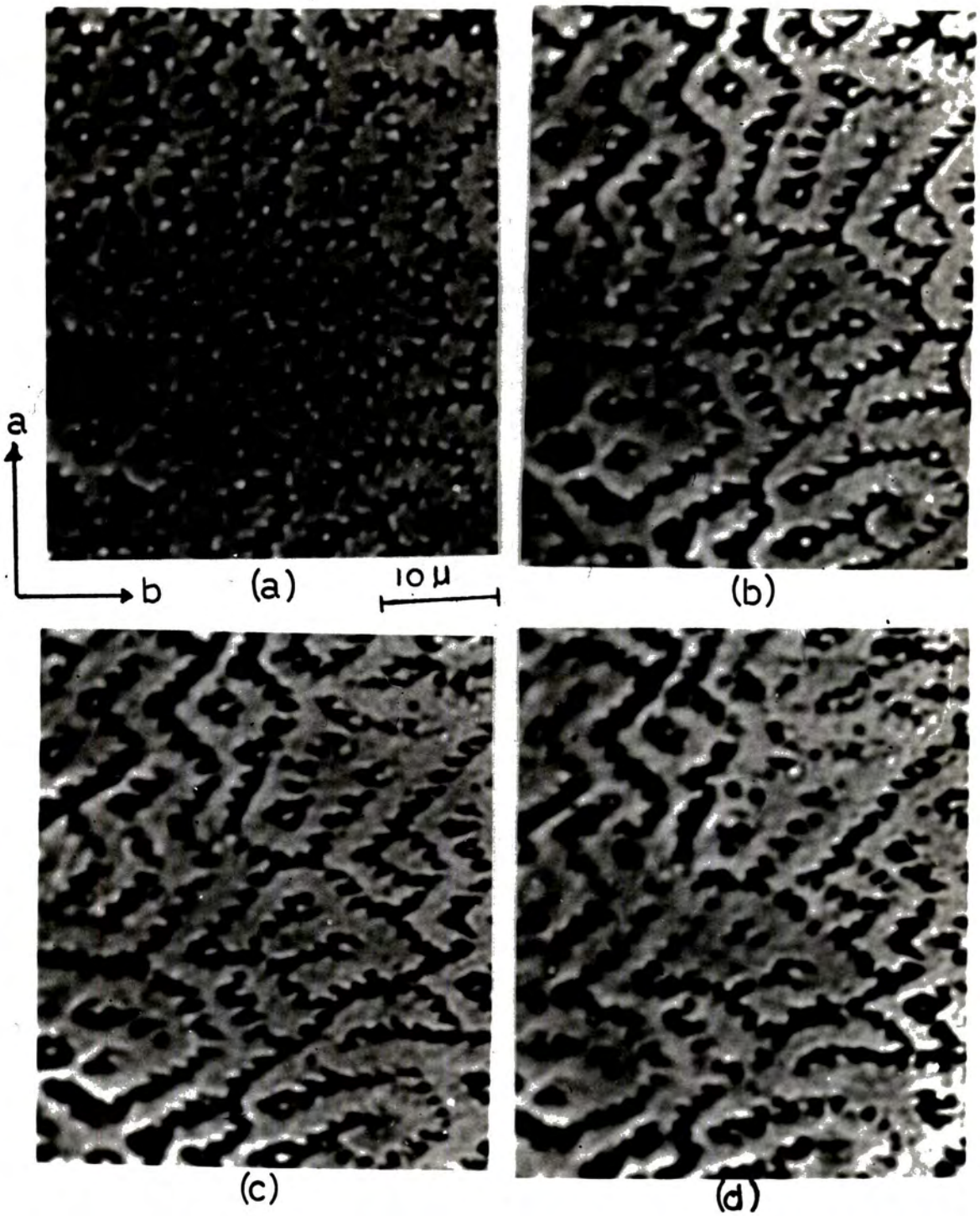

Fig. 5.9. (a-d) Domain Structure on Basal Plane. Magnetic field applied along b-axis.

a- 120 Oe., b- 560 Oe., c- 1000 Oe., d- 1400 Oe.

Up to 120 Oe there is no appreciable change in structure though the contrast of the pattern improves. An increase to 560 Oe produces a noticeable change in the secondary structure, the colloid free regions rotating so as to lie along the field direction, except where the main wall already lies along this direction when they disappear. The general pattern also expands slightly in the b-direction. This extension proceeds as the field strength is increased. In Fig.5.9c the structure retains the same features as in Fig. 5.9a but is subject to considerable distortion. At 1400 Oe, as in Fig. 5.9d, the structure is becoming less well defined, walls appear to be breaking up and the colloid-free secondary structure has either completely disappeared or become greatly modified. With higher fields it is difficult to obtain a satisfactory pattern and this may be due to the effect of the demagnetizing field associated with the oxide inclusions. The high field will produce an increased density of free poles at the ends of the inclusions adjacent to the surface of the specimen which will greatly effect the colloid pattern.

5.5.2 Effect of small normal applied field

The behaviour of basal plane structures under the influence of normal field is such that when a field of ± 300 Oe is applied the pattern obtained will be complementary. This is due to the presence

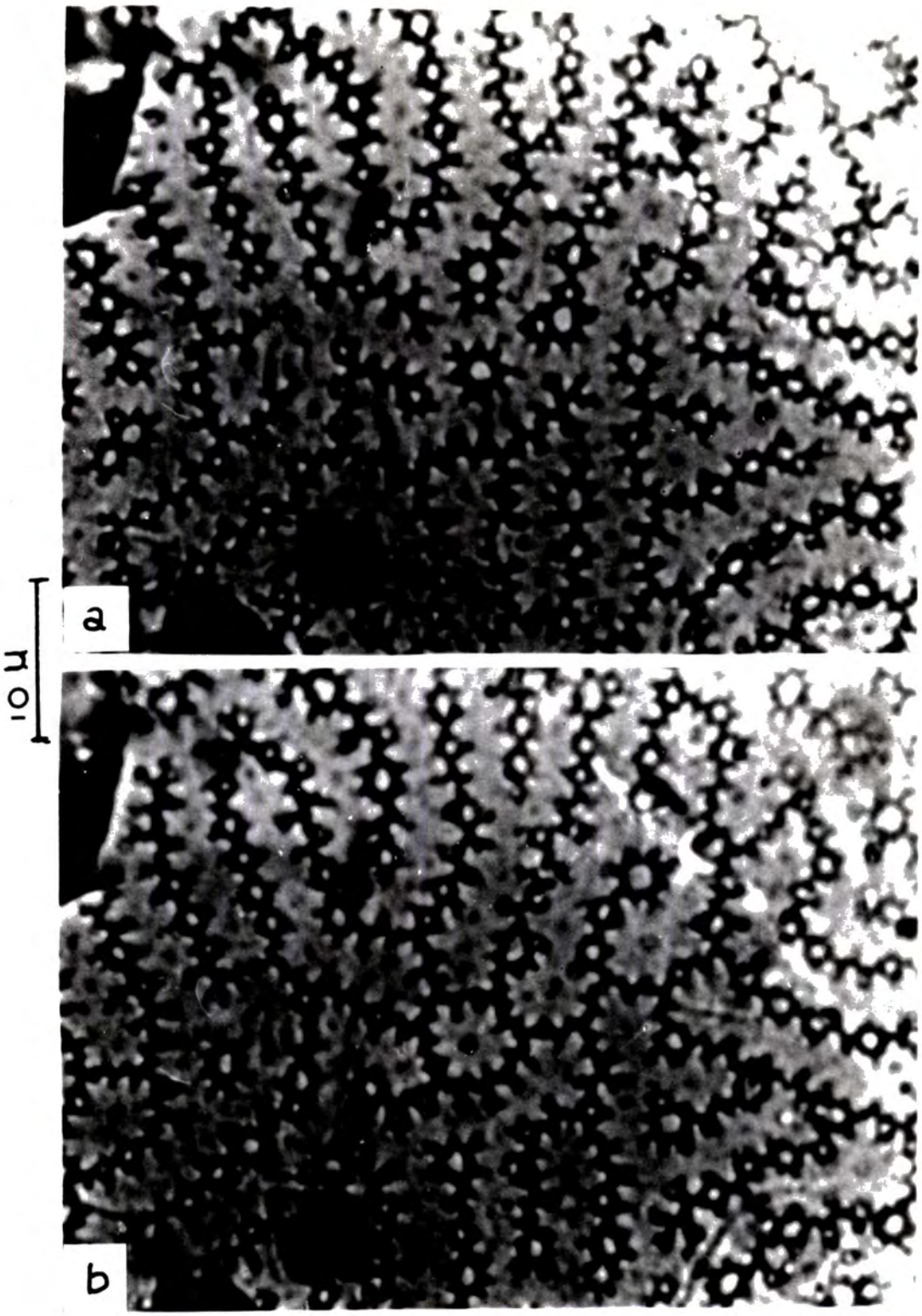

Fig. 5.10. Domain Structure on Basal Plane surface at 274° K with Magnetic field applied parallel to the c-axis.

a- -300 Oe. b- +300 Oe.

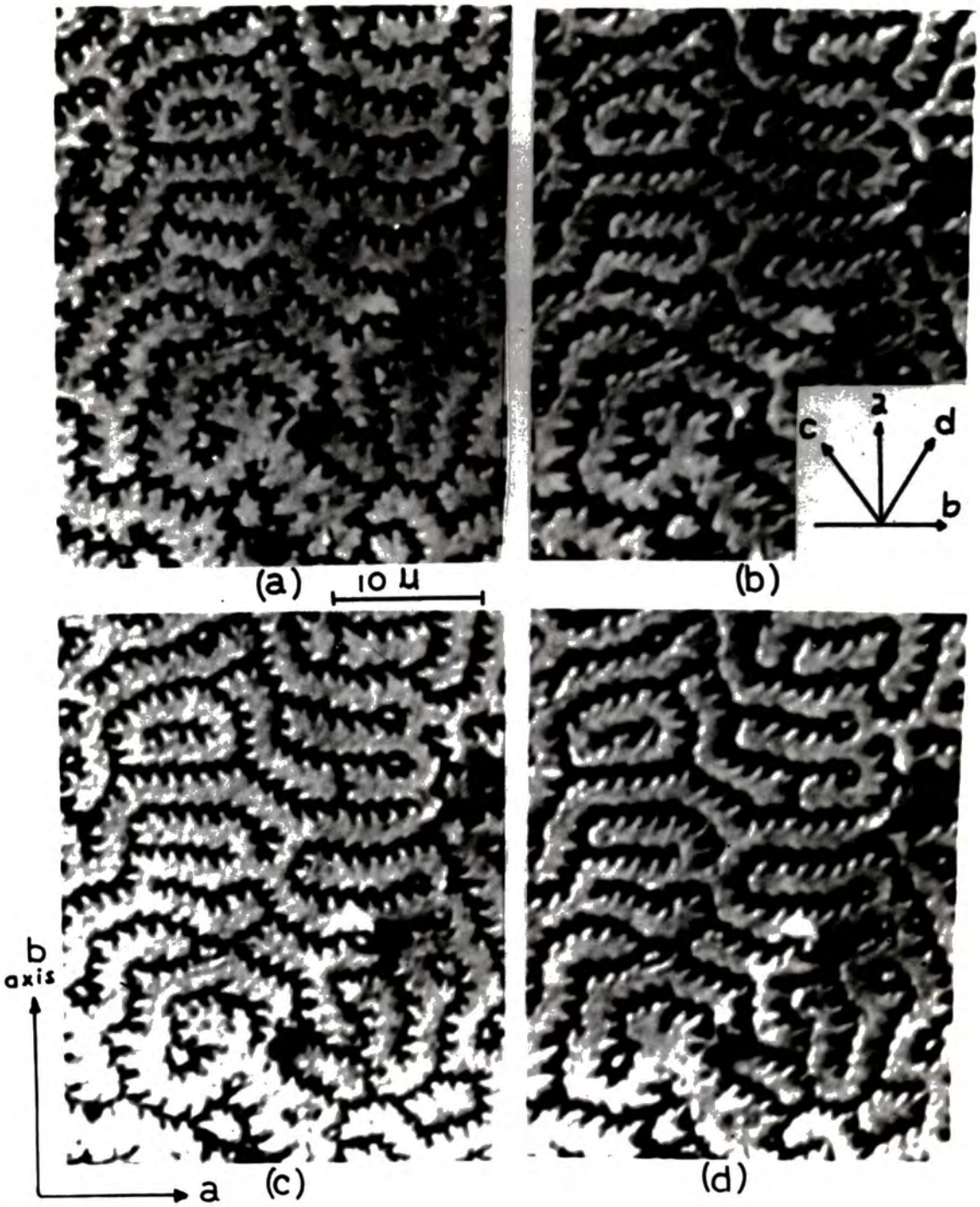

Fig. 5.11. (a-d) A series of patterns observed on Basal Plane showing the effect of rotation of the Magnetic field (300 Oe.). The direction of the applied field is indicated by the arrows.

of areas of free poles on the surface which selectively attract the polarised colloid. The end of reverse daggers are visible and there are also regions which do not collect colloid with either direction of magnetic field. These may be regions with magnetization parallel to the surface (closure structure) this is shown in Fig. 5.10(a,b).

5.5.3 Effect of the rotation of the field on the basal plane structure

The application of a magnetic field of about 300 Oe parallel to the surface would not be expected to produce any change in the main domain configuration on the basal plane but it might be expected to produce changes in the closure structures since the basal plane is magnetically isotropic at 274°K. Fig. 5.11(a-d) shows how the structure changes as a field of 300 Oe was applied parallel to the surface. There are changes in the orientation of the fine structure, but the general pattern remains unchanged.

5.6 Behaviour of Patterns at Lower Temperature

5.6.1 Surface containing C-axis

With the decreasing temperature, the anisotropy constant decreases rapidly and k_1 changes sign at about 245°K as shown in Fig. 5.1. As a result of this a drastic reorientation of domains takes place. The effect of reducing the temperature on the patterns on a $\langle 11\bar{2}0 \rangle$ plane is shown in Fig. 5.12(a-d). As the temperature falls the walls become

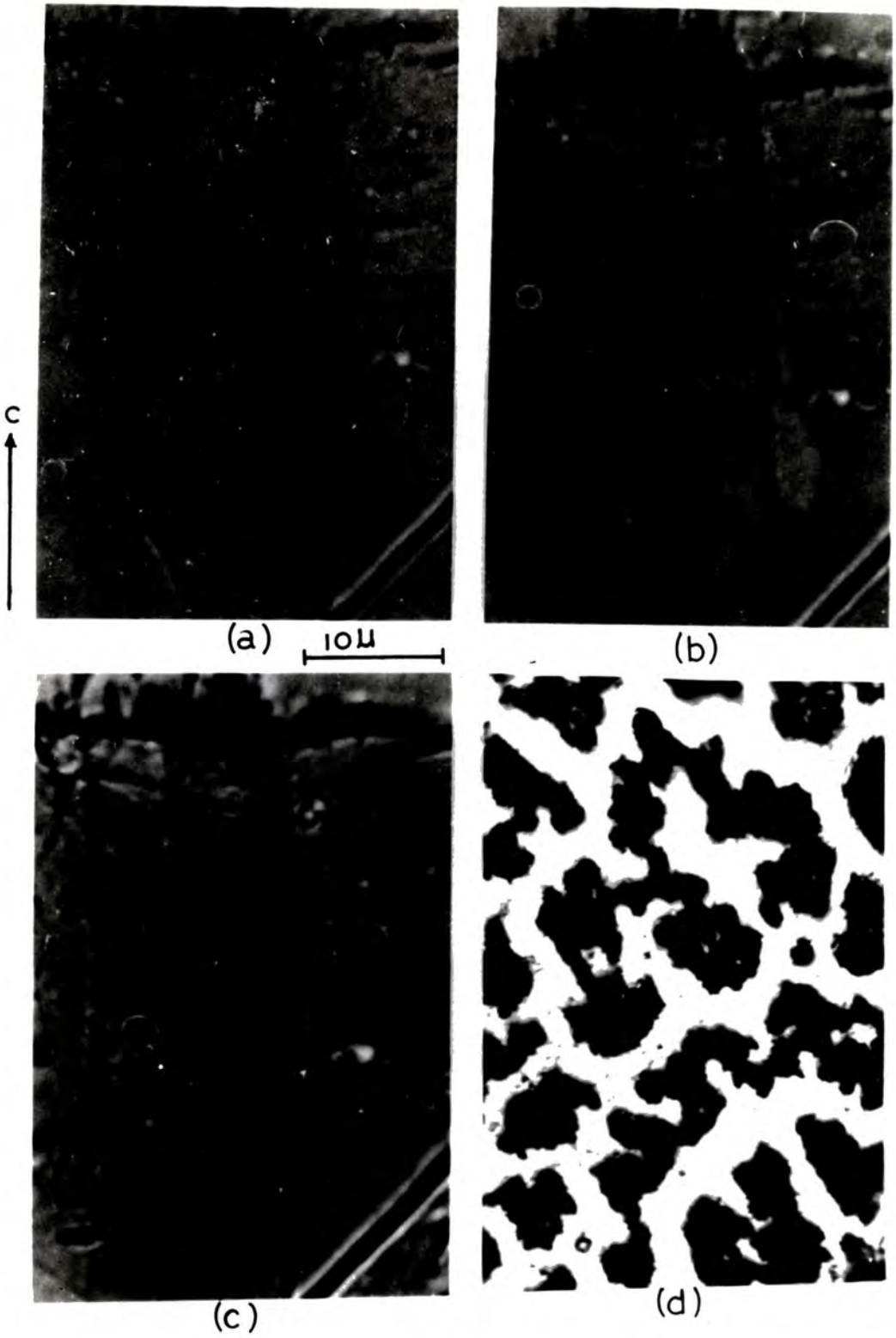

Fig. 5.12. (a-d) Effect of Temperature on Patterns observed on $\langle 11\bar{2}0 \rangle$ surface.

a- 270°K, b- 260°K, c- 250°K, d- 130°K (dry colloid)

less well defined and disappear completely at 240°K. Some wall motion takes place, but this is probably restricted by the presence of impurities. A limited degree of movement can be seen to have taken place in Fig. 5.12c. When the temperature falls below 240°K a new type of structure would be expected owing to the rotation of the easy direction away from the c-axis Fig. 5.2. A definite and repeatable pattern, such as that shown in Fig. 5.12d at 130°K is observed and a similar type of pattern was obtained at lower temperatures down to that of liquid nitrogen. These patterns were obtained by using a dry colloid technique. It is difficult to interpret such patterns and it is not clear if such observed patterns represent a true magnetic domain or just patterns resulting from the cooling of the specimen since the thermal expansion of pure gadolinium may be expected to be different from that of other impurities included in the specimen. This may give rise to a strain which may considerably modify the magnetic domain structure.

5.6.2 On basal plane

The behaviour of the basal plane pattern at low temperatures can be seen at Fig. 5.13(a-c). When the temperature is reduced from 274°K to 250°K the basal pattern becomes less well defined. At first the colloid-free region reduces in size and then the pattern becomes less definite, though it retains the general characteristics of the initial

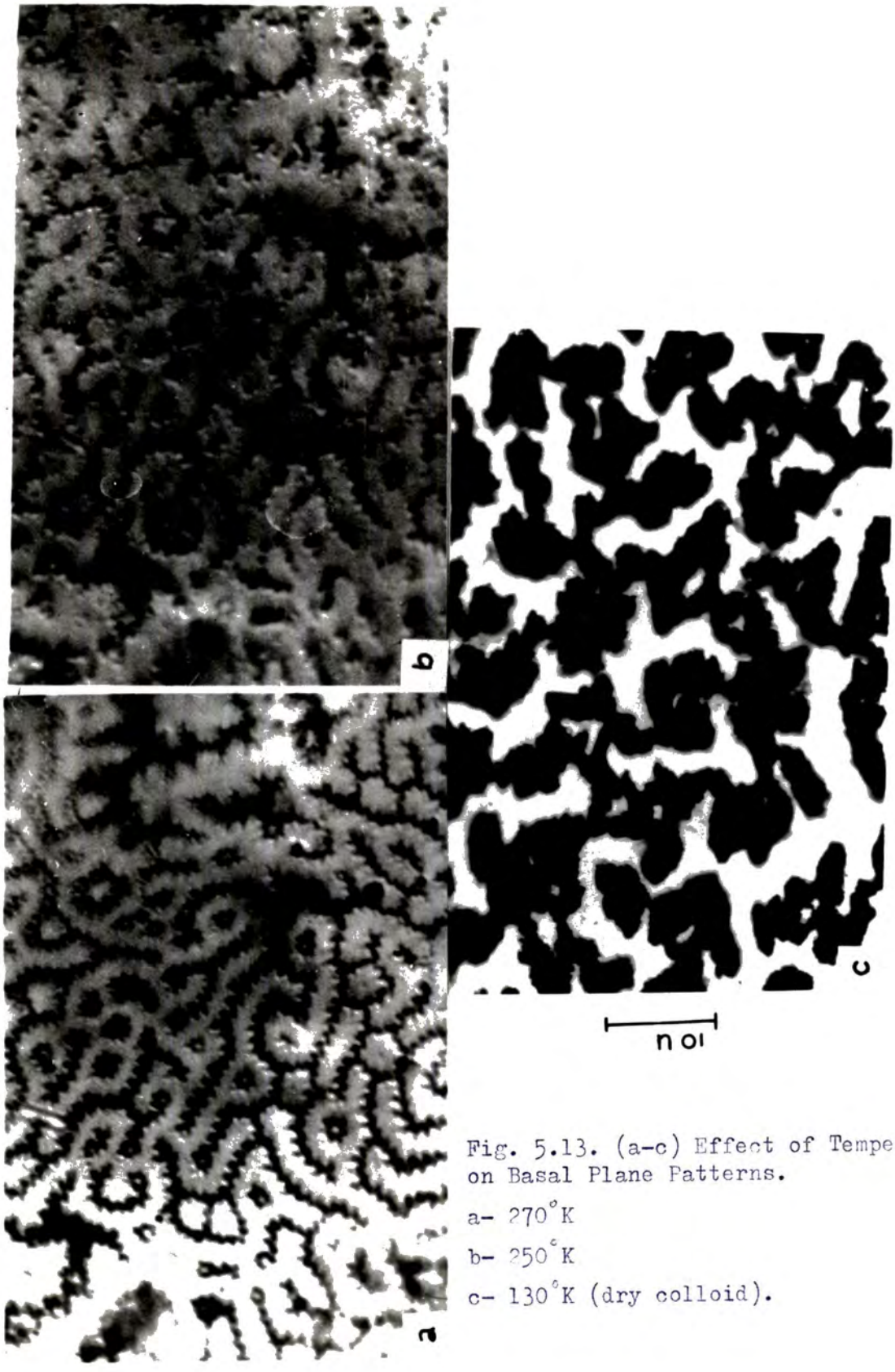

Fig. 5.13. (a-c) Effect of Temperature on Basal Plane Patterns.

a- 270°K

b- 250°K

c- 130°K (dry colloid).

pattern. Below 250°K patterns are difficult to observe owing to the rapid decrease in the anisotropy. When the region of conical magnetization is reached repeatable patterns can again be obtained. They have the same characteristics as those obtained on <11$\bar{2}$0> surfaces at the same temperature, a typical example being shown in Fig. 5.13c. It may again be said that these low temperature patterns are the result of thermal stresses due to cooling of the sample and perhaps a result of the differential thermal expansion of the metal and the oxide inclusions.

5.7 Variation of domain width with the specimen thickness

The complexity and the width of the domain structure in gadolinium is a function of the specimen thickness as in the case of other uniaxial ferromagnetic materials. Due to the presence of oxide inclusions in the gadolinium metal in the form of small sheets distributed inside the bulk material a layer of pure gadolinium may be sandwiched between one of these inclusions and the specimen surface. This might be considered as a film of varying thickness and the structure observed on the surface will depend on the thickness of this layer. To show that the variation of the pattern on the basal plane is due to the thickness change another experiment has been performed where the same region on the surface could be followed. Two pieces of set mounting materials were cut of identical shape. One

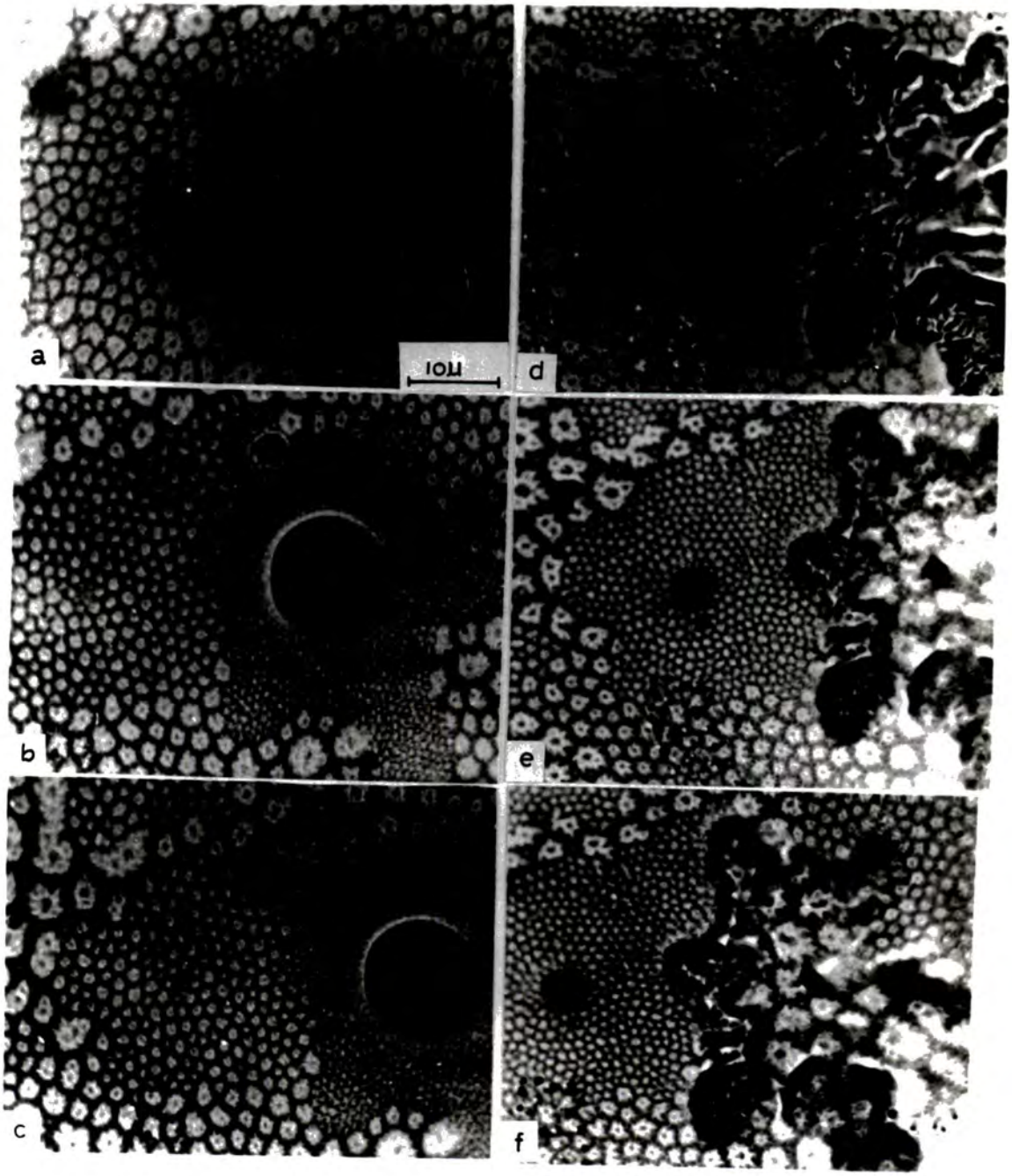

Fig. 5.14. (a-f) Series of Patterns on Basal Plane after successive layers of Gadolinium have been removed (dry colloid), at 274 K.

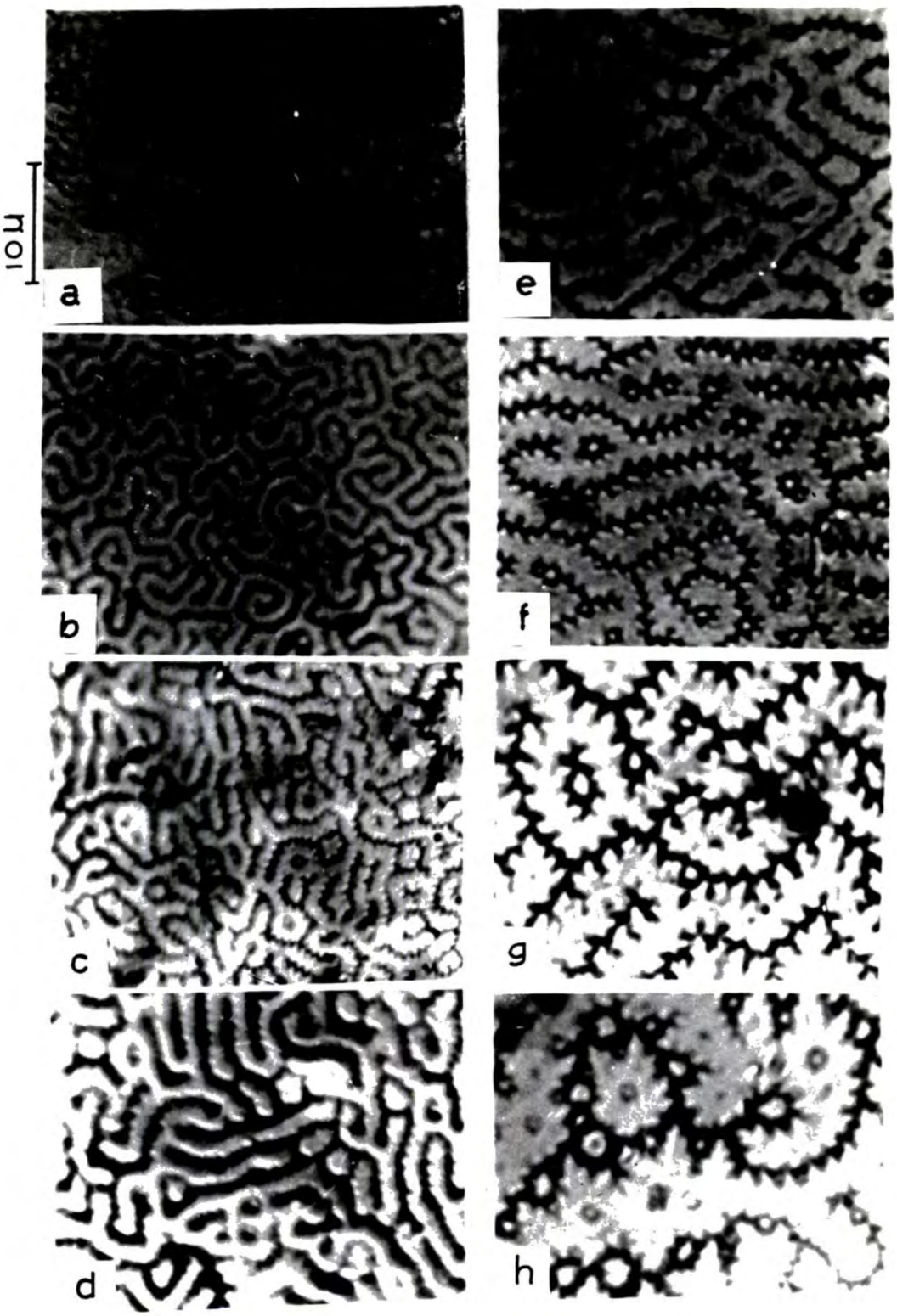

Fig. 5.15. (a-h) The variation of The Domain width with the Crystal thickness, the thickness increases progressively from a to h, 274°K.

piece was placed on the microscopic moving stage and had 3 pins mounted in it. These pins located in three corresponding holes in the other piece of mounting material in which was mounted the specimen (this mount was thinner than the specimen thus exposing part of the specimen for cooling purposes). By matching the pins to the holes the same position of the specimen under the microscope could always be achieved and the same region of its surface be seen for study. Figs. 5.14(a-f) show a series of patterns obtained after successive layers of the pure gadolinium had been removed by chemical polishing. Finally the pattern disappeared completely when the oxide inclusion appeared over the whole region which had been covered by a pattern of uniform type. This is evidence that the variation of the domain on basal plane is due to change in the thickness of the materials. A selected area from the surface was chosen which showed the variation of the domain width with thickness is shown in Fig. 5.15(a-h). In a thin film the patterns consist of smooth domains without a surface structure. As the specimen thickness increases the walls divide forming spikes of reverse magnetization and closure domains and these may be divided further forming a very complicated structure. This situation is confirmed in Fig. 5.6. This is one form of the complex pattern which may be observed at the $\langle 11\bar{2}0 \rangle$ surface.

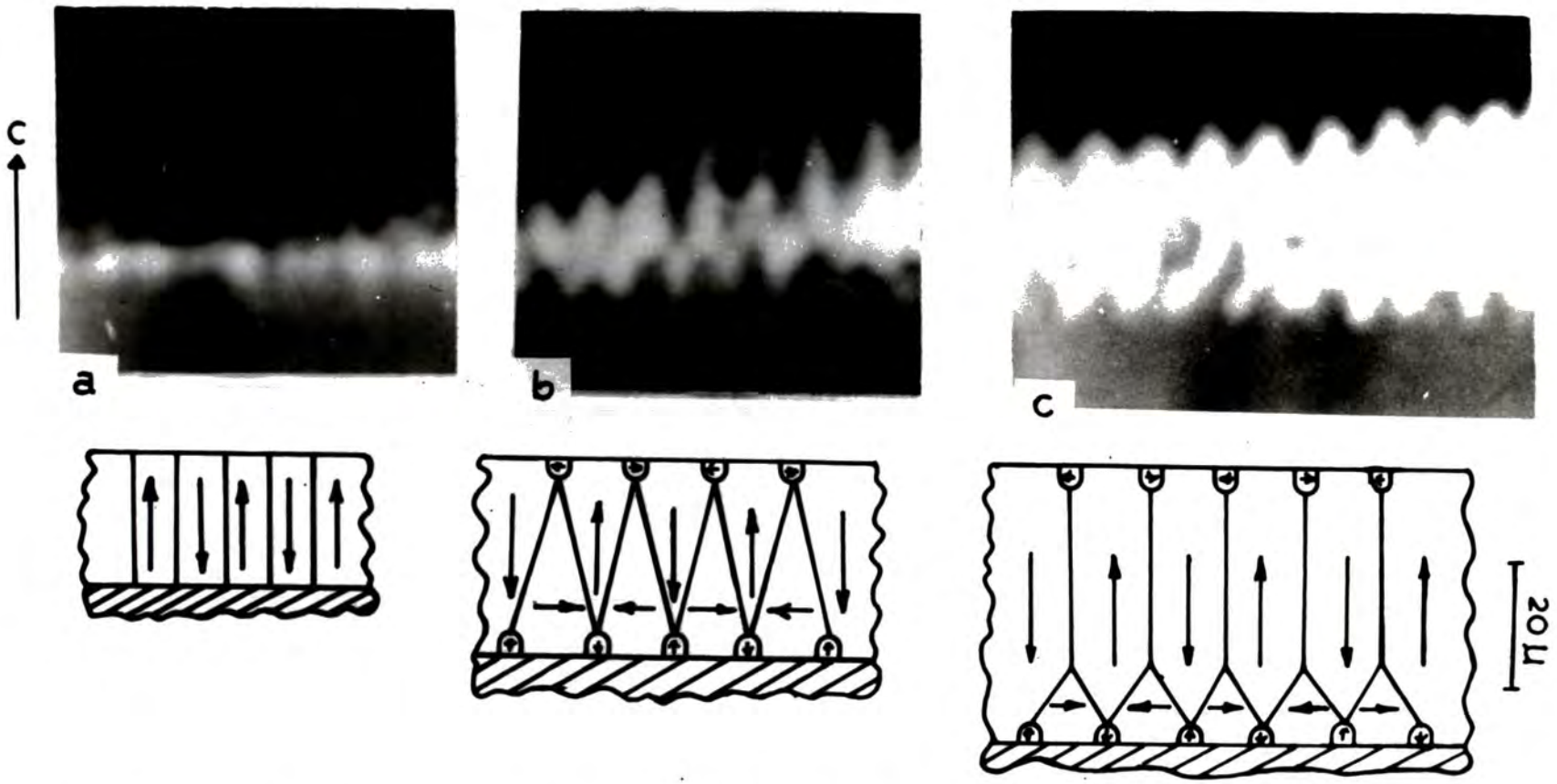

Fig. 5.16 (a-c) Modified Domain observed near the edge of $<10\bar{1}0>$ surface between layer of oxide inclusion and the specimen surface.

a - simple structure, b - intermediate structure, c - usual pattern observed on thick crystal.

(field 300 Oe. applied parallel to the C-axis)

Fig. 5.16(a-c) shows the pattern observed on a $<10\bar{1}0>$ surface near the basal plane where the inclusion separates the gadolinium metal in the form of a wedge shape, as shown schematically. The domain structure varies from a simple one Fig. 5.16a to a more complicated one as the thickness increases, Fig. 5.16c. An intermediate structure, Fig. 5.16b appears when the size of the domain region with magnetization perpendicular to the c-axis is comparable to the one with magnetization along the c-axis.

5.8 Honeycomb structure observed on Gd. single crystal

Honeycomb structures have been created and studied on various ferromagnetic crystals; on magnetoplumbite by Kaczer et al.(1961), on cobalt by Wyslocki et al. (1965), and on Mn_5Ge_3 crystal by Wrzeciono et al. (1966). The structures were dealt with as main domains running through the body of the specimen and not as merely superficial structures on a surface perpendicular to the c-axis. To create such a structure a field normal or parallel to the c-axis is needed, the magnitude of such a creation field is of a few thousand oersted dependent on the orientation of the specimen.

In the case of gadolinium it was found that a small field of the order of 100 Oe obtained from rod shaped permanent magnet produces a honeycomb structure. It was found that the same structure is obtainable with different lengths of the bar magnet giving fields of slightly

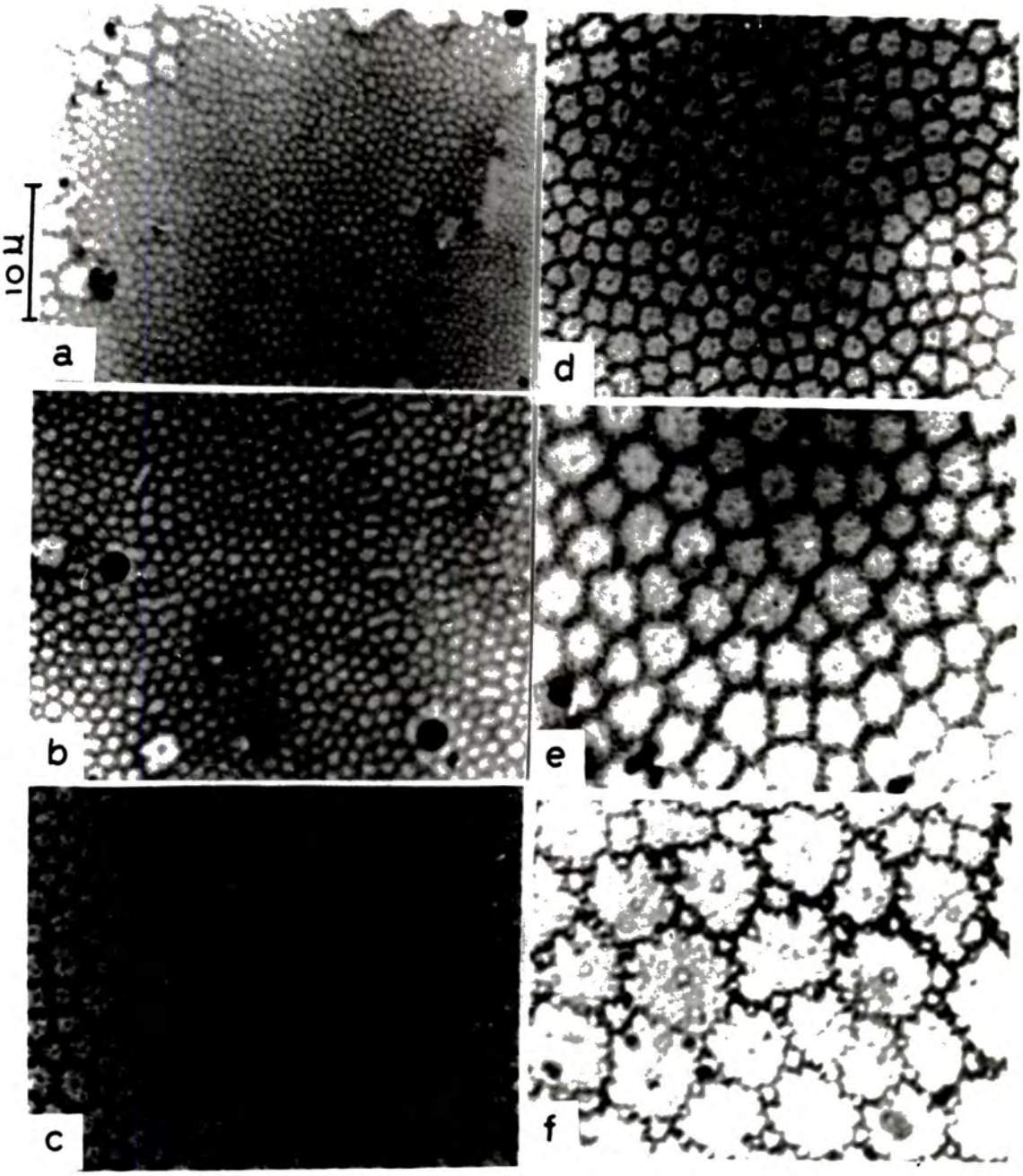

Fig. 5.17. (a-f) The variation of Honeycomb Domain width with Crystal thickness, the thickness increases progressively from a to f, at 274° K.

different magnitudes. Attempts were made to obtain such a pattern by applying to the surface a normal field produced by small electromagnets from zero up to a few hundred oersted. Only one type of domain, that is the typical domain shown before, were produced and there was no sign of honeycomb pattern. Though a field applied parallel to the basal plane has the same effect whether it originates from a permanent magnet or electromagnet, this structure may be created as a result of non-uniformity of the lines of force produced by the permanent magnets and since the spin directions within the closure domain are easily rotated with rotation of the field one would expect that a non-uniform field would accordingly create different patterns. Thus a field from a rod shape magnet created a hexagonal like structure. The honeycomb structure again is dependent on the crystal thickness as shown in Fig. 5.17(a-f). For small thicknesses the wall on the basal surface has the shape of hexagons but under a critical thickness this seems to be transferred to a cylindrical or rod shaped domain. With increasing thickness the domains grow and a surface structure begins to form and clear star shape patterns are formed. As the specimen thickness increases the domains grow further and the surface structure becomes more complicated and no longer looks like honeycombs. It seems that there is an intermediate structure as that obtained on the edge of $\langle 10\bar{1}0 \rangle$ surface. Fig. 5.18 shows a pattern obtained on basal plane with lower magnification.

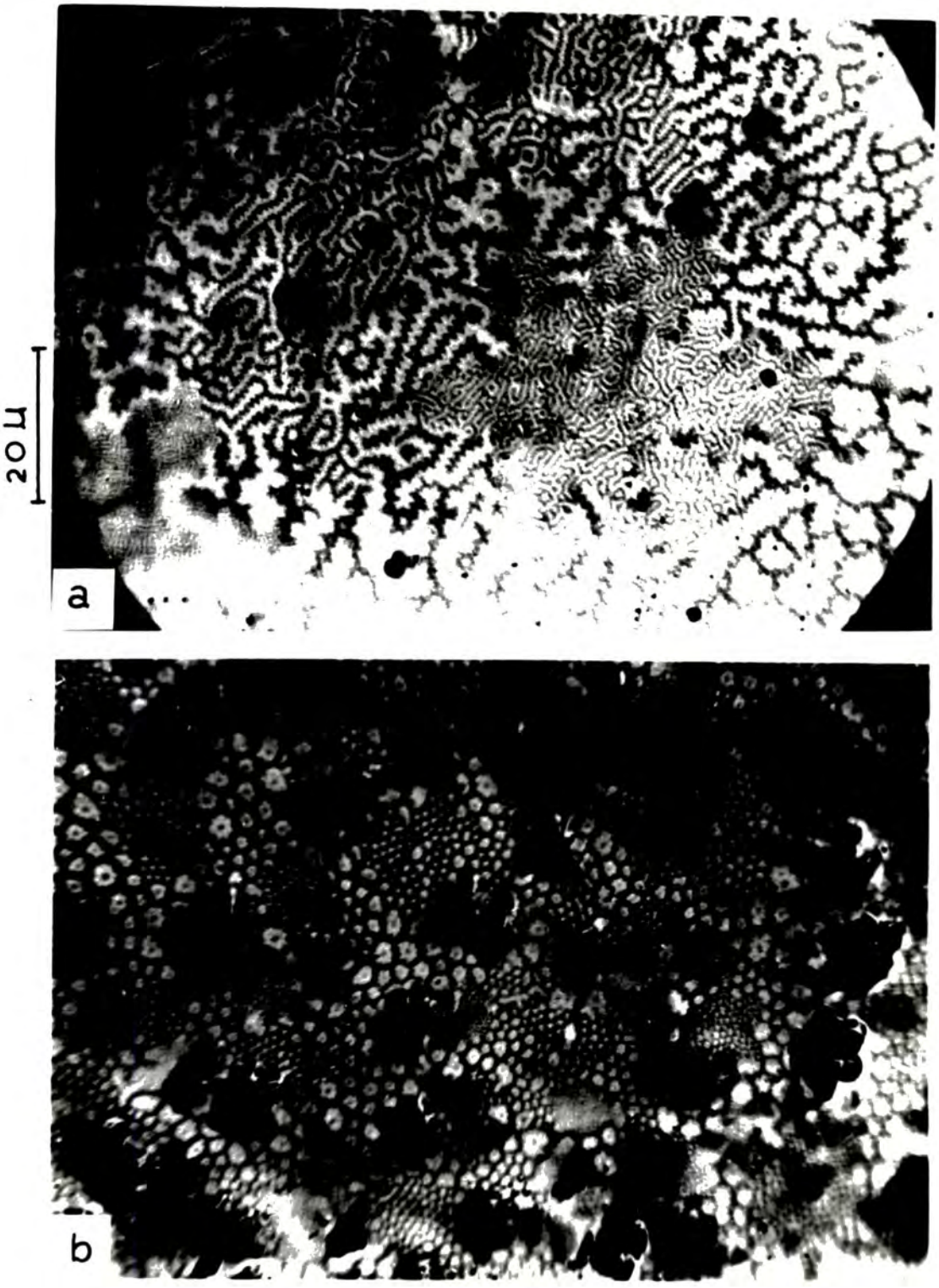

Fig. 5.18. Pattern on Basal Plane of Gadolinium observed at 274°K with field applied normal to the surface.

a- 300 Oe. from electromagnet.

b- 300 Oe. from permanent magnet.

5.9 Discussion

It was observed that when two surfaces in a gadolinium crystal each containing the c-axis were cut perpendicular to each other, both surfaces exhibited a structure of parallel 180° domain walls and the internal structure must therefore consist of arrays of 180° domains. These are not of a simple plane-parallel form, but of a wavy one as is shown by the form of the basal plane patterns. The wall of such a domain might not intersect a surface containing a c-axis but could be closed within the body of the specimen and this might contribute to the complexity of the structure on the basal plane. This type of domain structure has a lower energy than the checker board array. The problem has been discussed by Goodenough (1956); who showed that the wall area associated with the checker board array is considerably reduced without an appreciable increase in the surface pole energy if the corners are rounded. Then accordingly the total surface energy will decrease. Examining the edge of the $\langle 11\bar{2}0 \rangle$ surface near the basal plane it was possible to observe the structure of the closure domains. These consist of very small regions magnetized in a direction normal to the easy axis (c-axis). They grow mostly in those places where the stray field is large and make a smooth region for the transition of the magnetization from one domain to the other of opposite magnetization. Those closure domains will eliminate completely the effect of the free

poles at the places where they were produced and in turn reduce the magnetostatic energy, however, they will contribute to the magneto-crystalline anisotropy energy term. As can be seen from the photograph the closure domains are surrounded by an area of free poles. As a consequence of this a sub-division of these areas into smaller regions of different polarity will take place and spikes of reverse magnetization may form in order to reduce the density of the free poles at the surface which in turn will lower the magnetostatic energy. The spikes usually grow in the middle of domains where the surface charges have maximum demagnetization effect. The behaviour of the domain structure on the basal plane of a gadolinium crystal under the influence of magnetic field is also a good evidence of the presence of both closure and free pole effects. When field normal to the basal plane surface was applied into the paper and then reversed the dark bands on reversal of the field became the light bands showing that such a pattern is one of free poles at the surface. However, careful examination of the pattern on the surface reveals that some areas are not affected by reversal of the field and others are completely unresponsive to normal field. That is, some areas are not covered with colloid and those will change direction as a magnetic field parallel to the surface is rotated. Such a region clearly indicates an involvement of magnetization other than that parallel to the c-axis.

For gadolinium at 274^{o}K the magnetoelastic contribution may be neglected as it amounts to only about 1% of the total free energy. So

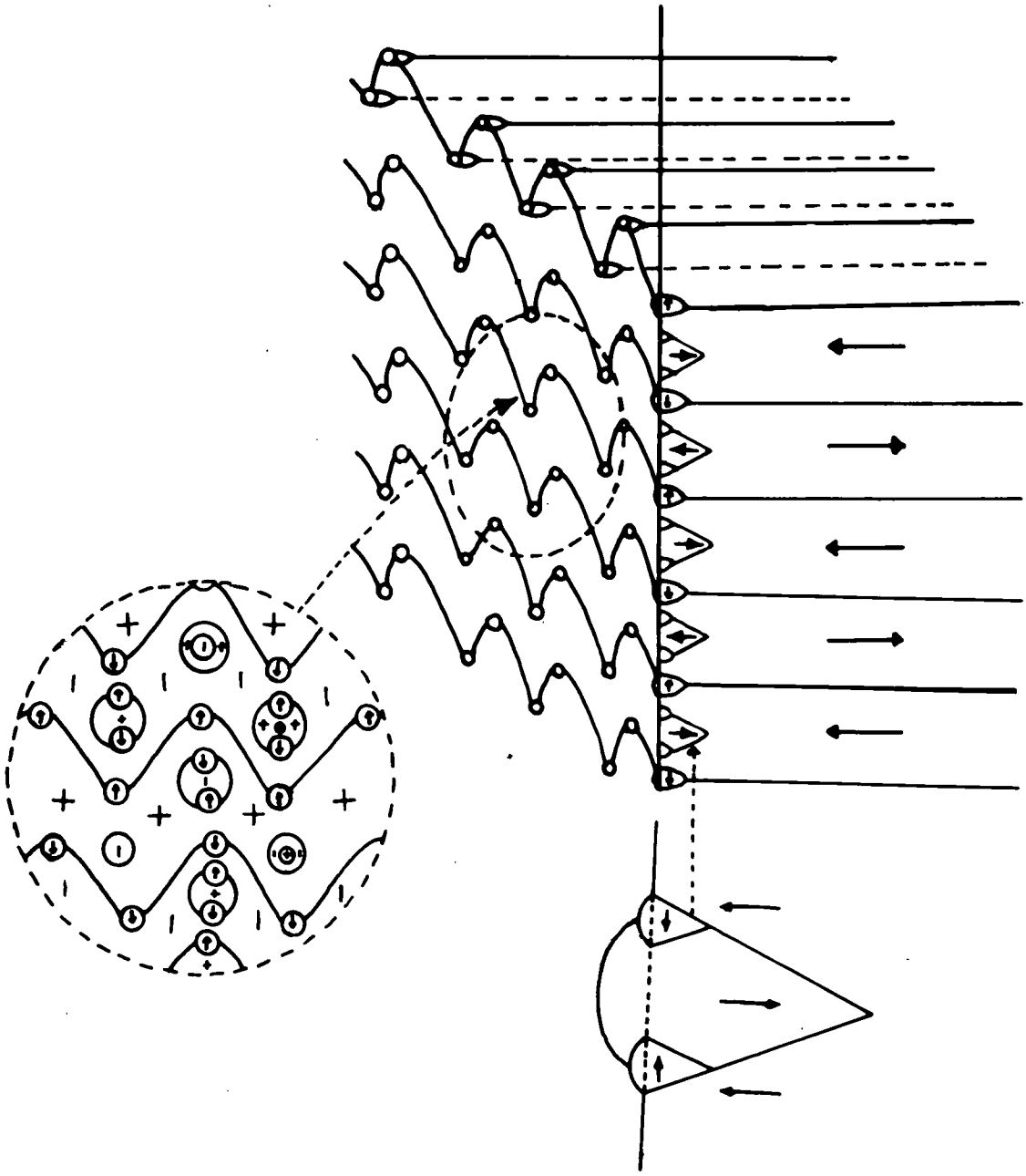

Fig. 5.19. Model representing the Domain structure on a Gadolinium single Crystal.

the value of the magnetostrictive energy will contribute very little to the total energy. The value of P is 0.28 compared to that in Cobalt at 274°K P ≃ .98. So it is reasonable to assume that closure domains and surface free poles will be present. Thus in gadolinium the surface structure consists of a mixed state. A representation of the different types of structure is given in Fig. 5.19. Gemperle et al. (1963) assumed a similar model for the surface structure of Cobalt at room temperature. Estimation of the energies involved in such a model is extremely difficult.

Creation of a honeycomb structure by the application of a normal field produced by a permanent magnet to the basal plane is not fully understood, but it could be due to the non-uniformity of the field. Though this type of structure has higher energy compared to the simple plate like structure, the change in thickness of the sample produced change in the honeycomb structure as observed on other uniaxial materials. This shows that the structure is the main body domain rather than a superficial pattern. It is believed that there are still regions of closure structure with magnetization parallel to the basal plane existing between the hexagonal structure but these regions disappear as the thickness of the specimen is reduced.

The presence of closure structures with magnetization different from that of the c-axis may contribute to the anomalies which appeared in the measurements of magnetization of Belov et al. (1962).

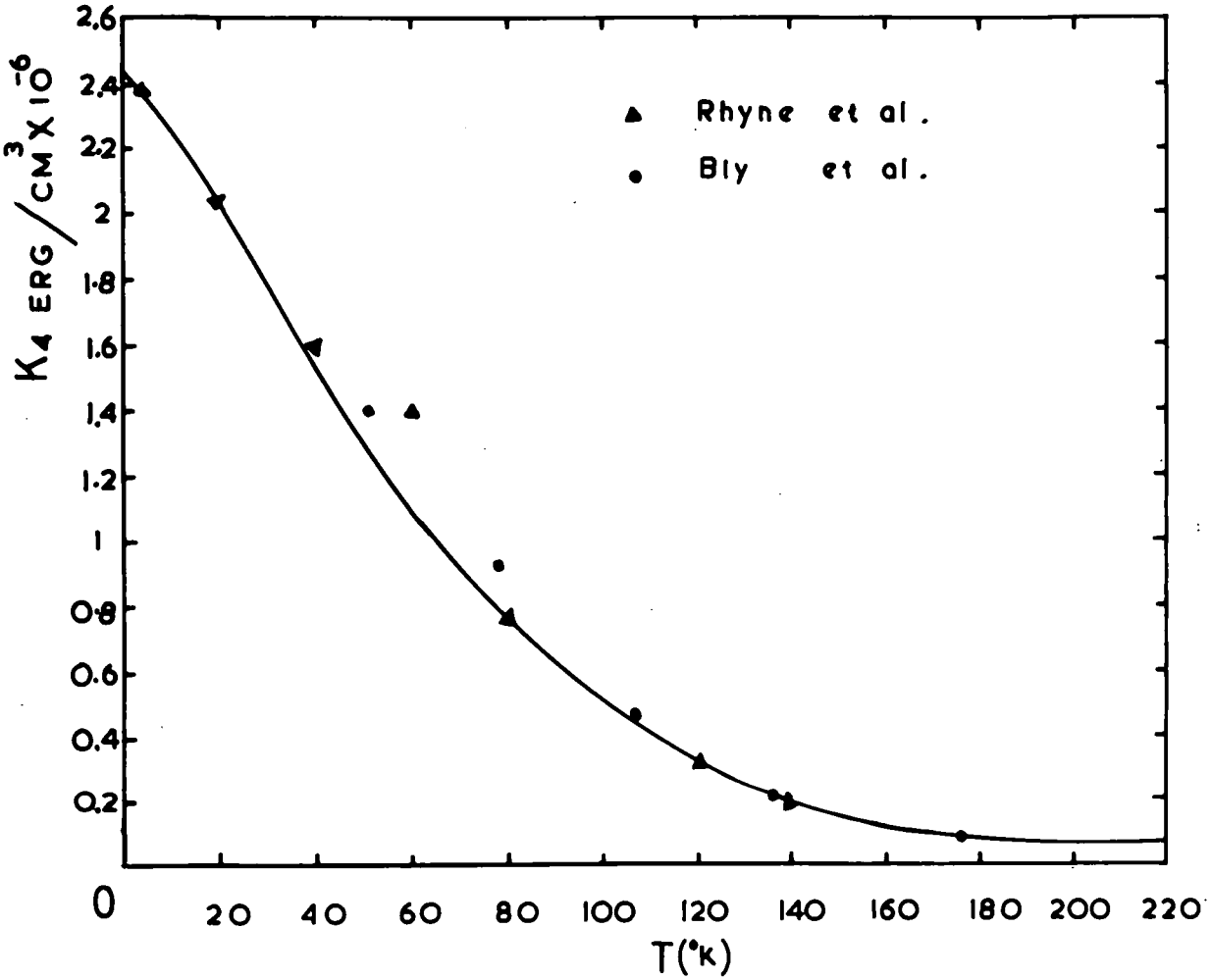

FIG. 6.1 Variation of Basal Plane Anisotropy K_4 with Temperature for Terbium.

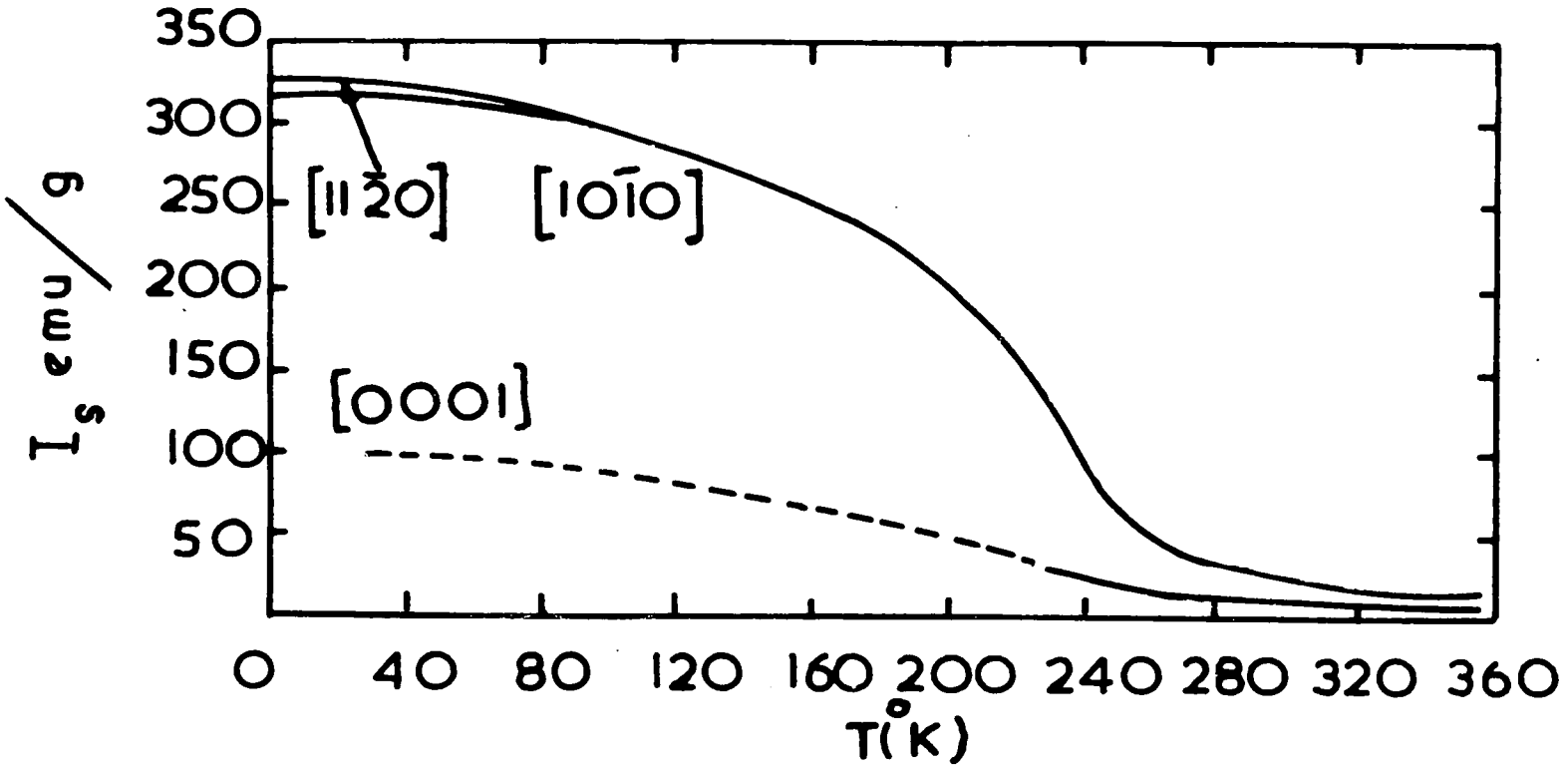

FIG. 6.2 Variation of Magnetization with Temperature for Terbium at 18KOe.

CHAPTER 6

DOMAIN STRUCTURE OF TERBIUM SINGLE CRYSTALS

6.1 Introduction

Terbium follows gadolinium in the heavy rare earth group, having properties similar in many ways to those of gadolinium. However, Terbium exhibits antiferromagnetism in the range of temperature 228°K to 222°K. Unlike gadolinium it has a high uniaxial anisotropy which strongly favours magnetization in the basal plane. In this plane there is a smaller anisotropy which favours magnetization along the b-axis. The value of basal plane anisotropy constant k_4 varies from 2.4×10^6 erg/cm^3 at 4°K to about 2×10^5 erg/cm^3 at 140°K while the uniaxial anisotropy constant k_1 changes from 5.5×10^8 erg/cm^3 at 411°K to 1.4×10^8 erg/cm^3 at 205°K. The anisotropy data have been reported by Rhyne et al. (1967) and Bly et al. (1968) and the variation of k_4 with temperature is shown in Fig. 6.1. Hegland (1963) reported on the magnetization data and Fig. 6.2 shows magnetization as a function of temperature. It is clear that there will be no rotation of magnetization to any direction other than the basal plane except for high applied fields, that is the easy direction remains in the basal plane and favours the $[10\bar{1}0]$ direction.

There has been no previous report of domain structure on Terbium and this is probably due not only to involvement of oxide in this metal

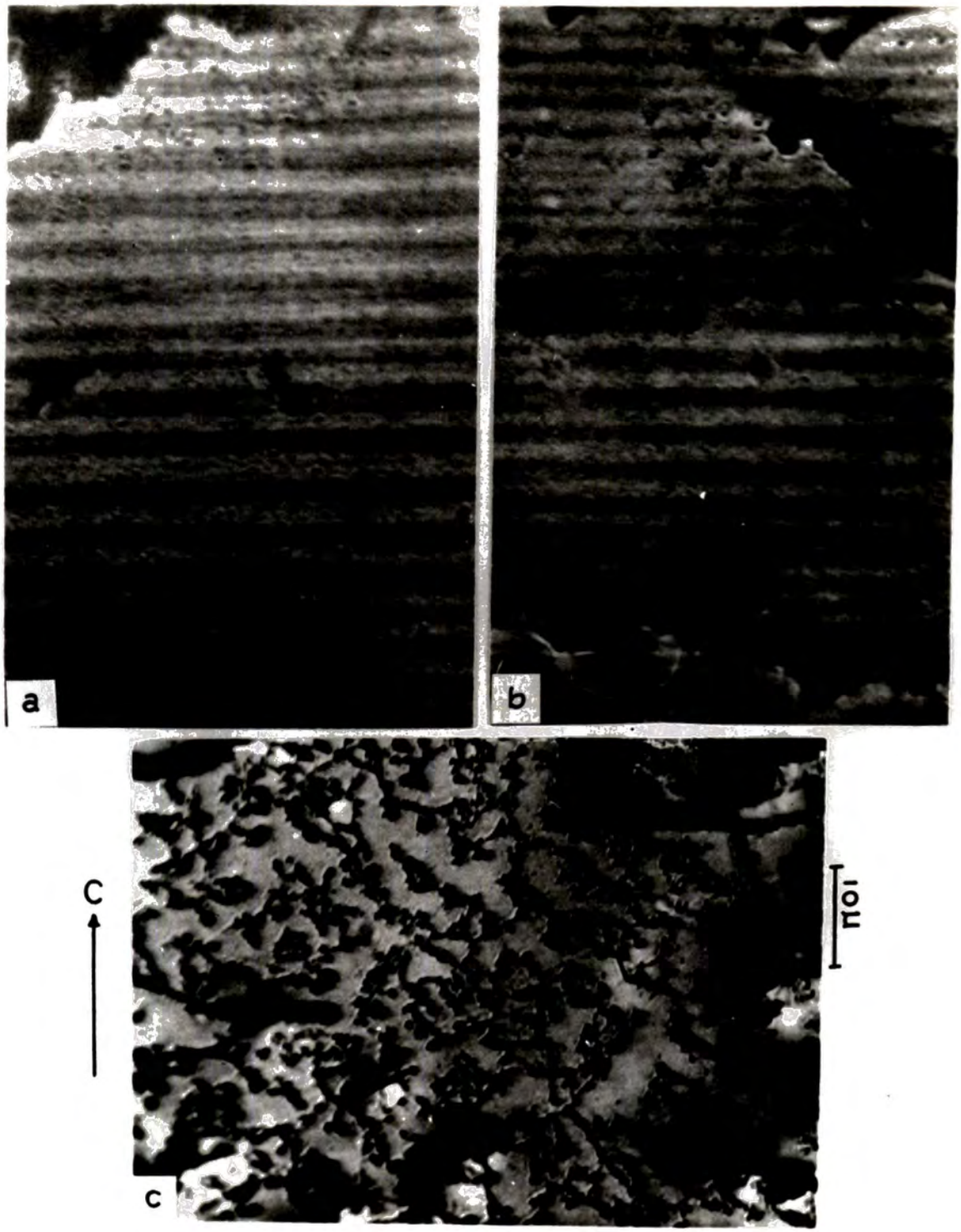

Fig. 6.3. (a-c) Domain pattern observed on Terbium single crystal (dry colloid)

a- on $\langle 11\bar{2}0 \rangle$ surface at 210°K.
b- on $\langle 10\bar{1}0 \rangle$ surface at 210°K.
c- on $\langle 11\bar{2}0 \rangle$ surface at 130°K.

but also to the Curie temperature being much below room temperature (T_c = 222°K).

6.2 Present work

Even though the Terbium specimen has been purified by the method of solid state electrolysis it was not possible to obtain as good a specimen as that of gadolinium. The oxide had not aggregated to form plates with the c-axis normal to their surface as in the case of gadolinium. There were still large amounts of inclusion in the form of small particles distributed all over the specimen except in a few regions where the surface was mirror like and where the domain structure of Terbium could be easily observed.

Observation of the domain structure was carried out using the dry colloid technique (evaporation of iron in a Helium atmosphere of 0.2 torr.). Attempts using a colloid suspension in secondary butyl alcohol as described in Chapter two, proved unsuccessful. No pattern was observed using dry colloid at 210°K but by applying a small field of the order of 150 Oe normal to the surface under investigation, a clear pattern was observed on both $\langle 11\bar{2}0\rangle$ and $\langle 10\bar{1}0\rangle$ surfaces. The results are shown in Fig. 6.3(a,b). Both surfaces show a plate like domain structure. Examination of the basal plane did not reveal any type of structure. An intensive investigation at 210°K was carried out in order to find

out if there are any closure structure present (structures magnetized in a direction other than the [10$\bar{1}$0] direction). Both the <11$\bar{2}$0> and <10$\bar{1}$0> surface show no such structure and this is not surprising since the anisotropy of Terbium is very high and any magnetization along the hard direction will involve a large anisotropy energy contribution to the total energy of the system.

6.3 Pattern at Lower temperature

As the temperature was lowered it became more difficult to obtain a satisfactory pattern even at 190°K. From 190°K down to 77°K a pattern like that shown in Fig. 6.3c was obtained. Whether or not this represents a domain pattern is not yet clear. It is most probably a strain pattern like those obtained on gadolinium at low temperatures, even though the pattern obtained on gadolinium at 130°K is different in nature from that obtained at the same temperature on Terbium. The difference in the two strain patterns may be due to the fact that in gadolinium the magnetization direction rotates from the c-axis to a cone of easy magnetization while in Terbium the magnetization always lies in the basal plane.

6.4 Discussion

Terbium has a preferred plane of magnetization. On the basis of this, assumptions may be made about the domain configuration. Kazer (1962)

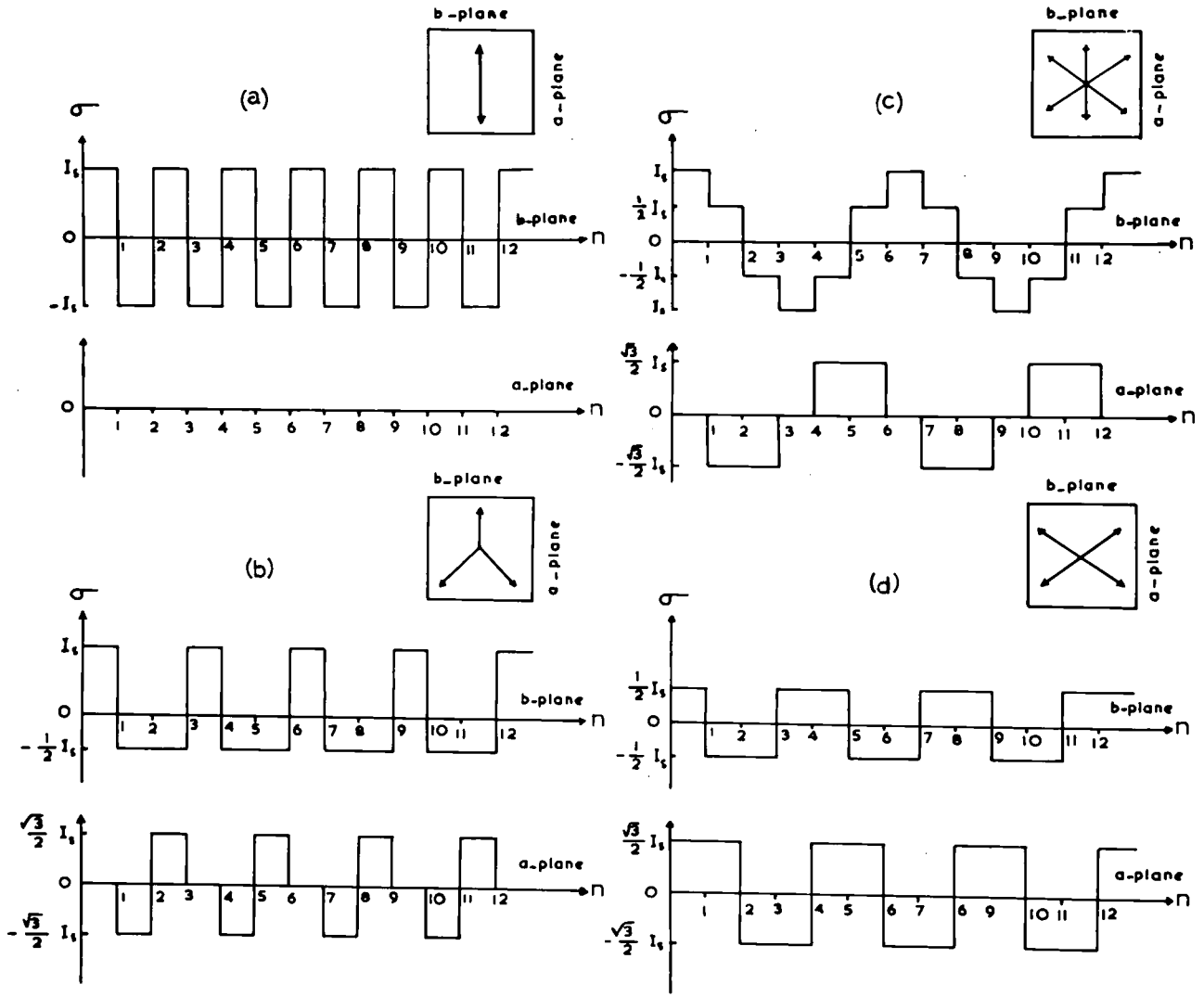

FIG. 6.4 POSSIBLE CONFIGURATION OF FREE POLE DENSITY σ ON a AND b PLANE OF A CUBE SHAPED TERBIUM SINGLE CRYSTAL. n IS THE NUMBER OF DOMAIN LAYERS.

proposed two possibilities for an infinite cylinder with an easy direction laid in the basal plane and non vanishing basal plane anisotropy ($k_4 \neq 0$). These are shown in Fig. 1.4b.

The sample of Terbium dealt with in this work is very nearly cubical with dimensions x = 0.257 cm., y = 0.302 cm., and z = 0.242 cm. There are several different possibilities for the domain configuration of a cube with easy plane of magnetization and $k_4 \neq 0$ these are -

1. When the magnetization lies along only one of the b-axes, as shown in Fig. 6.4a. The free pole density which appears on the surface is $I_s \cos\theta$ where $\theta = 0$ or 180° so $\sigma = \pm I_s$. The total energy of such a model is easily calculated since the structure simply represents a Kittel type configuration with free poles on a $\langle 10\bar{1}0 \rangle$ surface. While $\langle 11\bar{2}0 \rangle$ surface has a div $\vec{I} = 0$.

2. The second possibility is the one in which the magnetization rotates from one domain to the next by an angle $\theta = 120^\circ$, thus there will be free poles appearing on both $\langle 10\bar{1}0 \rangle$ and $\langle 11\bar{2}0 \rangle$ surfaces and and free pole distribution will look like the one represented in Fig. 6.4b.

3. In this possibility the easy direction of magnetization forms a six-fold symmetry and the rotation of magnetization from one domain to the next will be through $\theta = 60^\circ$. The distribution of free poles will be of the type represented in Fig. 6.4c.

4. Here the magnetization lies along two of the b-axes, but not along the axis perpendicular to surface under study. Such a structure will reduce the densities of the free poles. The walls will be a mixture of 60° and 120°. The distribution of free polarity is shown in Fig. 6.4d.

Observations on the Terbium single crystal cut with $\langle 10\bar{1}0 \rangle$ and $\langle 11\bar{2}0 \rangle$ surfaces perpendicular to each other show that a structure of the type shown in Fig. 6.4a is not probable since the patterns on both a - and b - planes show similar domain structure with approximately the same spacing. If the Fig. 6.4a structure were present one would expect to see alternate dark and light strips on the b-plane and separate domain boundaries on the a-plane.

The structure shown in Fig. 6.4b would give rise to alternating light and dark strips on the b-plane while in the a-plane there would be strips which collected no colloid under any condition.

The observed structures could not be accounted for by a structure of the type shown in Fig. 6.4c. It would give rise to different distributions of free pole density on the a- and b-planes, but there would be regions on the a-plane which never collected colloid. There is little visual evidence for this from Fig. 6.3. A calculation of the energy of such a structure has been carried out by Kazer for an infinite cylinder with axis parallel to the crystallographic c-axis. Though the boundary conditions are different for the sample used here the calculation

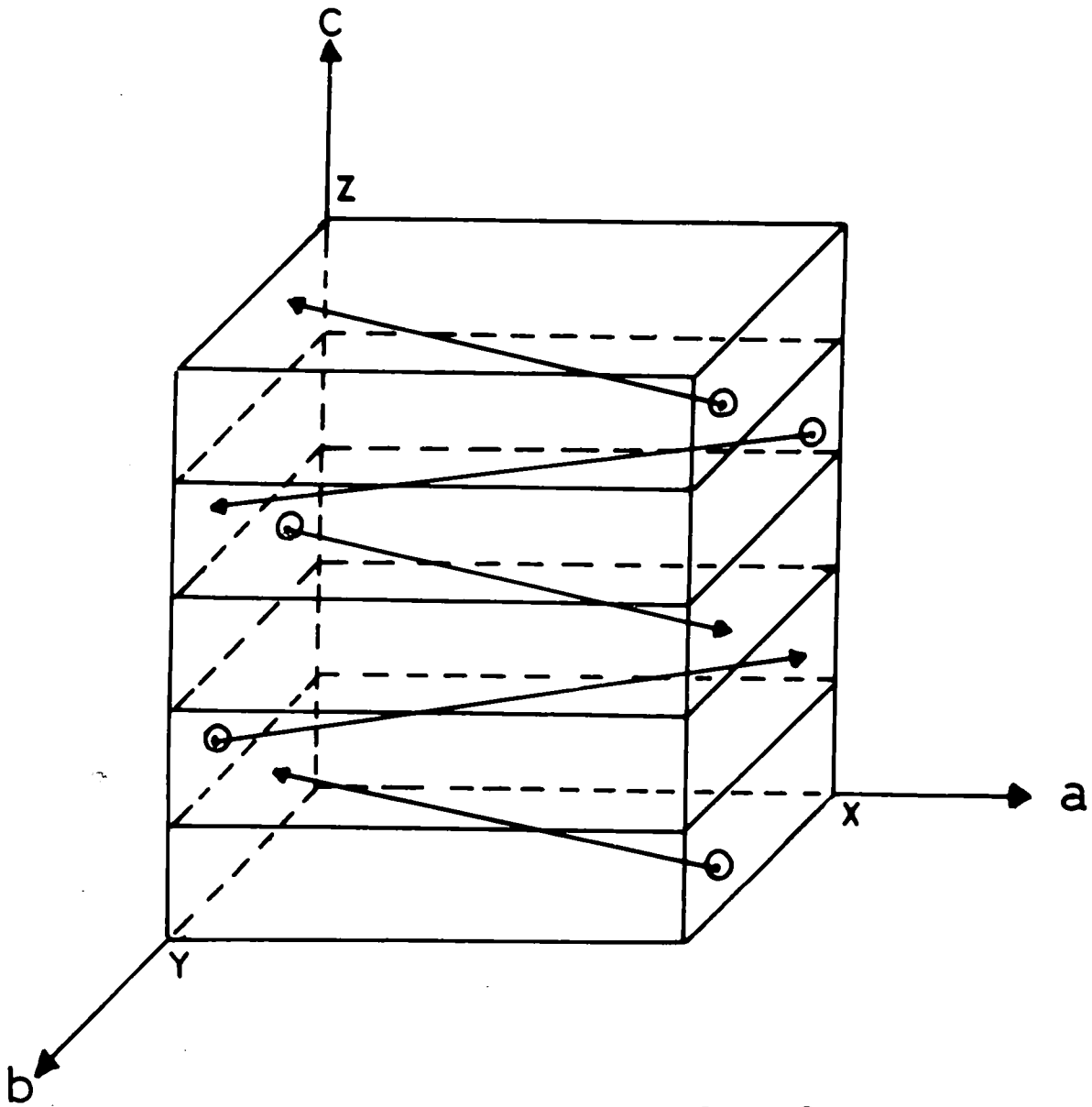

FIG. 6.5 Domain Structure of a Cube Shaped Terbium Single Crystal.

used in principle be repeated for the appropriate geometry.

A structure of the type illustrated in Fig. 6.4d could accord well with the domain patterns shown in Fig. 6.3 and calculations of the domain spacing and energy density have been made for this model.

6.5 Energy calculation

An estimate will be made of energy involved in the model shown in Fig. 6.5 where there is a mixture of domain walls of 120° and 60° type. The energy expression for this model contains terms representing the magnetostatic energy and the wall energy.

The magnetostatic energy due to the free poles on both $\langle 11\bar{2}0\rangle$ surfaces (a-planes) is

$$E_m = yz \cdot 1.7 \left(\frac{\sqrt{3}\, I_s}{2}\right)^2 \cdot 2D \quad \ldots\ldots\ldots\ldots (6.1)$$

The magnetostatic energy due to the free poles on both $\langle 10\bar{1}0\rangle$ surfaces (b-planes) is

$$E_m = xz \quad 1.7 \left(\frac{I_s}{2}\right)^2 \cdot 2D \ldots\ldots\ldots\ldots\ldots (6.2)$$

equal numbers of 60° and 120° walls are present in this model. Thus the wall energy is

$$E_w = \frac{xyz}{2D} \quad (\gamma_{60} + \gamma_{120}) \ldots\ldots\ldots\ldots\ldots (6.3)$$

Assuming that the γ_{120} (the wall energy of 120° wall) is $\frac{1}{3}\gamma_o$, where γ_o is the energy of a 360° wall, and γ_{60} (the energy of a 60° wall) is $\frac{1}{6}\gamma_o$.

Then $$E_w = \frac{xyz}{2D}\left(\frac{\gamma_o}{6} + \frac{\gamma_o}{3}\right) \quad \text{.....(6.4)}$$

The total energy thus

$$E_{total} = xz\ 0.85\ I_s^2\ D + 3yz\ \ 0.85\ I_s^2\ D + \frac{xyz}{4D}\ \gamma_o \text{....(6.5)}$$

The total energy per unit volume is

$$\frac{E_{total}}{V} = \left(\frac{.85\ I_s^2}{y} + \frac{2.55\ I_s^2}{x}\right) D + \frac{\gamma_o}{4D} \quad \text{.....(6.6)}$$

minimizing obtained for domain width

$$D_o = \left\{ \frac{\gamma_o}{3.4\ I_s^2 \left(\frac{1}{y} + \frac{3}{x}\right)} \right\}^{\frac{1}{2}} \quad \text{.....(6.7)}$$

substitute $\gamma_o = 8\sqrt{A\ k_4}$

where A is the exchange constant and k_4 basal plane anisotropy.

So $$D_o = \frac{2}{I_s}\left\{ \frac{xy\sqrt{A\ k_4}}{1.7\ (x + 3y)} \right\}^{\frac{1}{2}} \quad \text{.....(6.8)}$$

The minimum energy per unit volume is

$$E_o = 2\ I_s \sqrt{\frac{1.7(x+3y)}{xy}}\ \sqrt{A\ k_4} \quad \text{.....(6.9)}$$

Insert the value for

$$x = 0.257 \text{ cm}, \quad y = 0.302 \text{ cm}.$$

$$A = \frac{2k\ T_c}{a_o}$$

where Boltzmann constant $k = 1.38 \times 10^{-16}$ erg/deg.

Curie Temperature $T_c = 222^{\circ}K$

Lattice parameter $a_o = 3.6 \times 10^{-8}$ cm.

Thus $A = 1.7 \times 10^{-6}$ erg/cm.

The basal plane anisotropy constant at $210^{\circ}K$ is $k_4 = 0.18 \times 10^{6}$ erg/cm^3 and the saturation magnetization at this temperature

$$I_s = 1556 \text{ e.m.u./cm}^3$$

So the equilibrium domain width is

$$D_o = 1.97 \ \mu m$$

The average of a large number of domains width was taken and found to be

$$2D_o = 3.38 \ \mu m$$

so

$$D_o = 1.69 \ \mu m$$

The energy term is obtained from equations 6.8 and 6.9

$$E_o = \frac{\gamma_o}{2\ D_o}$$

put $D_o = 1.69 \ \mu m$

The corresponding energy term per unit volume is

$$E_o = 1.31 \times 10^4 \text{ erg/cm}^3.$$

Any disagreement between the calculated value and measured one may be due to the involvement of the oxide inclusion in the metal.

CHAPTER 7

CONCLUSIONS

7.1 Summary of Results

The work presented here deals with the domain structure of one of the transition metals, cobalt, and two elements belonging to the heavy rare earth subgroup, gadolinium and terbium. The cobalt single crystal is easily obtainable in a pure form while the rare earth elements were difficult to obtain in a pure form as far as the oxide and other impurities involved. It seems from the study of the surface of these metals that the inclusion percentage with respect to the metal is very high and must be taken as a serious factor to be considered whenever magnetic or physical properties are considered. A solid state electrolysis treatment was used on these metals in order to obtain satisfactory samples. This method was good for Gd and to a slightly less extentfor terbium while experiments with Dysprosium have not yet yielded samples of satisfactory quality. Therefore the domain structure of Dy could not be studied. A number of different types of domains configurations where observed including closure and honeycomb domains in gadolinium.

For cobalt crystals the structure observed on both $\langle 2\bar{1}\bar{1}0\rangle$ and $\langle 10\bar{1}0\rangle$ surfaces shows simple plate-shaped domains magnetized along the c-axis. This structure includes a large amount of free pole on the surface perpendicular to the c-axis and no closure structure

could be observed at the edge of the surface with the c-axis. Study of the surface structure (basal plane structure) proved that the surface is one of free poles with no magnetization parallel to the surface (perpendicular to the c-axis). However, the difference between the measured value of the domain width and the exchange constant and the calculated one could be due to the fact that part of the surface structure might possess a closure structure and as a consequence of this a different equilibrium value must be derived. The variation of the energy density ratio P with temperature gives a value at high temperature which is in favour of partial closure domain development. A very interesting relationship was found between the length of a dagger of reverse magnetization and the width of its base; for both simple and complex daggers these were in direct proportionality. For the vanishing value of the length there will still be a value for the base which is of a diameter of 0.18 μm and these might represent a region where the magnetic moment is directed in the hard direction. Variation of domain width with the temperature was obtained and compared with that of Kittel and Landau and Lifshitz model. It was shown to be in agreement with the Kittel model.

It was much easier to derive a model for the domain structure of gadolinium than for cobalt. Domain structure on both $\langle 10\bar{1}0 \rangle$ and $\langle 11\bar{2}0 \rangle$ surfaces proves that the domain consists mainly of plates of a wavy type magnetized along the c-axis which change to a complex type

of pattern below 240°K. Very interesting results were observed at the edge of the specimen near the basal plane where the closure structure appeared clearly. A complex pattern was observed near the edge which gave explanation for the complex nature of the basal plane pattern. However the closure structure made a partial closure of flux and did not completely eliminate the free poles on the surface. Investigation of the basal plane structure shows that it is one of a mixed type, that is free poles as well as closure domains are present. The variations of domain structure with temperature and field were studied on all the three surfaces and these add more evidence to the mixed nature of this structure. Between 240°K and 77°K the domain patterns were difficult to analyse, this was due to the complex nature of the pattern and this may be due to the interaction of the strain induced by cooling with the magnetic moment. Thus the nature of such a pattern is not yet understood. A surprising and unexpected pattern was observed when a small field from a rod shaped permanent magnet was applied normal to the basal plane. This was a honeycomb structure. A model was suggested based on the observed pattern and its behaviour under the field. To derive an equilibrium width for such a structure is complicated by the mixed nature of the pattern. No calculation of domain width or the energy of the system could be obtained.

The domain structure of terbium was expected to be of more interest than that of cobalt or gadolinium since the crystal has the easy direction of magnetization laid along the b-axis. A variety of possibilities were suggested for a Tb single crystal in the form of a cube. Agreement between the suggested model and the patterns observed on Tb is seen in the model in which the domains are magnetized along the b_1 and b_2-axes but not the b_3 axis which is perpendicular to one of the cube surfaces; this will be favourable since it will achieve an appreciable reduction in magnetostatic energy. Thus the domains observed on $<10\bar{1}0>$ and $<11\bar{2}0>$ surface were similar and were of a plate shape magnetized along b_1 and b_2 axes. There was no structure observed on basal plane which in turn confirmed the suggested model. The study of the domain structure of Tb at low temperature presents the same difficulties as that of gadolinium. A pattern was obtained down to $77^{\circ}K$, but it is very complex. It is not possible to interpret this in terms of any simple model for the magnetization. Again it was supposed that such a pattern is due to the strain induced by cooling as in the case of Gd. An energy term was formulated in which two types of domain walls were involved, that of 60° and 120° walls. An equilibrium domain width was derived and calculated. The domain width measured experimentally agreed well with that calculated for the suggested model.

Unfortunately it was not possible to obtain a pure dysprosium sample in order to investigate its domain structure. Although six samples subjected to the method of purification were received none of them was in a suitable condition for domain study.

7.2 Suggestions for further work

It will be a very difficult task to carry out any further work on domain structure on any member of the rare earth group unless very pure metal is obtained. It is suggested that if a sublimed crystal be obtained which could be treated by the application of the solid state electrolysis method of purification a specimen would result with higher purity than that used in present work. If this was made available then it will be of great interest to study the domain structure of gadolinium between 240°K and 4°K where the easy direction lies on a cone of easy magnetization. An investigation of the honeycomb produced by the small permanent magnets and the application of a large normal field to the basal plane produced by such magnets might give more detailed information about the nature of this pattern. A pure sample of Tb will make it easy to investigate the nature of the pattern at low temperature. A study of the domain structure in the antiferromagnetic range with applied field necessary to produce a ferromagnetic alignment will be of interest, also the

effect of applied field on the domain structure of Tb seems important. The dependence of the domain structure in the single crystal terbium on the shape of the sample is of interest since in the case of a cube the magnetization took direction along b_1 and b_2-axis, but not along the b_3-axis which is perpendicular to the surface. It would thus be very interesting to obtain a single crystal of Tb in shape of a disc or a cylinder and examine the possibilities of other domain configurations. Calculation of the magnetostatic energy for models, a, b, and c, in Fig. 6.4 could be compared to the energy for Fig. 6.4d and to show that the latter is the more favourable one.

A study of the domain configuration in a thin film prepared by epitaxial growth on a suitable substrate, will allow the use of the Kerr effect technique and by this the change in the magnetization during cooling will follow easily and thus a full understanding of low temperature patterns will be achieved. Variation of domain structure with the film thickness and the effect of shape anisotropy in a very thin film would provide further interesting study.

A study of domain structure on other rare earth metals might prove to be interesting and useful.

ACKNOWLEDGEMENTS

I would like to express my sincere thanks to Dr. W. D. Corner who has supervised and guided me throughout this work.

Thanks are also due to Professor G. D. Rochester for facilities granted.

I am also grateful to the Technical Staff of the Physics Department for their help and to my fellow Research Students. Thanks are also due to Mrs. J. Moore for typing this thesis.

The author also wishes to express his gratitude to Metals Research Limited for providing the single crystals of Gadolinium and Terbium.

Finally, thanks are due to the Government of Iraq for a Scholarship which has enabled me to carry out the work.

T. Al-Bassam

REFERENCES

Andrä, W. (1954) Ann. Phys. Lpz., 15, 135

(1956) " " " 17, 233

Bates, L. F., and Craik, D.J.

(1962) J. Phys. Soc. Japan, 17, 535

Bates, L.F., and Spivey, S.

(1964) Brit. J. App. Phys., 15, 705

Becker, R., and Doring, W.

(1939) Ferromagnetismus (Springer Berlin)

Belov, K.P., Levitin, R.Z., Nikitin, S.A., and Ped'ko, A.V.

(1961) Soviet Phys., Jetp., 40, 1562

Belov, K.P., and Ped'ko, A.V., and Eksp, Zh.

(1962) Soviet Phys. Jetp., 15, 62

Birss, R.R., and Wallis, P.M.

(1963) Phys. Letters, 4, No. 6., 313

Bloch, F. (1932) Phys. Z. 74, 295

Bly, P.H., Corner, W.D., Taylor, K.N.R., and Darby, M.I.

(1968) J. App. Phys., 39, 1336

Bozorth, R.M., and Wakiyama, T.

(1962) J. Phys. Soc. Japan, 17, 1669

Brown, W.F. (1962) Magnetostatic Principle in Ferromagnetism,

North-Holland Pub. Co., Amsterdam.

Cable, J.W., Moon, R.M., Koehler, W.C., and Wollan, E.O.

(1964) Phys. Rev. Letts. 12, 553

Cable, J.W., and Wallon, E.O.

(1968) Phys. Rev. 165, 733

Cable, J.W., Wollan, E.O., Koehler, W.C., and Wilkinson, M.K.

(1961) J. App. Phys., 32, 493

Chikazumi, S.

(1964) Phys. of magnetism, Edit. John Wiley & Son.

Corner, W.D., Roe, W.C., and Taylor, K.N.R.,

(1962) Proc. Phys. Soc., 80, 927

Cooper, B.R.

(1968) Solid State Phys., Advance in Research and Application, Academic Press. 21, 393

Craik, D.J. (1956) Proc. Phys. Soc. 69, 647

Craik, D.J., and Tebble, R.S.

(1965) Ferromagnetism and Ferromagnetic Domains, North Holland Publishing Company, Amsterdam.

Carey, R., and Isaac, E.D.

(1964) Brit. J. App. Phys., 15, 551

(1966) Magnetic Domainsand Techniques for their observation English University Press Limited.

Darby, M.I., and Taylor, K.N.R.

(1964) Proc. Int. Conf. on Magnetism, Nottingham, England, p. 742

Davis, D. D., and Bozorth, R.M.

(1960) Phys. Rev. 118, 1543

Davis, K.G., and Teghtsoonian, E.,

(1962) Acta Met. 10, 1189

Elliott, J.F., Legvold, S., and Spedding, F.H.

(1953) Phys. Rev. 91, 28

(1955) " " 100, 1595

Elmore, W.C.

(1938) Phys. Rev. 54, 310

Fowler, C.A., and Fryer, E.M.

(1955) Phys. Rev. 98, 270

(1954) " " 94, 310

Fox, M., (1956) The preparation and properties of ferromagnetic single crystals.
Thesis University of Leeds.

Fox, M., and Tebble, R.S.

(1958) Proc. Phys. Soc. 72, 765

Gemperle, R., Gemperle, A., and Bursuc, I.

(1963) Phys. State. Sol. 3, 2101

Goodenough, J.B.

(1956) Phys. Rev. 102, 356

(1954) " " 95, 914

Germer, L.H.

(1942) Phys. Rev. 62, 295

Graham, C.D., Jr.

(1962) J. Phys. Soc. Japan, 17, 1310

(1967) J. Appl. Phys., 38, 1375

(1963) " " " 36, 1135

Grundy, P. J.

(1965) Phil. Mag. 12, 335

Grundy, P.J., and Tebble, R.S.

(1964) J. Appl. Phys., 35, 923

Hale, M.E., Fuller, W.C., and Rubinstein, H.

(1959) J. Appl. Phys., 30, 789

Hall, E.O. (1956) Proc. Phys. Soc., B.2, 254

(1957) Acta Met., 5, 110

Heisenberg, W.

(1928) Z. Phys., 49, 619

Hegland, D.E., Legvold, S., and Spedding, F.H.

(1963) Phys. Rev. 131, 158

Hubert, J. (1968) J. Appl. Phys., 39, 444

Hund, F. (1925) Z. Physik. 33, 855

Hutchinson, R.I., Lavin, P.A., and Moon, J.R.
(1965) J. Scientific Instruments 42, 885

Jacquet, P. (1935) Comptes Rendus 201, 1473
(1936) " " 202, 403

Kaczér, J. (1958) Bulletin of Academy of Sciences of U.S.S.R.
21, No. 8, 1161
(1963) Symposium on Ferromagnetism and Ferroelectricity,
Leningrad 30 - 5 to 5 - 6
(1962) J. Phys. Soc., Japan, 17, 530
(1962) Czech. J. Phys. B.12, 354

Kaczér, J., and Gemperle, R.
(1961) Czech. J. Phys., B11, 510
(1960) " " " B10, 9614

Kaczér, J., Gemperle, R., and Hauptman, Z.
(1958) Czech. J. Phys., 6, 608

Kittel, C. (1949) Rev. Mod. Phys., 21, 541

Koehler, W.C.
(1961a) J. Appl. Phys. 31, 20S
(1961b) Acta Cryst. 14, 535

Koehler, W.C., Cable, J.W., Wollan, E.O., and Wilkinson, M.K.
(1962a) J. Phys. Soc. Japan, 17, B-111, 32
(1962b) Phys. Rev. 126, 1672

Koehler, W.C., Child, H.R., Wollan, E.O., and Cable, J.W.

(1963) J. Appl. Phys. Supp. 34, 1335

Koehler, W.C.

(1965) J. Appl. Phys. 36, 1078

Koepke, B.G., and Scott, T.E.

(1966) Usaec Rept. Is - 1337

Kranz, J. (1956) Naturwissenshaften 43, 370

Landau, L., and Lifshitz, E.,

(1935) Physik, Z., Sowjet 8 , 153

Legvold, S., Spedding, F.H., Barson, F., and Elliott, J.F.

(1953) Rev. Mod. Phys. 25, 129

Lifshitz, E.

(1944) J. Appl. U.S.S.R., 8, 337

Lilley, B.A.

(1950) Phil. Mag. 41, 792

Mayer, L. (1967) J. Appl. Phys., 28, 975

Mee, C.D. (1950) Proc. Phys. Soc. A 63, 922

Metals Research Limited, Melbourn, Royston, Herts., England

Moon, R.M., Cable, J.W., Koehler, W.C.

(1964) J. Appl.Phys., Suppl. 35, 1041

Néel, L. (1955) Compt. Rend. Acad. Sci., Paris, 241, 533

(1944) J. Phys. Radium 5, 265

Nigh, H.E., Legvold, S., and Spedding, F.H.

(1963) Phys. Rev. 132, 1092

Osborn, J.A. (1945) Phys. Rev. 67, 351

Pauthenet, R., Barnier, Y., and Rimet, G.

(1962) J. Phys. Soc. Japan, 17, B.1, 309

Rhyne, J.J., and Clark, A.E.

(1967) J. App. Phys., 38, 1379

Rhodes, B.C., Legvold, S., and Spedding, F.H.

(1958) Phys. Rev. 109, 1542

Roman, W.A. (1965) The metallographic preparation of some rare earth metals by R.R. Russel

General Electric Technical Information series.

Report No. 65 - C - 017.

Salkovitz, E.

(1951) J. of Metals, 189, 1951

Shur, J.S., Glazer, A.A., Dragochanskii, Yu. N., Zaikova, V.A., and Kandaurova, G.S.

(1964) Izv. Akad. Nauk. U.S.S.R., 28, 553

Spedding, F.H., and Daane, A.H.

(1961) The Rare Earths - Edit. J. Wiley & Sons

Spedding, F.H., Legvold, S., Daane, A.H., and Jenning, L.D.

(1957) Progress in low temperature physics - Edit. C.J. Gorter, Vol. 11, Chapt.12, North Holland Publishing Co. Amsterdam.

Spedding, F.H., and Daane, A.H.

(1954a) J. Metals, 6, 504

Spedding, F.H., Voight, A.F., Gladrow, E.M., and Sleight, N.R.

(1947) J. Am. Chem. 69, 2777

Spedding, F.H., and Powell, J.E.,

(1954b) J. Metals, 6, 1131

Stoner, E.C. (1950) Rep. Progs. Phys. 13, 82

Sucksmith, W., and Thompson, J.E.

(1954) Proc. Roy. Soc., A225, 362

Suhl, H.T. (1968) Magnetism III. - Edited by G.T. Rado. H. Suhl.

Academic Press, N.Y., and London, pp.415

Takata, Y. (1962) J. Phys. Soc. Japan, 18, 87

Tannenwald, P.E., and Weber, R.

(1961) Phys. Rev. 121, 715

Tebble, R.S.

Proc. of Int. Conf. on Magnetism, Nottingham,

(1965) Inst. of Phys. & The Phys. Soc., London p.859

Van Hamos and Thiessen, P.A.

(1932) Z. Physik, 71, 442

Van Vleck, J.H.

(1952) Rev. Mod. Phys. 23, 213

Weiss, P. (1907) J. Phys. Theo. Appl. 6, 661

Will, G., Nathans, R., and Alperin, H.A.

(1969) J. App. Phys. Suppl. 35, 1045

Williams, H.J., Foster, F.G., and Wood, E.A.

(1951) Phys. Rev. 82, 119

Williams, H.J., Bozorth, R.M., and Shockley, Y.W.

(1949) Phys. Rev. 75, 155

Wilkinson, M.K., Koehler, W.C., Wollan, E.O., and Cable, J.W.

(1961a) J. Appl. Phys. 32, 48

Wilkinson, M.K., Child, H.R., McHargne, C.J., Koehler, W.C., and Wollan, E.O.

(1961b) Phys. Rev. 122, 1409

Wilkinson, M.K., Child, H.R., Koehler, W.C., Cable, J.W., and Wollan, E.O.

(1962) J. Phys. Soc. Japan, 17, B-111, 27

Wrzeciono, A., and Gemperle, R.

(1966) Phys. State. Sol. 14, 491

Wysolocki, B., and Zietek, W.

(1965) Acta Phys. Polon. 27, 716

(1963) Phys. Stat. Sol. 3, 1333